540

NITROGEN DIOXIDE OXIDATIONS

A Thesis submitted by

EDWARD HUMPHREY CROWSTON

in partial fulfilment of the requirements for the degree of Doctor of Philosophy of the University of London.

September 1986

Department of Chemistry

Imperial College

South Kensington

LONDON SW7

Abstract

The chemistry of NO_2 and N_2O_4 and the role of gaseous NO_2 as an environmental pollutant are briefly discussed.

A systematic study of the reactions of dilute ($\langle$2000 ppm) gaseous NO_2 with aqueous solutions of several substrates is reported. Quantitation of NO_2^- and NO_3^- yields by Ion Chromatography is shown to be a useful method for investigating these reactions.

In water at pH$\rangle$5, hydrolysis of gaseous NO_2 produces equimolar quantities of NO_2^- and NO_3^- which are best explained as a reaction of the thermodynamically stable N_2O_4 dimer (O_2N-NO_2). In the presence of oxidisable substrates, an excess of NO_2^- is produced. This is shown to arise from electron transfer from the substrate rather than by hydrogen abstraction. The $[NO_2^-]/[NO_3^-]$ ratio is a simple method of detecting electron transfer by gaseous nitrogen dioxide.

Analysis of the data suggests that both NO_2 and a kinetically stable dimer (probably ON-OO-NO) are one-electron oxidants of various substrates.

By varying the pH the reactive form of the substrate in solution has been identified as the phenoxide ion and unprotonated DABCO and aniline. The studies have been extended to aqueous-organic solvent mixtures to solubilise water insoluble substrates (e.g. phenothiazine) and to employ dielectric effects as confirmation for the electron transfer processes.

These studies have been applied to the reaction of gaseous NO_2 with serum. Excess NO_2^- is produced and serum proteins are shown to be reactive due to their tyrosine and tryptophan content. A synergistic effect, the redox reaction between tryptophan radical cation and tyrosinate, is proposed to account for these observations.

Product analyses of a number of phenols at pH 13 are consistent with the electron transfer oxidation proposed.

Acknowledgements

I would like to thank my supervisor Dr. B.C. Challis for his guidance and enthusiasm during this project and the SERC for a Quota Award.

I acknowledge the friendly advice of my colleagues in the Harwood Laboratory, and the academic and technical staff of the Chemistry Department.

Finally, my thanks to Caroline, my wife, for her understanding, and the typing of this Thesis.

Contents

Chapter/Section	Title	Page
1.	Introduction and Historical Review	1
1.1.	Introduction	2
1.2.	The Chemistry of NO_2 and N_2O_4	3
1.2.1.	Physical Properties	3
1.2.2.	Addition and Hydrogen Abstraction	4
1.2.3.	Nitrosation	6
1.2.4.	Nitration	10
1.3.	Nitrogen Dioxide as a Pollutant	11
1.3.1.	Introduction	11
1.3.2.	Measurement of Ambient NO_2	12
1.3.3.	Fate of Inhaled Nitrogen Oxides	16
1.4.	Oxidation of Phenols	18
1.5.	Conclusion	21
2.	Electron Transfer Reactions of Nitrogen Dioxide and Dinitrogen Tetraoxide	22
2.1.	Introduction	23
2.2.	HPLC Analysis of Nitrite and Nitrate Ions	23
2.3.	Hydrolysis of Nitrogen Dioxide	26
2.3.1.	Nitrite and Nitrate Ion Stability	26
2.3.2.	Effect of Nitrogen Dioxide Concentration	27
2.3.3.	pH Dependence	29

Chapter/Section	Title	Page
2.3.4.	Conclusions	33
2.4.	Reactions of Gaseous Nitrogen Dioxide with Organic Substrate in Aqueous Solution	34
2.4.1.	Observation of Excess Nitrite Ion	34
2.4.2.	Hydrogen Abstraction vs Electron Transfer	37
2.4.3.	Dependence on Substrate Concentration	38
2.4.4.	Dependence on Nitrogen Dioxide Concentration	41
2.4.5.	The Reaction Model	41
2.4.6.	Electron Transfer to Dinitrogen Tetraoxide	59
2.4.7.	Rate Coefficients	61
2.5.	Summary	62
3.	Factors Governing Substrate Reactivity	64
3.1.	Reduction Potentials	65
3.2.	The Reactive Moiety in Solution	74
3.2.1.	Phenol	74
3.2.2.	DABCO	76
3.2.3.	Aniline	76
3.2.4.	Conclusion	80
3.3.	Radical Cation Basicities	80
3.3.1.	Thiol Reactivity	87
3.4.	Summary	88

Chapter/Section	Title	Page
4.	The Reactions of Gaseous Nitrogen Dioxide with Organic Substrates in Aqueous-Organic Solvent Mixtures	89
4.1.	Introduction	90
4.2.	Electron Transfer in Aqueous-Organic Solvent Mixtures	90
4.3.	Water Insoluble Substrates	96
4.4.	Solvent Effects	97
4.5.	Micelles	99
4.6.	Summary	101
5.	Biological Substrates	102
5.1.	Introduction	103
5.2.	The Reaction of Nitrogen Dioxide with Serum	103
5.2.1.	Antioxidant Capability	104
5.2.2.	Serum Proteins	106
5.2.3.	Reactions in Serum	111
5.2.4.	Synergistic Effect	113
5.2.5.	Plasma	115
5.2.6.	Biological Effects of Gaseous Nitrogen Dioxide	116
5.3.	Product Analyses	116
5.3.1.	3-Methylindole - GC/MS Studies	118
5.4.	Summary	127

Chapter/Section	Title	Page
6.	Phenol Oxidations	128
6.1.	Introduction	129
6.2.	The Reaction of Gaseous Nitrogen Dioxide with Phenol	129
6.3.	The Reaction of Gaseous Nitrogen Dioxide with 2,4,6-Trimethylphenol	133
6.4.	The Reaction of Gaseous Nitrogen Dioxide with 2,4,6-Trichlorophenol	137
6.4.1.	Halide Displacement	138
6.5.	Polymer Formation	140
6.5.1.	Crystallisation of Dimers and Trimers	140
6.5.2.	Gel-Permeation Chromatography (GPC) Studies	140
6.5.3.	Oligomers	142
6.6.	Dioxin Formation	144
6.6.1.	Synthesis of 2-(2'-Chlorophenoxy)-phenol	144
6.6.2.	The Reactin of 2-(2'-Chlorophenoxy)-phenol with Gaseous NO_2	144
6.7.	Summary	145
7.	Concluding Remarks	147
8.	Experimental	149
8.1.	Reactions with NO_2	150
8.1.1.	Gas Circulation Apparatus	150

Chapter/Section	Title	Page
8.1.2.	NO_2 Line	152
8.1.3.	Bubbler Design	153
8.1.4.	Typical Reaction Conditions	154
8.2.	Analytical Protocol	155
8.2.1.	HPLC Analysis	155
8.2.1.1.	General and Instrumentation	155
8.2.1.2.	Nitrite and Nitrate Ion Analysis	156
8.2.1.3.	Nitrophenols	158
8.2.1.4.	Nitroanilines	159
8.2.2.	GC Analysis	159
8.2.2.1.	General and Instrumentation	159
	Capillary GC	159
	2-Methylindole/3-Methylindole Analysis	160
8.2.2.2.	Work-up Procedures	162
	Phenol Product Analysis	162
	Dioxin Production	162
8.2.3.	GC/MS	163
8.2.4.	GPC Analysis	163
8.3.	Biological Fluids	164
8.4.	Preparative	165
Appendix	Standard Reactivity Index	172
	References	178

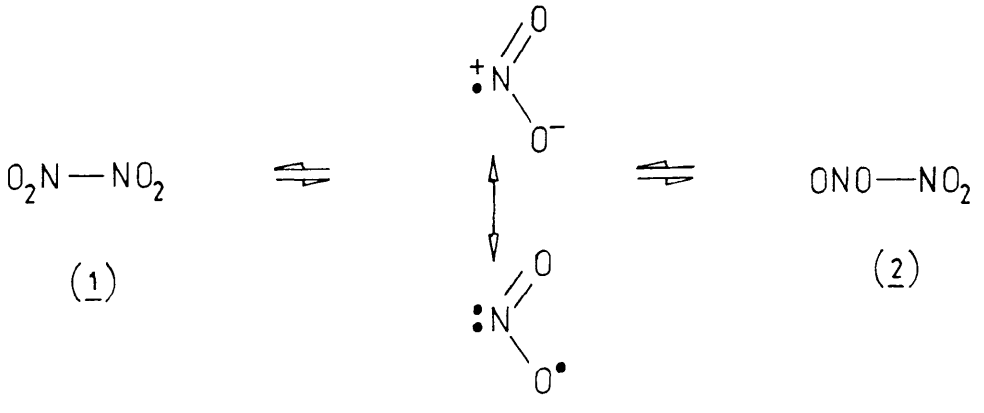
Chapter 1

Introduction and Historical Review

1.1. Introduction

NO_2 is a simple but important radical. It is a primary pollutant in acid rain[1] and the formation of toxic compounds[2,3]. It is a component of cigarette smoke[4] and could be a factor in lung cancer.

NO_2 has been widely investigated[5,6] and is known to act as an oxidant, nitrating and nitrasating agent. All the studies are complicated by dimerisation to N_2O_4 which may have either a symmetrical[7,8] (1) or unsymmetrical[9] (2) structure. Further, NO_2 has the potential to react either at the O- or N- atom (Scheme 1).



Scheme 1. Isomers of NO_2 and N_2O_4

Since NO_2 is in equilibrium with N_2O_4[10] one would expect to observe reactions of NO_2 mainly at high temperature and high dilution. Factors influencing reaction at either the O- or N- atoms are not well defined and most recent estimates suggest 49%[7] of the unpaired electron resides on the O-atoms.

1.2. The Chemistry of NO_2 and N_2O_4

1.2.1. Physical Properties

The equilibrium between brown paramagnetic NO_2 and colourless diamagnetic N_2O_4 is strongly temperature dependent in both solution and the gas phase. The equilibrium constant $K_{N_2O_4}$ (= $[NO_2]^2/[N_2O_4]$) is 1.51×10^{-1} mol dm^{-3} in the gas phase at 25°C[11]. Dissociation of N_2O_4 to NO_2 is less in solution[10,11] as the constants in Table 1 indicate.

Solvent	$K_{N_2O_4}$ (25°C)/mol dm^{-3}
Cyclohexane	1.77×10^{-4}
Carbon Tetrachloride	1.78×10^{-4}
Acetonitrile	3×10^{-5}
Water	1.53×10^{-5}

Table 1. $K_{N_2O_4}$ in Solution[10]

In the solid state the oxide is wholly N_2O_4. Partial dissociation occurs in the liquid; it is pale yellow at the freezing point and contains 0.01% of NO_2, which increases to 0.1% in the deep red-brown liquid at the boiling point, 21.15°C. In the vapour at 100°C the composition is NO_2 90% N_2O_4 10% and dissociation is complete above 140°C. At higher temperatures the position is complicated by decomposition to nitric oxide (Scheme 2), which begins at 150°C and is complete at 600°C[12].

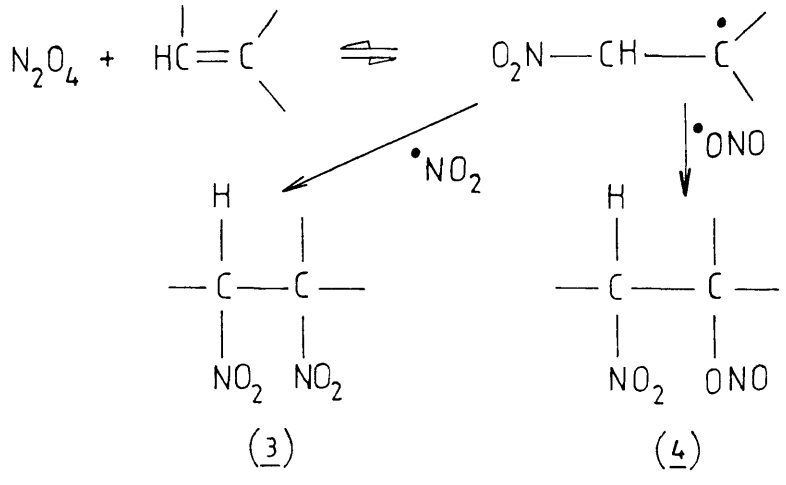
$$2NO_2 \rightleftharpoons 2NO + O_2$$

Scheme 2. Dissociation of NO_2

NO_2 is oxidised fairly readily to NO_2^+, an intermediate in acid catalysed nitration. Salts like NO_2BF_4 and N-nitrocollidinium tetrafluoroborate have been isolated and are known to be good nitrating agents in organic solvents[13].

1.2.2. Addition and Hydrogen Abstraction

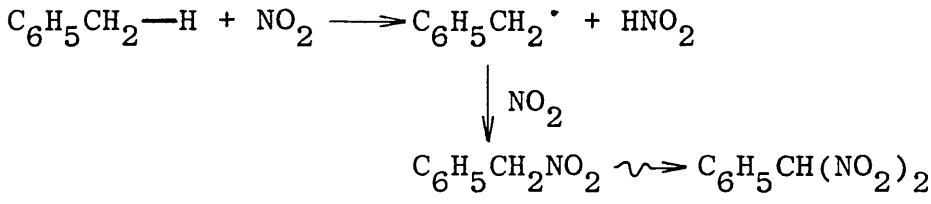
At relatively low temperatures[5,14] (-10 to 25°C) in solvents such as diethyl ether, ethyl acetate and dioxane[14], high concentrations of nitrogen dioxide react with alkenes by addition to the double bond. Addition always occurs to give a C—N bond and the most substituted radical, both factors confuring greater stability[14]. The product forming step is less selective leading to dinitrocompounds (3) or nitronitrates (4) (Scheme 3).



(3) (4)

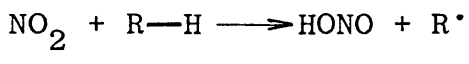
Scheme 3. Addition to olefins

In contrast, NO_2 reacts with toluene[15] by abstraction of benzylic hydrogen atoms following Scheme 4 from Yoshida's study[16]. For ortho and para MeC_6H_4R (R=MeO, Me,



Scheme 4. Hydrogen Abstraction from toluene

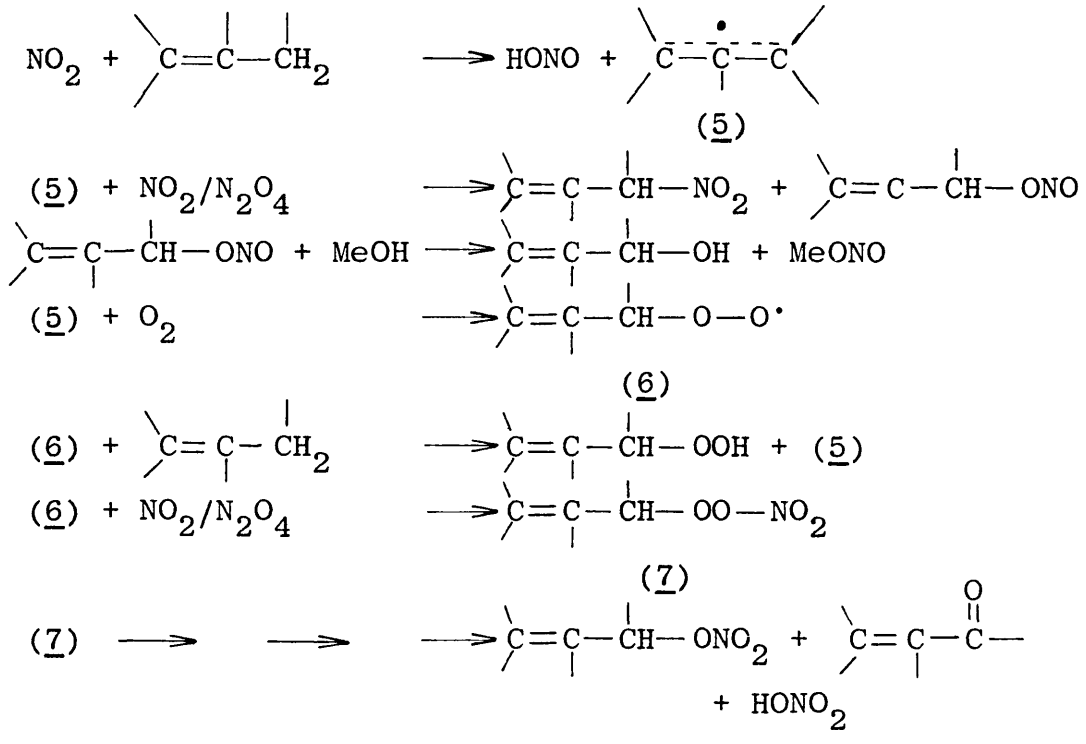
Cl, CHO, CN or NO_2) in C_6H_6, the rate of side chain nitration correlated with Hammett σ^+ parameters with ρ= -1.40, correlation coefficient= -0.99. Gas-Phase nitration and oxidation of hydrocarbons occurs via this route[5] which is generalised in Scheme 5. Rates of reaction decrease in line with the stability of the intermediate radical i.e. $R_3CH \rangle R_2CH_2 \rangle RCH_3$[15].



Scheme 5. Hydrogen Abstraction

Recently Pryor et al[17] studied the reaction between gaseous NO_2 (70ppm to 50%) and alkenes in hexane at 30°C. They found that at high concentrations addition to the double bond is the predominant process. Below 10000ppm (1%), however, hydrogen abstraction is more important. Scheme 6 shows the proposed mechanism for the formation of the allylic substitution products observed. It was seen that autooxidation occurs in the presence of oxygen at low NO_2

concentrations which was also rationalised by the same mechanism.



Scheme 6. Hydrogen Abstraction Mechanism[17]

The dependence of the reaction mechanism on the NO_2 concentration was attributed to competition between reversible addition and irreversible H-abstraction.

Unsaturated fatty acid esters i.e. methyl linoleate were shown to react by hydrogen abstraction[17]. It was suggested that reaction of inhaled NO_2 with polyunsaturated fatty acids (PUFA) in the lung initiated PUFA autooxidation and formed nitrous acid in lung tissue.

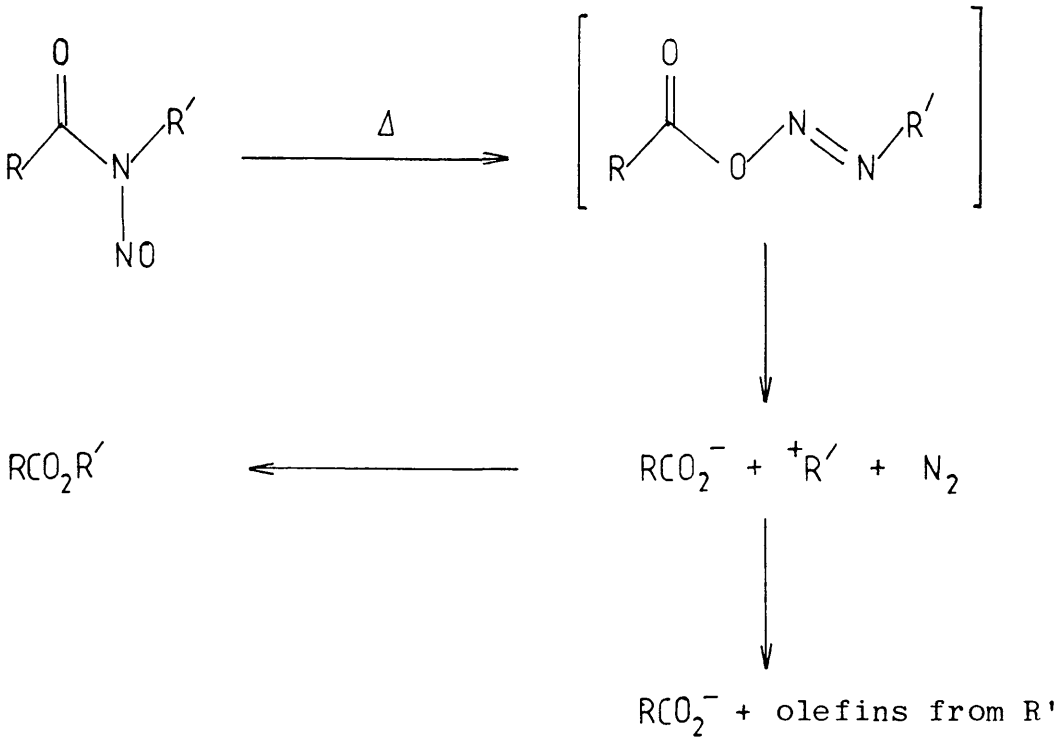
1.2.3. Nitrosation

In 1955 White investigated the suitability of several reagents for the preparation of N-alkyl-N-nitrosamides[18] and found that N_2O_4 in CCl_4 with an excess of sodium acetate gave good yields of many N-nitrosamides

after 10 mins at $0^{o}C$.

Concurrently White[19,20] and Huisgen and his colleagues[21,22] showed that N-alkyl-N-nitrosamides thermolyse by only two pathways; ester formation by loss of nitrogen, and the formation of a carboxylic acid with olefinic products. The dominant pathway is a function of several variables, most importantly the substitution at the R'-group (Scheme 7) and the solvent polarity. Temperature is of secondary importance, and the nature of the acyl fragment has relatively little effect. Ester formation tends to dominate in non-polar solvents and to decrease with increasing substitution - to the amide nitrogen atom. The mechanism of this elimination of nitrogen has been thoroughly investigated, and is considered to involve slow rearrangement to a diazoester intermediate with subsequent rapid collapse to a carboxylate anion and carbonium ion (Scheme 7). Further reactivity has been rationalized by carbonium ion instability and solvent basicity, and has been discussed in detail by White[23].

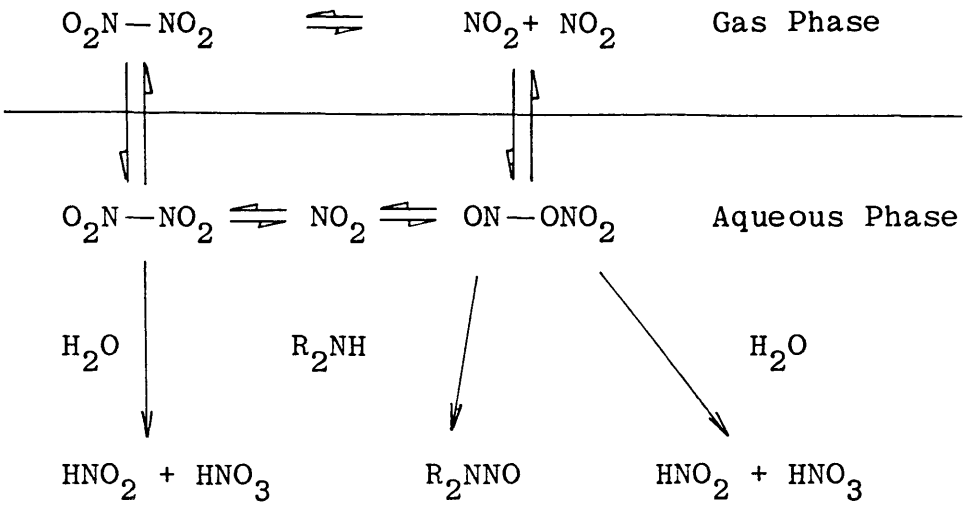
In 1957 White and Feldman[24] communicated the nitrosation of amines by N_2O_4 in CH_2Cl_2. Subsequently, the nitrosation of amines in neutral and alkaline aqueous solutions with gaseous N_2O_4 and N_2O_3 has been reported by Challis and Krytopoulos[9,25]. Secondary amines such as piperidine or morpholine gave N-nitroso compounds, aniline and substituted anilines were diazotised[26]. The reactions were fast, but little dependency on the basicity of the amines of nitrosation yields were seen (1.5-2% diazotisation of anilines), which suggested diffusion or



Scheme 7. Thermolysis of N-Alkyl-N-Nitrosamides

encounter controlled reactions. Prior to dissolution, N_2O_4 in the gas phase is substantially dissociated into NO_2 radicals. N_2O_4 dissolved in solution is less dissociated[10] and therefore NO_2 radicals may combine in solution to give the reactive metastable isomer $ONONO_2$ the predominant nitrosating agent in solution[9]. The rate-limiting step for the nitrosation would then be the radical coupling to give $ONONO_2$ or the diffusion of N_2O_4 into the aqueous phase. This is illustrated together with competing hydrolysis reactions in Scheme 8.

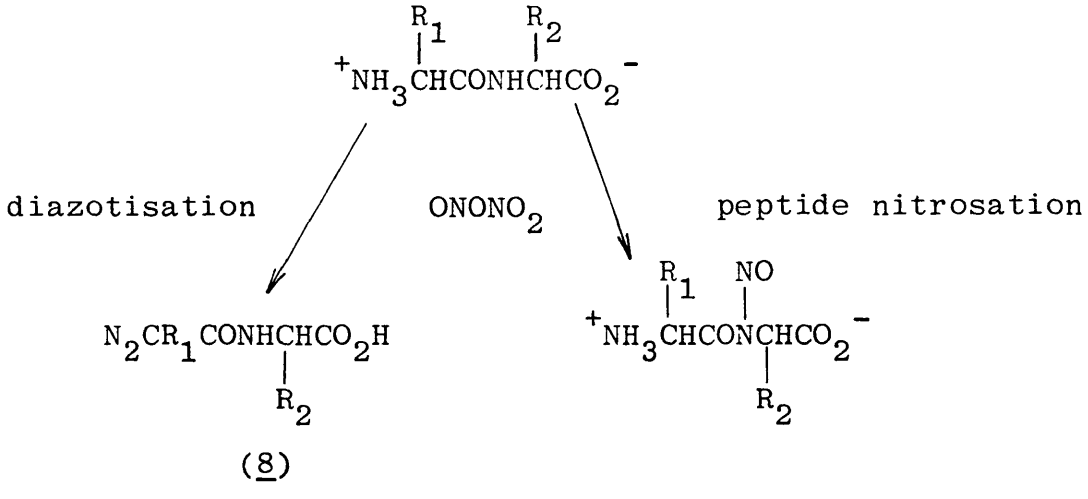
N-Nitrosopeptides recently synthesised and authenticated by Challis et al[27], have been formed by the reaction of gaseous nitrogen dioxide with terminal primary amino protected amino-acids and peptides at -20°C in the



Scheme 8. Nitrosation by $ONONO_2$

presence of sodium acetate in dichloromethane[28].

Diazopeptides (8) are formed on passing N_2O_4 through solutions of small peptides in neutral and alkaline aqueous solutions[29]. This is presumeably in competition with the formation of N-nitrosopeptides, as shown for a dipeptide in Scheme 9. Some N-nitrosopeptides[30] and diazopeptides[31] exhibit *in vitro* mutagenic activity.

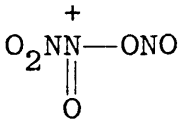


(8)

Scheme 9. Peptide nitrosation and diazotisation

1.2.4. Nitration

Treatment of polycyclic aromatic hydrocarbons with dinitrogen tetraoxide in dichloromethane solution leads to the clean production of mononitro derivatives with high positional selectivity in almost quantitative yields[32]. An electron-transfer mechanism involving NO_2^+ or NO^+ has been considered. The former was predicted to undergo nitration via a Wheland intermediate not *via* electron transfer, whilst the latter species was predicted to be an effective non-bonding electron transfer oxidant[33]. Electron transfer to nitrogen dioxide has also been postulated[2]. It is thought improbable because of the rapid reverse reaction for naphthalene[10] and perylene[34] and because the reaction between perylene radical cation and nitrogen dioxide does not lead to clean formation of mononitroperylenes[34]. Eberson and Radner[3] have recently suggested the formation of a σ-complex by the attack of a novel nitrosated dinitrogen tetraoxide species (*9*) as an initial step and it is suggested that nitrous acid catalysed nitration follows the same pathway.



(*9*)

Recently Ridd[35] has published kinetic evidence for the nitrous acid-catalysed nitration of p-nitrophenol in aqueous nitric acid going through the p-nitrophenoxy radical, and has suggested *Scheme 10* as being consistent with all the experimental evidence. The first-step being rate

determining at low nitrous acid concentrations and the second step at high concentrations, explaining the zeroth order with respect to nitrous acid as the concentration of nitrous acid is increased.

$$ArO^- + NO^+ \underset{k_{-1}}{\overset{k_1}{\rightleftharpoons}} ArO^\cdot + NO^\cdot$$

$$(NO^\cdot + NO_2{}^+ \overset{K}{\rightleftharpoons} NO^+ + NO_2{}^\cdot)$$

$$ArO^\cdot + NO_2{}^\cdot \xrightarrow{k_2} \text{Dinitroproduct}$$

Scheme 10. Nitrous Acid-Catalysed Nitration of p-Nitrophenol

Clearly the mechanism of nitrous acid-catalysed nitration is unproven and further evidence is required to differentiate between the electrophillic[3] and electron transfer[35] pathways proposed.

Nitration of phenols by NO_2 is reviewed in Section 1.4.

1.3. Nitrogen Dioxide as a Pollutant

1.3.1. Introduction

Nitric oxide and nitrogen dioxide play an important role in the atmospheric chemistry of the troposphere. They are essential components of the ozone production cycle and also control the concentrations of other important photochemical oxidants, the hydroxyl radical and hydrogen peroxide[1] (Scheme 11). These oxidants are responsible for the conversion of SO_2 to acidic products and the oxidation of the nitrogen oxides to nitric acid. A recent study by Cocks and Crane[36] has assessed the contributions of the various natural, agricultural and fossil fuel combustion sources to total NO_x emissions in Europe and in

the UK. The fossil fuel source, which includes vehicle emissions, dominates, contributing about 95% to the total UK and 85% to total European emissions averaged over a year. In summer the corresponding proportions are around 90% and 70%. Substantial reductions of NO_x levels in the UK and Europe are possible through stringent emission controls. Such controls will reduce to a minimum any further environmental damage akin to that already observed in Scandanavia, West Germany and Wales[1].

$$NO_2 + h\nu \longrightarrow NO + O$$
$$O + O_2 + M \longrightarrow O_3 + M$$
$$NO + O_3 \longrightarrow NO_2 + O_2$$
$$O + H_2O \longrightarrow 2HO^{\bullet} \longrightarrow H_2O_2$$
$$HO^{\bullet} + NO_2 + M \longrightarrow HNO_3 + M$$
$$HO^{\bullet} + SO_2 + M \longrightarrow HSO_3 + M$$
$$HSO_3 + O_2 \longrightarrow HO_2 + SO_3$$
$$HO_2 + NO \longrightarrow HO^{\bullet} + NO_2$$
$$HO_2 + HO_2 \longrightarrow H_2O_2 + O_2$$
$$RCH_3 + 4O_2 \longrightarrow RCHO + H_2O + 2O_3$$

Scheme 11. Production of Atmospheric Oxidants[1]

1.3.2. Measurement of ambient NO_2

Nitrogen dioxide is an atmospheric pollutant and could be harmful in its own right and as a precursor to carcinogens (e.g. N-nitrosamines). The atmospheric determination of nitrogen dioxide has been made internationally for many years using the Saltzman method[37]

or a modification of it. The Saltzman method involves the absorption of nitrogen dioxide in a mixture of sulphanilic acid, N-(1-naphthyl)ethylenediamine dihydrochloride and acetic acid. A stable direct colour is produced. The sulphanilic acid is diazotised by nitrous acid and the resulting diazosulphanilic acid is coupled with the naphthylamine to give an azo dye, the intensity of which is quantitatively determined spectrophotometrically.

If the nitrite produced in these reactions was solely the result of the classical hydrolysis reaction (Equation 1) the ratio of nitrite to nitrogen dioxide

$$2NO_2 \rightleftharpoons N_2O_4 \xrightarrow{H_2O} HNO_2 + HNO_3 \qquad ..(1)$$

would be 0.5. This ratio is termed the 'Saltzman Factor' and was originally reported as 0.72 by Saltzman[37]. Subsequent research has shown it to vary between 0.5 and 1[38-59].

Early work showed no general pattern in the value of the Saltzman Factor, however is soon emerged that reducing the nitrogen dioxide concentration (in the ppm range) increased the Saltzman Factor[42,44,45,48,49,51,52,54,57]. These results led to the postulation of the following two step mechanism for the hydrolysis reaction[48,49,52,54,59]. The first step is proposed to be a hydrogen abstraction followed by the reaction of the radical formed with another molecule of NO_2 (Scheme 12), the combination of which results in the classical Saltzman Factor of 0.5.

$$NO_2 + H_2O \longrightarrow HO^{\cdot} + HNO_2$$
$$HO^{\cdot} + NO_2 \longrightarrow HONO_2$$

Scheme 12. Hydrogen Abstraction from Water

It can be seen that decreased nitrogen dioxide concentration reduces the yield of the second step in relation to other reactions of the hydroxyl radical i.e. dimerisation, thereby increasing the observed Saltzman Factor. Hydrogen abstraction[48,60] and electron transfer[46] from solutes have also been proposed but not proven to account for these observations.

Yanagisawa and Nishimura have reported[56] that the Saltzman Factor increased with increased hydroxyl ion concentrations in the absorbing solution on passing 1.2 ppm gaseous NO_2 at ca. 600 ml/min using a fritted-glass bubbler. This may indicate the increased reactivity of HO^- (Equation 2) over H_2O towards NO_2, although further work is necessary to establish that these results are not artifactual.

$$HO^- + NO_2 \longrightarrow HO^{\cdot} + NO_2^- \qquad ..(2)$$

It must be emphasised that all this work must be critically reviewed because of the wide variety of experimental conditions used. Results reported using this method may be erroneous due to incomplete understanding of the reactions taking place.

Recently[61] nitric oxide and nitrogen dioxide concentrations have been determined with instruments that utilise the chemiluminescent reaction between nitric oxide

and azone. A converter inside the instrument reduces NO_2 to NO so that the total oxides of nitrogen can be determined (Scheme 13). NO_2 levels are calculated from

Catalytic Converter	$NO_2 \longrightarrow NO$
Flow Reactor	$NO + O_3 \longrightarrow NO_2^* + O_2$
	$NO_2^* \longrightarrow NO_2 + h\nu$

Scheme 13. Operation of Chemiluminescent Reaction Instruments

simultaneous NO and NO_x measurements by the instrument. A novel application of this analyser has been marketed by Sievers and co-workers[62,63] in the form of a specific gas chromatography detector. They observe selective oxidation of many organic compounds by nitrogen dioxide over a gold catalyst and detect the NO produced.

Selected[4,61,64] ambient NO_2 levels are given in Table 2. It is seen that the maximum environmental concentration is about 1 ppm.

Situation	NO_2 concentration / ppm
Rural	0.005
Urban, off-street	0.01-0.04
Urban, kerbside	-0.12
Smoke-filled room	0.10
Kitchen, gas cooker	0.25-1.1
Cigarette smoke (inhaled)	trace

Table 2. Ambient NO_2 levels

1.3.3. Fate of inhaled nitrogen oxides

In animal studies a significant proportion of inhaled nitrogen oxides is retained to be excreted in the urine, but not expired[60]. Chiodi and Mohler[65] found evidence that NO_2 diffuses slower through tissue than NO suggesting that retention in the trachea and bronchi as well as in the vascular space is feasible for the more reactive NO_2. The transformations of NO in blood are reasonably well understood. Under strict anaerobic conditions NO can combine with haemoglobin (Hb) to form nitrosyl haemoglobin (NOHb) without any methaemoglobin (MetHb) formation[65]. NO is not a Hb oxidant and to become one it needs the presence of O_2. On exposure to O_2, NOHb is converted to MetHb[65] but at a slower rate that the aerobic reaction of NO with oxyhaemoglobin (HbO_2)[66]. Production of methaemoglobin decreases the oxygen transporting capability of the blood[67] and may account for the toxicity of nitrogen oxides. Both reactions presumeably form nitrate (Scheme 14) which suggests that inhaled NO primarily contributes to the bodily intake of nitrate.

$$NOHb + O_2 \longrightarrow Met\text{—}Hb + NO_3^-$$

$$HbO_2 + NO \longrightarrow Met\text{—}Hb + {}^-OONO \longrightarrow NO_3^-$$

Scheme 14. Nitrate production

The fate of inhaled NO_2 is less well understood. NO_2 hydrolyses to nitrite and nitrate therefore the

reactions of nitrite may be important. Nitrite reacts with HbO_2 to give MetHb and nitrate[68-70]. The reaction is autocatalytic with an induction period but the mechanism is not fully understood. NO_2 has recently been proposed as an intermediate[69,70], the reaction being accelerated by NO_2 addition[69]. The reaction is inhibited by antioxidants[69] and by amines (e.g. morpholine and triethylamine) in aqueous phosphate buffer at pH 7.0[70]. Kosaka and Uozumi conclude that the latter results establish NO_2 involvement as amines are known to react with nitrogen dioxide to yield nitrosamines but no evidence of nitrosamine formation is given and the results may only indicate the oxidation of the amines by an unknown oxidant. Equation 3 illustrates the stoichiometry of this reaction.

$$4HbO_2 + 4NO_2^- + 4H^+ \longrightarrow 4MetHb + 4NO_3^- + O_2 + 2H_2O \quad ..(3)$$

A few animal inhalation experiments have been performed. Postlethwait and Mustafa[71] showed NO_2 absorbed in isolated perfused rat lungs gave only nitrite in the absence of erythrocytes and mainly nitrate (65%) in their presence. They concluded that absorbed NO_2 in the lung is converted predominately into nitrite which is then oxidised to nitrate by the erythrocytes after diffusion into the vascular space. Saul and Archer[60] estimated that 3.5 mg nitrite would be formed in the human lung each day from air containing 0.1 ppm NO_2 from urinary nitrate studies of rats exposed to NO_2 over 24 hours.

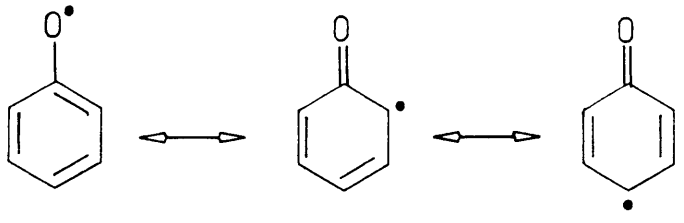
Oda et al[72] found that the nitrate and nitrite blood levels of mice rose quickly to constant values on exposure to 40 ppm NO_2, both declined after exposure with half-lives of 60 and 10 minutes respectively. The production of nitrite exclusively on exposure to NO_2[71] suggests that hydrolysis is not the only route of formation, this merits further investigation of the reactions of NO_2 with body fluids.

1.4. Oxidation of Phenols

The oxidation of phenols has been extensively reviewed[73-76]. Phenol oxidative coupling reactions are important in biosynthesis[76]. Phenol coupled products are given by a wide variety of oxidants e.g. potassium ferricyanide, ferric chloride, manganese (III), vanadium (V), manganese dioxide, lead dioxide, silver oxide, silver carbonate, chromate, nitric acid and organic nitrites[73]. The generally accepted mechanism for product formation is by radical coupling of phenoxy radicals although only the two former oxidants are known to react by one electron transfer and non-radical pathways have been suggested[73].

From the reaction of a simple phenoxy radical and because of its radical delocalisation (spin density $\rho_4 > \rho_2 > \rho_{oxygen} > \rho_3$[76]) as illustrated in Scheme 15 the possible dimeric couplings and subsequent products are shown in Table 3. Formation of Pummerer's ketone is well established[77] and the O,4'-dimer $\rightleftharpoons$ 2PheO· has often been investigated[78]. Recently spectroscopic evidence has been presented for the formation of the 2,2'-dimer by the

reaction of $N_3^{\bullet}$ with the phenolic dipeptide glycyltyrosine[79], about a 60 per cent yield was obtained but the product was not isolated. The same product was also seen in the oxidation by pulse radiolysis generated NO_2 by the same workers[80], however the major products at intermediate pH (7 to 9) were of nitration postulated to be via radical coupling. Nitration products were also seen spectrometrically from tyrosine containing peptides. Generation of NO_2 by this method requires dedicated expensive equipment and it is unclear as to whether NO_2 or N_2O_4 is the reactive species.



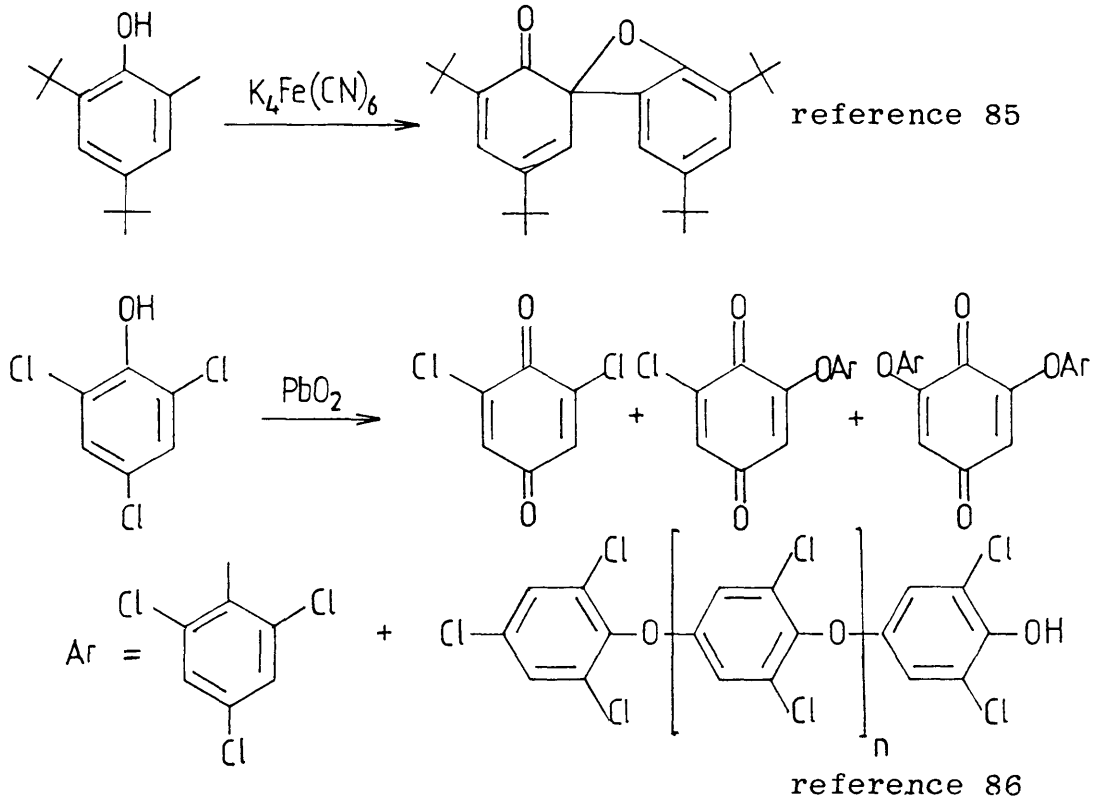
Scheme 15. Phenoxy Radical Delocalisation

Coupling	Dimer	Product
O,2'	phenoxy-phenol	
2,2'	biphenol	
4,2'	quinolyl-quinol	⟶ Pummerer's Ketone
O,4'	phenoxy-quinol	⇌ 2PheO$^{\bullet}$
O,O'	peroxide	⟶ ?
4,4'	biquinol	

Table 3. Likely Dimeric Products

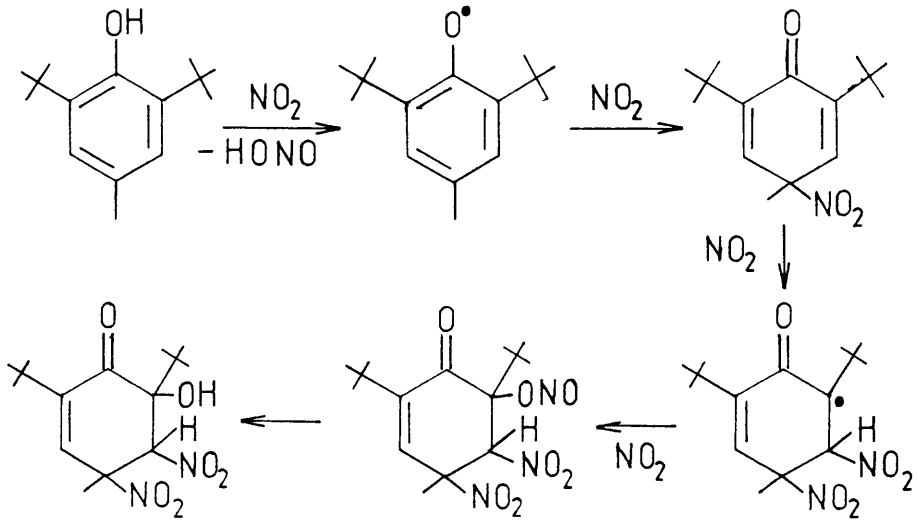
Many phenol oxidations give low yields of characterised products which has been attributed to polymer formation. Little data exists on these polymers. Lingren[81] measured the molecular weight of a proposed polymeric phenyl ether and although there was significant discrepancy in repeat measurements gave an upper limit of 1900 a.m.u. No other molecular weight distribution data is available.

Radical coupling generally occurs at unsubstituted positions, however when this is not possible there have been some cases of coupling at halide substituted positions these are illustrated in Scheme 16. There are no cases of displacement of halides or any other groups by phenoxy radical substitution (as opposed to direct radical coupling then halide loss).



Scheme 16. Coupling at Halide Substituted Positions

NO_2 also oxidises 4-methyl-2,6-ditertbutylphenol[82] to different products depending on the amount of NO_2 employed as illustrated in Scheme 17. Oxidation was postulated to occur via hydrogen abstraction.



Scheme 17. Oxidation of 4-Methyl-2,6-ditertbutylphenol[82]

1.5. Conclusion

The chemistry of NO_2 and N_2O_4 has been reviewed. There is a lack of systematic study of the reactions of gaseous NO_2 with aqueous solutions. Such studies may be complicated by the hydrolysis of NO_2 (N_2O_4). It is unclear whether measurements of ambient NO_2 by the Saltzman method are complicated by hydrogen abstractions from water, reactions of solutes or any other mechanism. The reactions of inhaled NO are well understood whilst those of inhaled NO_2 are at present uncertain. The work described in this Thesis is directed towards rectifying these deficiencies.

Chapter 2

Electron Transfer Reactions of Nitrogen Dioxide and Dinitrogen Tetraoxide

2.1. Introduction

Investigations of the atmospheric sampling of nitrogen dioxide stemming from the paper by Saltzman in 1954[37] are confused about the reactions of nitrogen dioxide in aqueous solutions (Section 1.3.2.). The work reported in this chapter is concerned with the nature of these reactions and whether they involve the solute and / or the solvent.

Throughout the text reference is often made to a ratio known as the 'Saltzman Factor'. This factor is defined as;

$$\text{Saltzman Factor} = \frac{[NO_2^-]}{[NO_2^-] + [NO_3^-]}$$

2.2. HPLC Analysis of Nitrite and Nitrate Ions

The quantitative analysis of nitrite (NO_2^-) and nitrate (NO_3^-) ions in aqueous solution was essential to the study. The common method for the analysis of NO_2^- is a colorimetric procedure involving formation of an azo dye first introduced by Griess and subject to several minor modifications. NO_3^- can then be analysed by reduction to NO_2^- which is again determined colorimetrically[45,57]. More recent hplc assays have reversed the concept in so far as NO_3^- is determined as a 2-nitrophenol derivative and NO_2^- is determined similary after oxidation with hydrogen peroxide[83]. Aqueous NO_2^- has also been determined by hplc *via in situ* formation of methyl nitrite[84].

A major goal of the present study was the

development of a simple hplc assay for NO_2^- and NO_3^- which could be carried out on a single column without preliminary derivatisation.

There are several published methods for the quantitation of NO_2^- and NO_3^- by hplc. All rely for separation on the different affinity of NO_2^- and NO_3^- for the tetra-alkylammonium cation. For Strong Anion eXchange (SAX) and Ion Chromatography (IC), this is achieved by incorporating the tetra-alkylammonium ion in the packing material. For Reversed-Phase Ion Chromatography (RPIC), however, the ODS resin packing has an affinity for the tetra-n-butylammonium hydroxide which is added to the eluent.

The published methods differ in regard to their resolving power, speed of analysis and eluent pH. The chromatograms in Figure 1 illustrate the first two factors. SAX chromatography employs a bonded silica packing which operates at an optimum pH of 3.0. At this pH, however, NO_2^- can be oxidised to NO_3^- by hydrogen peroxide. The generation of peroxy radicals in the hydrolysis of NO_2 is feasible (Section 1.3.2.) and quantitation at pH 3 is therefore circumspect. RPIC uses a phosphate buffer eluent at pH 6 for ODS columns and a borax buffer eluent at pH 9 for styrene/divinylbenzene (e.g. Hamilton PRP-1[87]) columns. The oxidation of NO_2^- to NO_3^- does not take place at pH $\geqslant$ 6 and both are therefore convenient alternative procedures to the preferred IC method discussed below. These alternatives were used to overcome occasional interferences from reactant

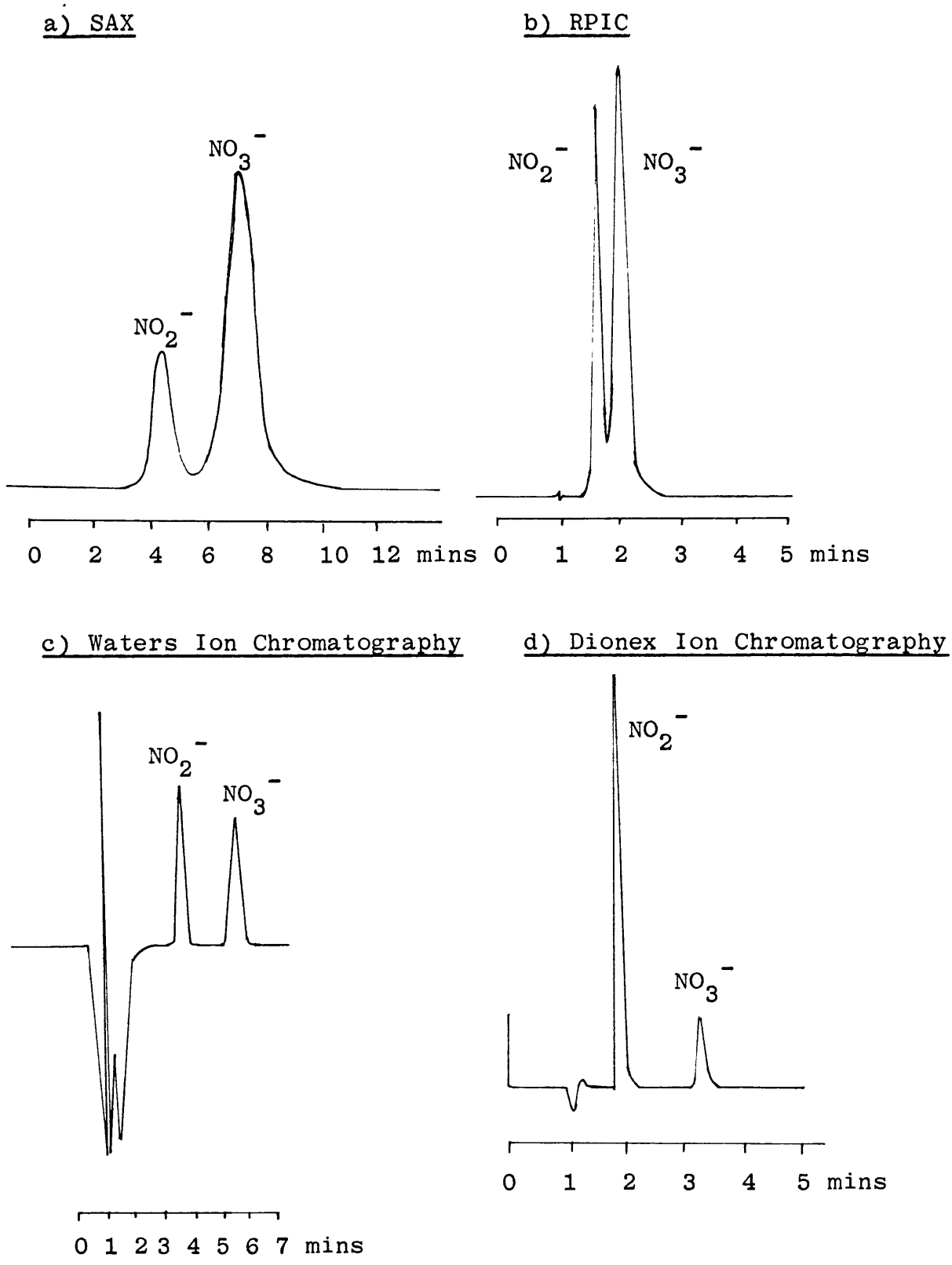


Figure 1. HPLC Analysis of Nitrite and Nitrate

or product peaks. Most of the NO_2^- and NO_3^- assays were carried out by IC using a Waters Anion Column (polymethacrylate resin) and a phosphate buffer eluent at pH 6.0. This method gave high resolution and fast analysis, without the need for time-consuming column equilibration arising from the presence of tetra-n-butylammonium hydroxide in the eluent. All of the hplc analysis used uv detection at 214 nm to quantify NO_2^- and NO_3^-. The sensitivity of the Waters IC column with uv detection is exceptional and sub μM levels of NO_2^- and NO_3^- can be quantified sequentially.

In general, all the hplc assays required a carefully buffered eluent to give good reproducibility. To achieve this analytical samples at pH 1 and 13 were neutralised with phosphate buffer (Section 8.2.1.2.) prior to injection on the column. This pretreatment was unnecessary for samples at $1 < pH < 13$.

Further practical details of all these assays are given in Chapter 8.

2.3. Hydrolysis of Nitrogen Dioxide

The reactions with dilute NO_2 were performed either using the Gas Circulation Apparatus or the Dilute NO_2 Line. Both systems are described in Chapter 8.

2.3.1. Nitrite and Nitrate Ion Stability

The stability of NO_2^- and NO_3^- in mildly alkaline conditions was examined independently. Aqueous solutions of sodium nitrite and sodium nitrate were placed in the reaction flask and nitrogen passed through at 80 ml/min. The variation

of NO_2^- and NO_3^- concentrations with time are summarised in Figure 2. NO_2^- and NO_3^- are seen to be stable under conditions typical of most of the reactions reported in this Thesis.

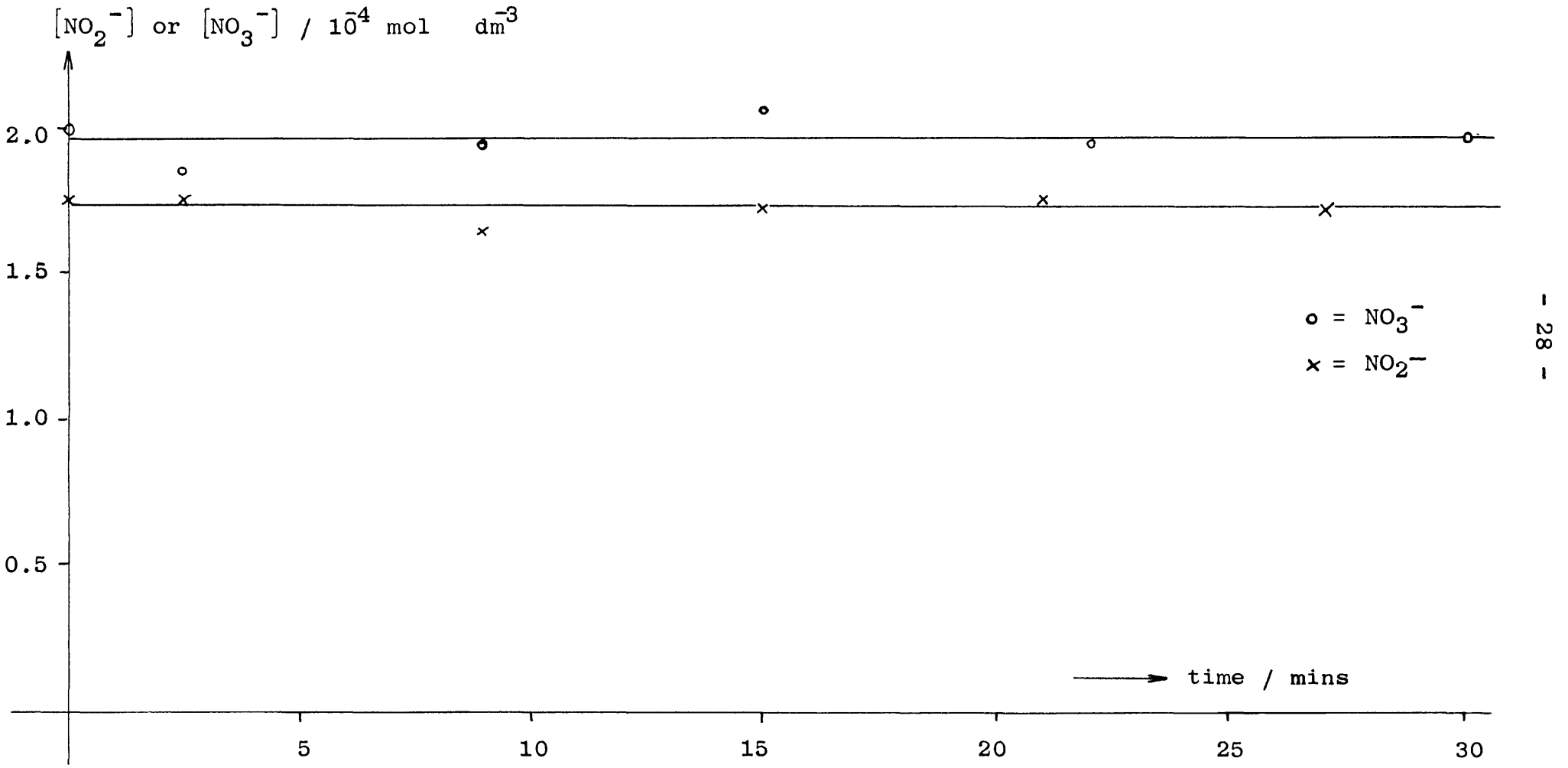
2.3.2. Effect of Nitrogen Dioxide Concentration

The hydrolysis of 5 - 100,000 ppm NO_2 in 0.1M NaOH produces equimolar concentrations of NO_2^- and NO_3^- as shown in Table 4. These experiments revealed the necessity to distill N_2O_4 for the Gas Circulation Apparatus. Undistilled N_2O_4 gave a NO_2^- to NO_3^- ratio greater than unity ($[NO_2^-]/[NO_3^-] > 1$). This is thought to result from a small NO impurity which gives excess NO_2^- via the hydrolysis of N_2O_3 (Scheme 18).

$[NO_2]$ / ppm	$[NO_2^-]/[NO_3^-]$	$[NO_2]$ / ppm	$[NO_2^-]/[NO_3^-]$
5	0.85	500	1.00
10	1.08	700	1.00
20	0.85	900	1.00
50	0.89	1500	1.02
100	0.96	2000	0.98
150	1.04	10000	1.05
200	1.04	100000	1.03
330	1.00		

Table 4. Hydrolysis of Nitrogen Dioxide in 0.1M NaOH at 25°C - Variation of Nitrogen Dioxide Concentration

Figure 2. Nitrite and Nitrate Stability at pH 9.7 with N_2 flow at 80 ml/min



$$NO + NO_2 \rightleftharpoons N_2O_3$$

$$N_2O_3 \xrightarrow{H_2O} 2HNO_2$$

Scheme 18. Excess Nitrite Ion from Nitric Oxide Impurity

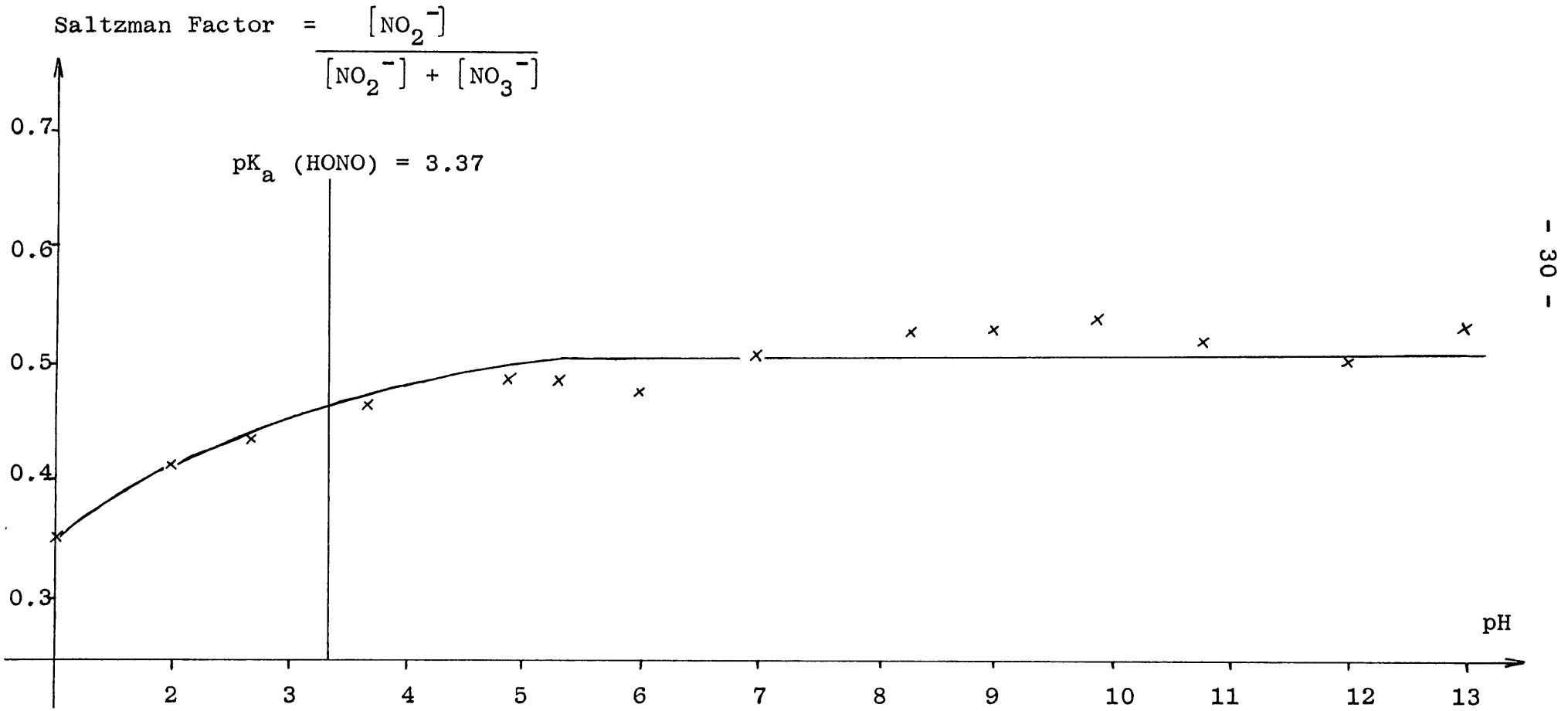
2.3.3. pH Dependence

Figure 3 shows the variation in the Saltzman Factor on reacting 200 ppm NO_2 with aqueous solution at different pH. There is a clear tendency to form excess NO_3^- at low pH. Colorimetric (Shinn's[88]) assay showed that NO_2^- was stable at pH $\gg$ 1 when the solutions were left to stand at 25°C. On bubbling nitrogen through a solution at pH 1 however, $[NO_2^-]$ decreased and $[NO_3^-]$ increased. The oxidation was quantitative at high nitrogen flow rate (300 ml/min) but less important at lower flow rates. These points are illustrated in Figure 4 and Table 5.

Bayliss and Watts[89] have shown that aspiration with nitrogen increases the decomposition rate of NO_2^- in aqueous acid. They found that with low nitrogen flows the decomposition was roughly dependent on the aspiration rate whereas with high nitrogen flow the decomposition was first order in nitrite, the slow step being the production of NO^+.

Agitation in our studies increases both the rate of NO_2^- decomposition (Figure 4) and the yield of NO_3^- (Table 5). It seems probable that nitrous acid evaporates (via N_2O_3) from our solutions and oxidation

Figure 3. Hydrolysis of 200ppm NO_2^- - Variation of pH



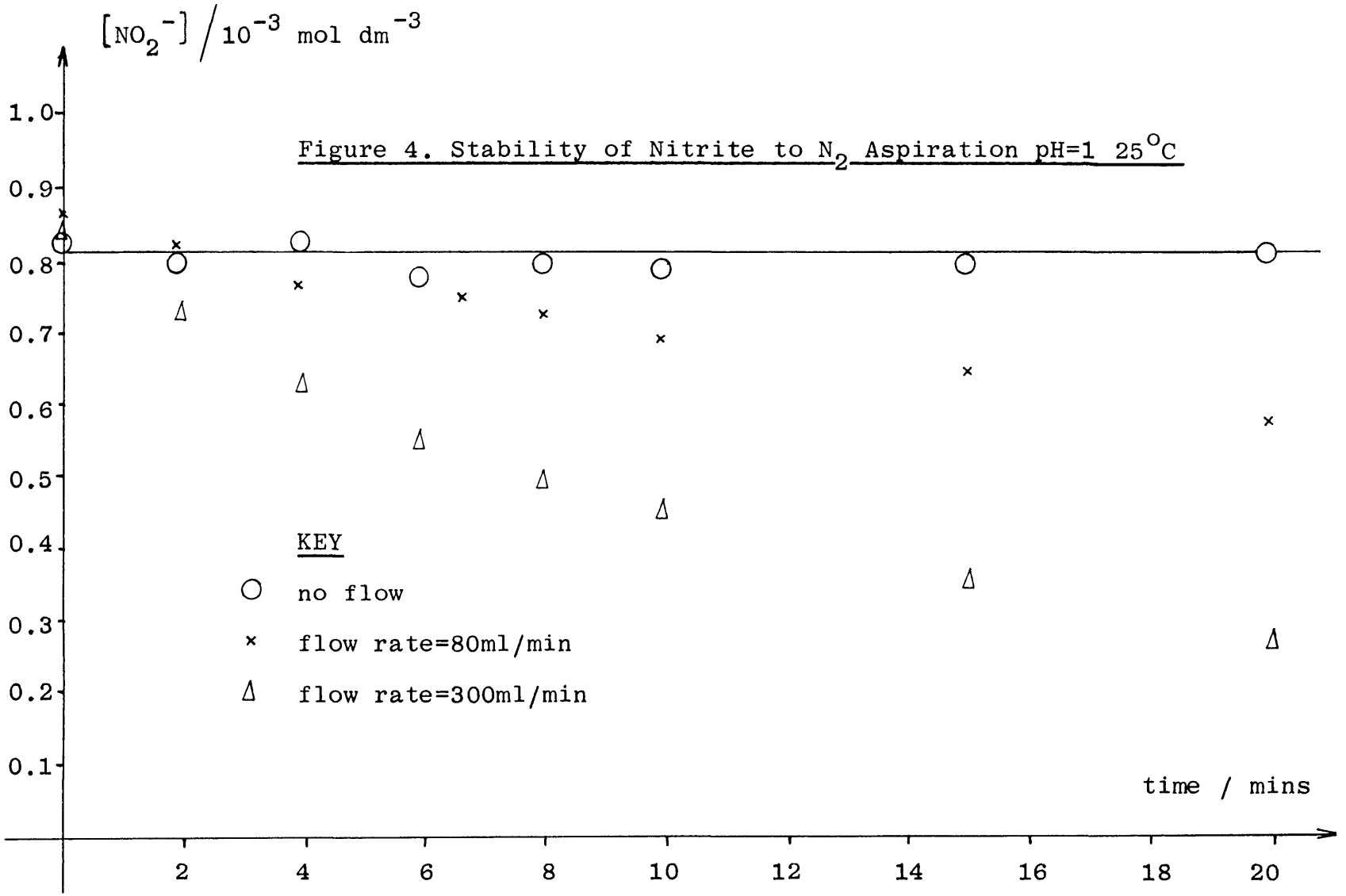


Figure 4. Stability of Nitrite to N_2 Aspiration pH=1 25°C

N_2 Flow Rate / ml/min	Time /mins	$[NO_2^-]$ /10^{-4} mol dm^{-3}	$[NO_3^-]$ /10^{-4} mol dm^{-3}
80	0	8.59	-
	10	7.19	0.58
	20	6.30	1.34
300	0	9.74	-
	10	4.07	5.42
	20	2.41	6.72

Table 5. Oxidation/Evaporation of Nitrite pH=1 25°C

of NO_2^- to NO_3^- also occurs with high flow rates. Scheme 19 shows the equilibria that account for the loss of NO_2^-.

$$NO_2^- + H^+ \rightleftharpoons HNO_2$$

$$2HNO_2 \rightleftharpoons N_2O_3 + H_2O$$

$$N_2O_3 \rightleftharpoons NO + NO_2$$

$$NO + O_2 \longrightarrow NO_2 \rightleftharpoons N_2O_4 \xrightarrow{H_2O} HNO_2 + HNO_3$$

Scheme 19. Oxidation of Nitrite in Acid

The increase in $[NO_3^-]$ is more difficult to explain but a key step may be the oxidation of nitric oxide to nitrogen dioxide (Scheme 19). There is enough oxygen in the white spot nitrogen used to produce this oxidation which is known to exhibit third order kinetics with the rate equation as defined in Equation 4 and a decreasing

rate with increasing temperature[90]. This can be

$$\text{Rate} = k_3[NO]^2[O_2] \qquad ..(4)$$

rationalised by the pre-equilibrium formation of $(NO)_2$ followed by bimolecular oxidation as shown in Scheme 20. The overall negative temperature dependence for oxidation is explained by a large inverse dependence for $K_{(NO)_2}$ outweighing a smaller normal dependence for k_3, and the reaction follows overall third-order kinetics. This implies $(NO)_2$ is the intermediate undergoing oxidation rather than $NO_3^{\cdot}$, which is unclear from frozen matrix studies[91-93].

$$NO + NO \overset{K_{(NO)_2}}{\rightleftharpoons} (NO)_2$$

$$(NO)_2 + O_2 \xrightarrow{k_3} 2NO_2$$

$$\frac{d[NO_2]}{dt} = k_3[(NO)_2][O_2] = k_3K[NO]^2[O_2]$$

Scheme 20. Oxidation of Nitric Oxide

2.3.4. Conclusions

NO_2^- and NO_3^- are stable under the reaction conditions (i.e. pH $>$ 5) used for most of the following experiments.

The reaction of gaseous NO_2 with aqueous media at pH $\gg$ 7 produces equimolar quantities of NO_2^- and NO_3^-, supporting the classical hydrolysis reaction via N_2O_4 (Equation 5).

$$NO_2 \rightleftharpoons N_2O_4 \xrightarrow{H_2O} HNO_2 + HNO_3 \qquad ..(5)$$

Excess NO_3^- is found at pH $<$ 5 due to an oxidation reaction promoted by the gas stream.

There is no evidence for the production of excess NO_2^- by reaction of NO_2 with either water or HO^-.

2.4. Reactions of Gaseous Nitrogen Dioxide with Organic Substrates in Aqueous Solution

2.4.1. Observation of Excess Nitrite Ion

Initially, the reaction of 5 structurally different substrates with 200 ppm NO_2 in 0.1M NaOH was examined. The 5 substrates were phenol, thiophenol, aniline, piperazine and 1,4-diazabicyclo[2,2,2]octane (DABCO). Excess NO_2^- was seen for all these compounds and the $[NO_2^-]/[NO_3^-]$ ratio increased with increasing substrate concentration. Figure 5 summarises these data and Figure 6 shows the large differences in the hplc chromatograms obtained for the hydrolysis of 330 ppm gaseous NO_2 in the absence and presence of 0.01M phenoxide ion. The data in Figure 5 show that the ability of the 5 substrates to increase the Saltzman Factor in 0.1M NaOH decreases in the order phenolate, thiophenolate, aniline, piperazine, DABCO.

Additionally n-butylamine, tert-butanol and n-butanol were found to have no effect on the Saltzman Factor (i.e. equimolar quantities of NO_2^- and NO_3^-

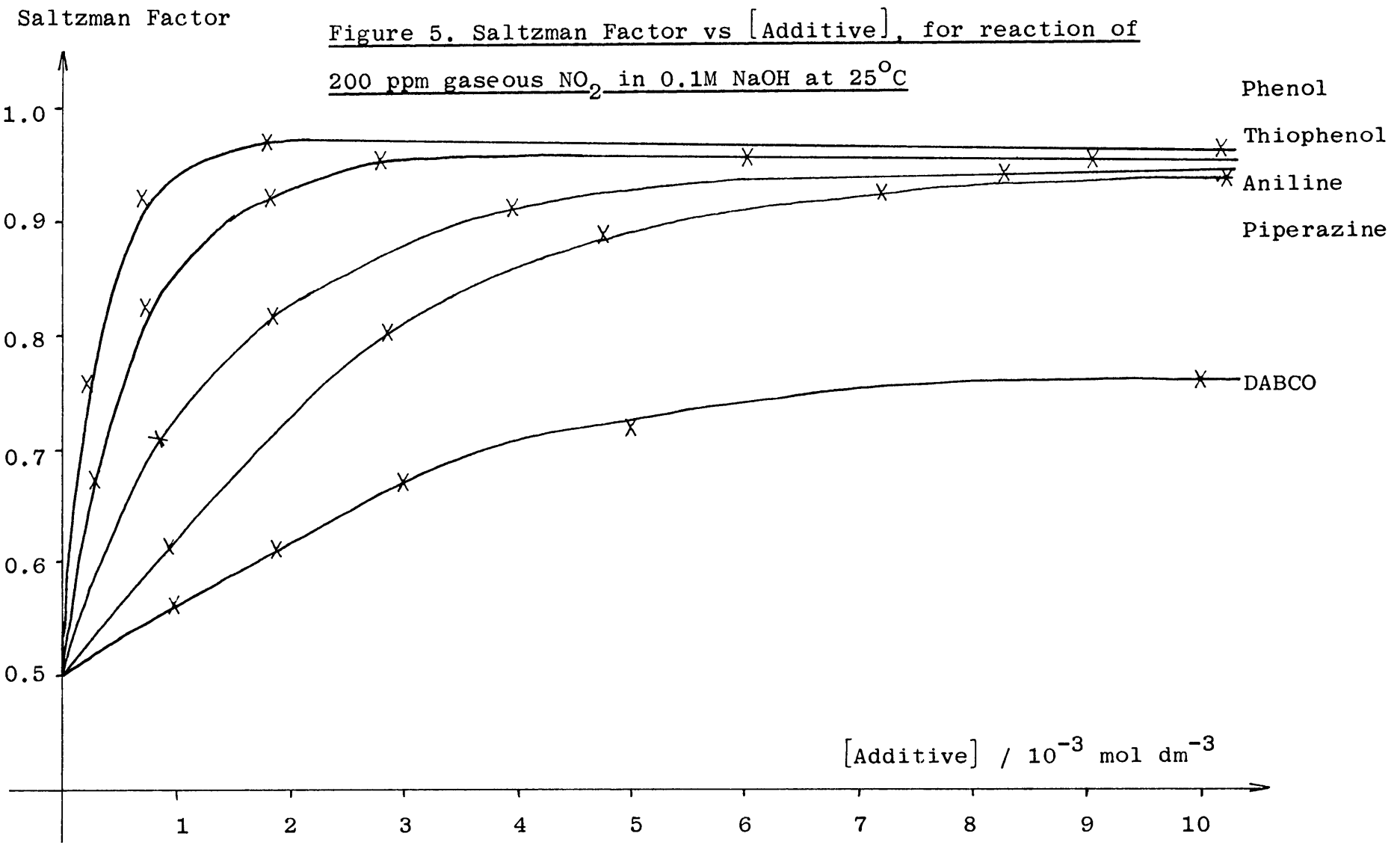
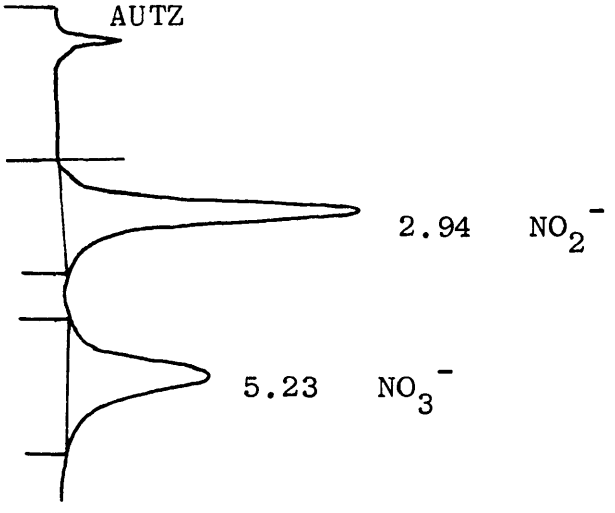


Figure 5. Saltzman Factor vs [Additive], for reaction of 200 ppm gaseous NO_2 in 0.1M NaOH at 25°C

Figure 6. Sample Chromatograms, 330 ppm NO_2 0.1M NaOH

Hydrolysis

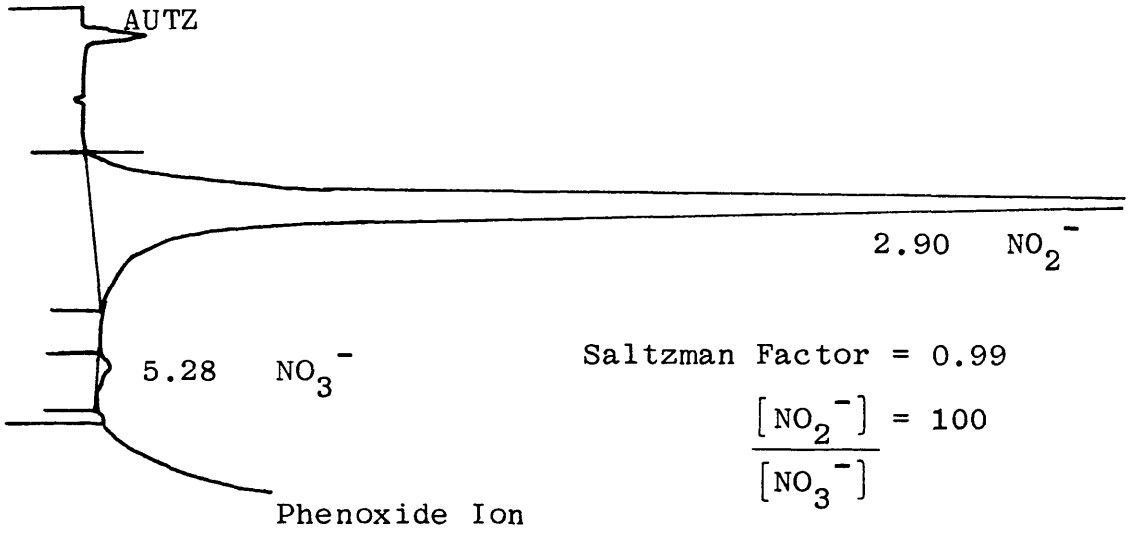


7.00 mins

Saltzman Factor = 0.50

$$\frac{[NO_2^-]}{[NO_3^-]} = 1.00$$

With 0.01M Phenoxide Ion



7.00 mins

Saltzman Factor = 0.99

$$\frac{[NO_2^-]}{[NO_3^-]} = 100$$

were obtained).

2.4.2. Hydrogen Abstraction[48] vs Electron Transfer[46,60]

Two possible explanations can be envisaged for the reaction of gaseous NO_2 with organic species to produce excess NO_2^-. They are electron transfer and hydrogen abstraction as illustrated in Scheme 21.

$$Org + NO_2 \longrightarrow Org^{+\cdot} + NO_2^-$$

Radical Cation

$$Org^- + NO_2 \longrightarrow Org^{\cdot} + NO_2^-$$

Radical

} Electron Transfer

$$Org{-}H + NO_2 \longrightarrow HNO_2 + Org^{\cdot}$$

Hydrogen Abstraction

Scheme 21. Electron Transfer or Hydrogen Abstraction by Gaseous NO_2 to Produce NO_2^-

The hydrogen abstraction pathway requires the substrate to possess active hydrogen. Neither phenol and thiophenol at pH 13 nor DABCO fulfil this condition, and these substrates must therefore react by electron transfer. Further support for an electron transfer pathway comes from the reactions of aniline, N-methylaniline and N,N'-dimethylaniline with 200 ppm NO_2 in 0.1M NaOH (Table 6). The order of their reactivity (N,N'-dimethylaniline $\rangle$ N-methylaniline $\rangle$ aniline) parallels the electron donating ability of the lone pair N-electrons.

Compound	$[NO_2^-]/[NO_3^-]$
Aniline	3.0
N-Methylaniline	4.1
N,N'-Dimethylaniline	9.6

Table 6. Aniline Reactivity with 1.0×10^{-3}M substrate and 200 ppm NO_2 at 25°C

A wide variety of other substrates were found to react with gaseous NO_2 in aqueous base to produce excess NO_2^-. The reactions were examined under a standard set of conditions (200 ppm NO_2 was passed at a flow rate of 80 ml/min through 10 ml of a 1.0×10^{-2}M solution of the substrate in 0.1M NaOH in the fritted-glass bubbler for 10 mins at 25°C) to allow comparison of their relative reactivity. These data are tabulated in the Standard Reactivity Index (Appendix) along with substrates which do not react with gaseous NO_2.

2.4.3. Dependence on Substrate Concentration

The dependence of the $[NO_2^-]/[NO_3^-]$ ratio on substrate concentration was studied for phenol and DABCO and results for 0.1M NaOH and 200 ppm gaseous NO_2 are shown in Figures 7-8. Both plots are linear with unit intercepts. The intercept values were confirmed by several independent experiments at the lower substrate concentrations. The gradient for phenol (phenoxide ion) is much greater than that for DABCO which reflects their relative reactivity. The results

Figure 7. Substrate dependence for reaction of phenol in 0.1M NaOH with 200 ppm gaseous NO_2 at 25°C

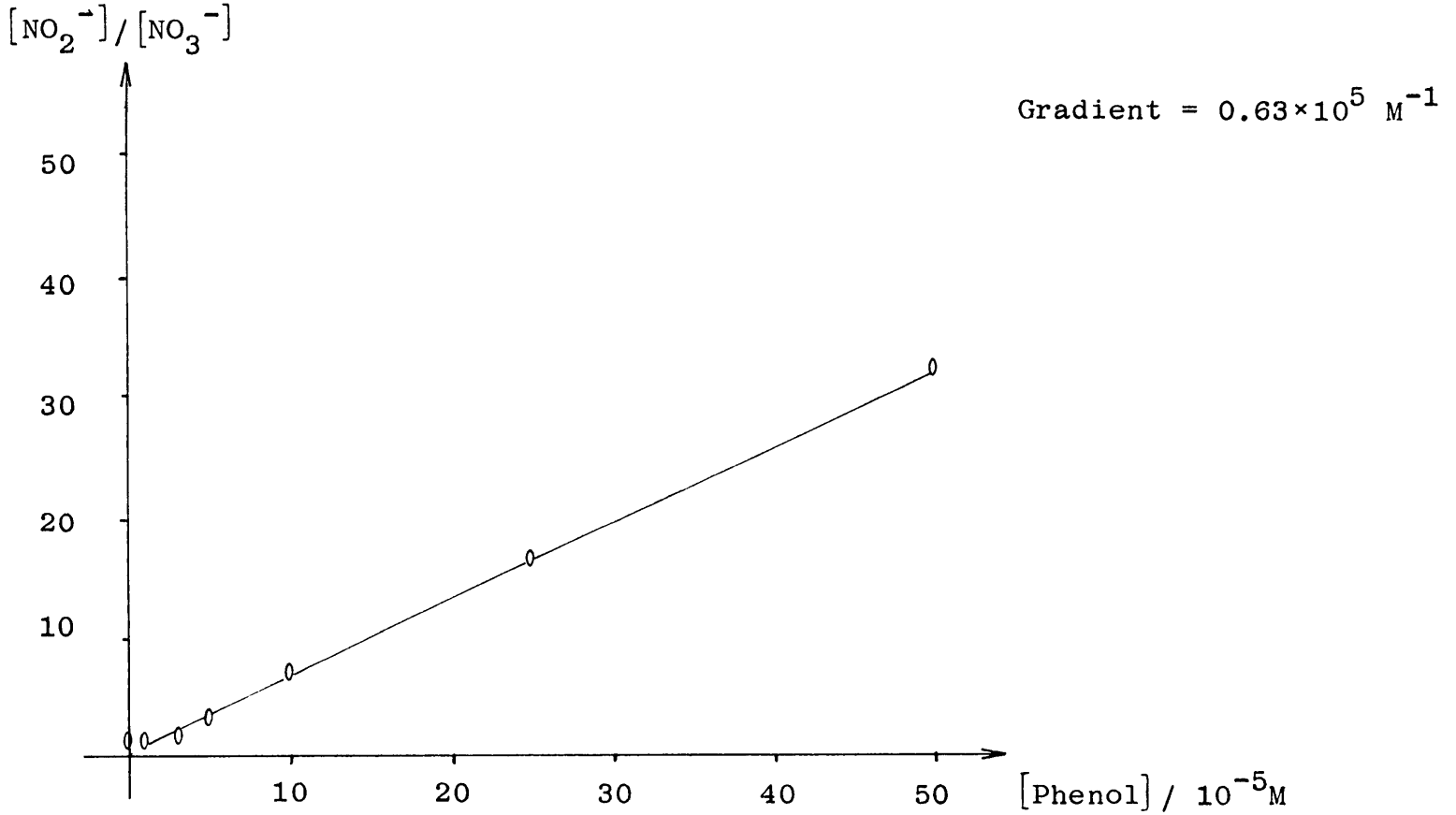
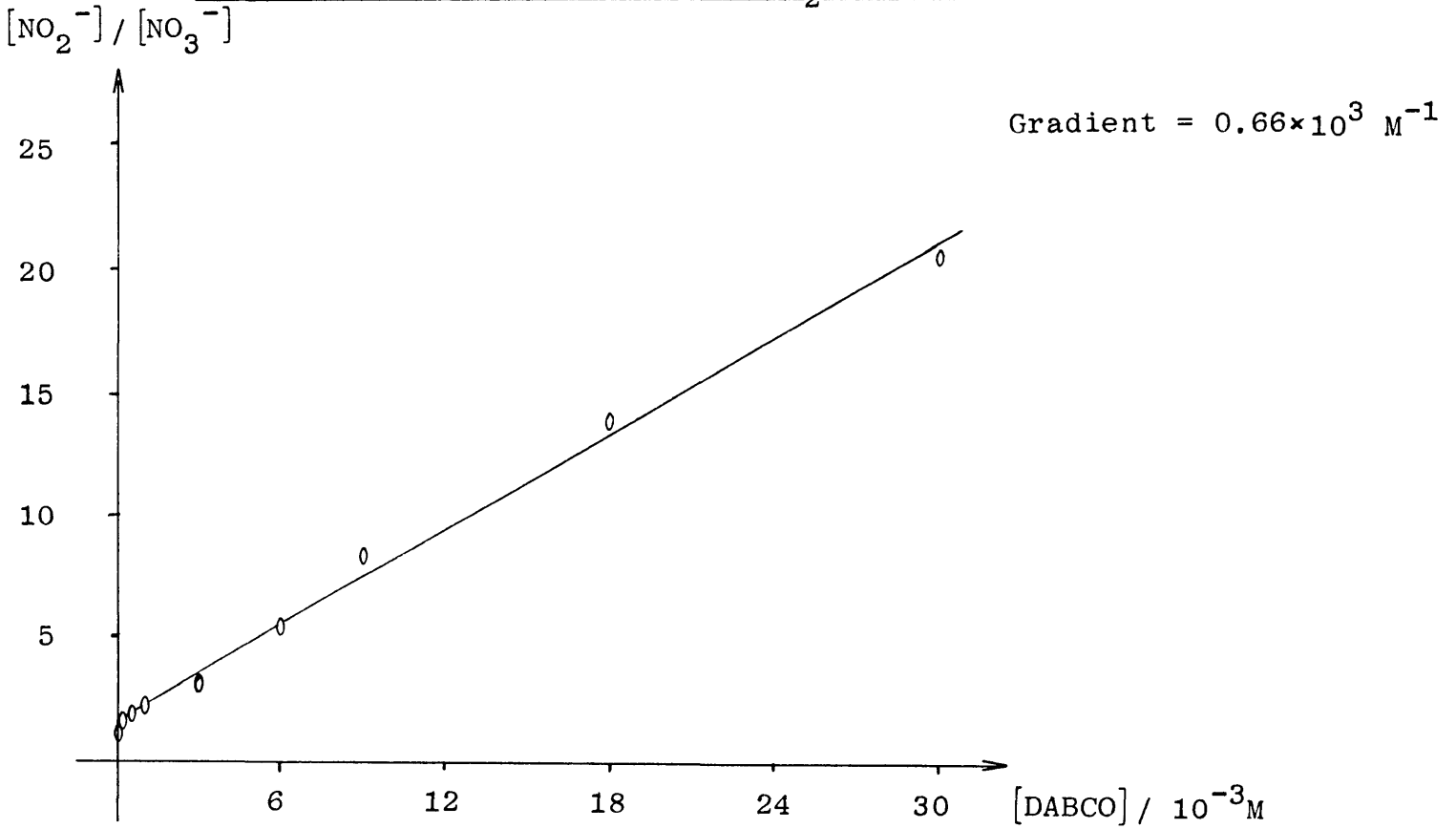


Figure 8. Substrate dependence for reaction of DABCO in 0.1M NaOH with 200 ppm gaseous NO_2 at 25°C



in Figures 7-8 show that at constant $[NO_2]$ the $[NO_2^-]/[NO_3^-]$ ratio is proportional to [substrate].

2.4.4. Dependence on Nitrogen Dioxide Concentration

The dependence of the $[NO_2^-]/[NO_3^-]$ ratio on NO_2 concentration was studied for DABCO, 2,4,6-trichlorophenol and 4-nitrophenol in 0.1M NaOH. To avoid artifactually low values of the $[NO_2^-]/[NO_3^-]$ ratio arising from the predominance of the normal hydrolysis of N_2O_4 over electron transfer to NO_2, ractant concentrations were selected to ensure that $[\text{substrate}]/[NO_2] \gg 10$. The variation of the $[NO_2^-]/[NO_3^-]$ ratio with $[NO_2]$ is shown in Figure 9 for DABCO, 2,4,6-trichlorophenol and 4-nitrophenol respectively. The plots are seen to be non-linear.

2.4.5. The Reaction Model

The dependence of the $[NO_2^-]/[NO_3^-]$ ratio on the presence of oxidisable substrates can be related to reaction of gaseous NO_2 by two independent pathways. One is electron transfer by the substrate to NO_2 to give NO_2^-, the other hydrolysis of N_2O_4 to give equimolar amount of NO_2^- and NO_3^-. The processes are illustrated in Scheme 22 for DABCO and it follows that the rates of formation of NO_2^- and NO_3^- are given by Equations 6 and 7 respectively.

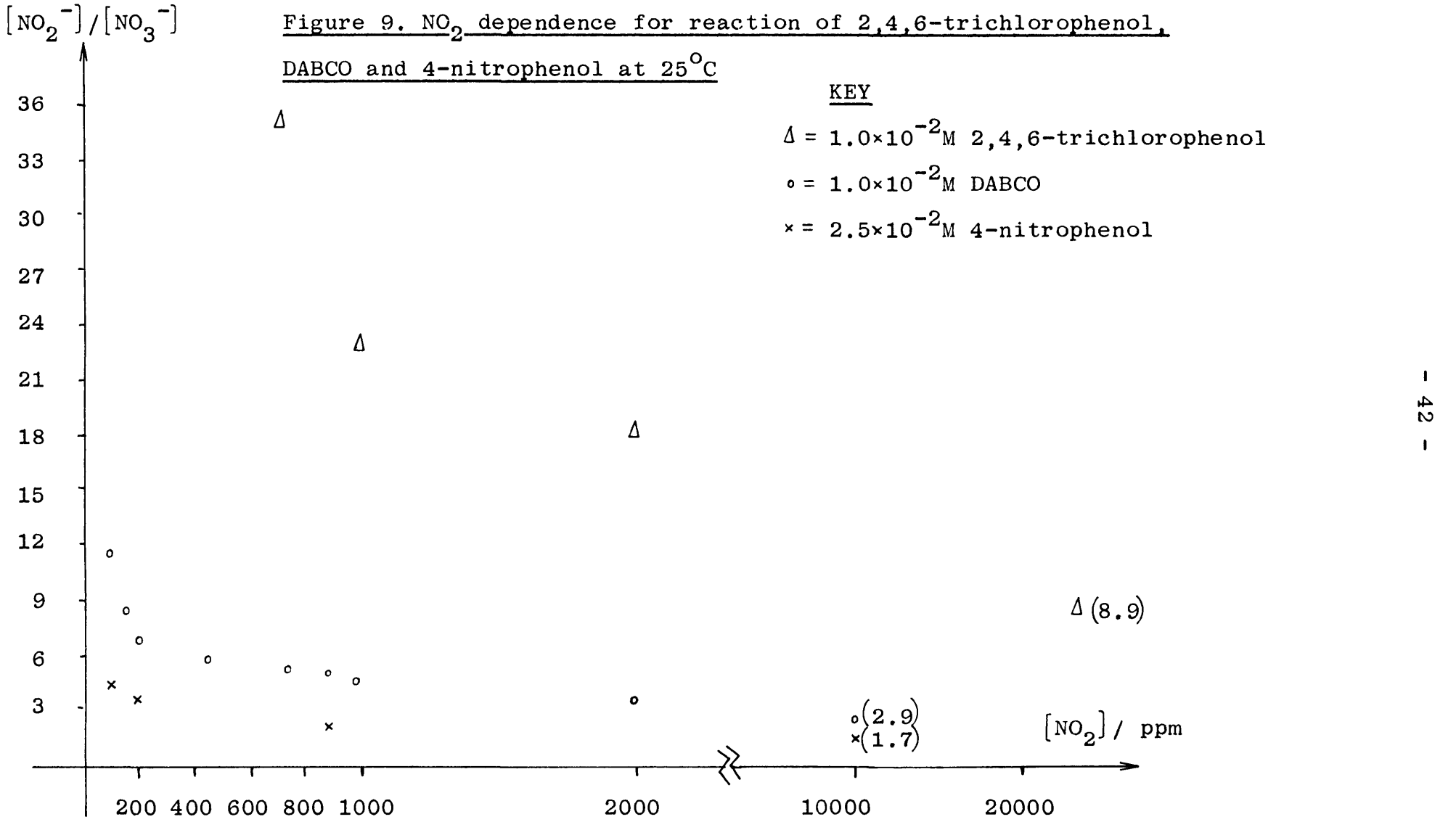
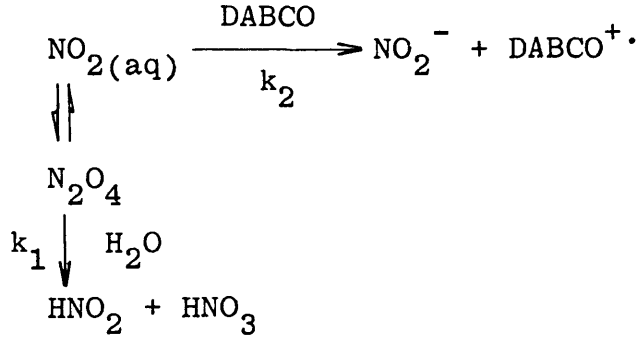


Figure 9. NO_2 dependence for reaction of 2,4,6-trichlorophenol, DABCO and 4-nitrophenol at 25°C



Scheme 22. Competition between Electron Transfer and Hydrolysis

$$\frac{d[NO_2^-]}{dt} = k_1[H_2O][N_2O_4] + k_2[DABCO][NO_2] \quad ..(6)$$

$$\frac{d[NO_3^-]}{dt} = k_1[H_2O][N_2O_4] \quad ..(7)$$

Unfortunately, it is not possible to measure the rates of NO_2^- and NO_3^- formation, but a more useful relationship dependent on product and substrate concentrations (Equation 8) is obtained by dividing Equation 6 by Equation 7.

$$\frac{[NO_2^-]}{[NO_3^-]} = 1 + \frac{k_2[DABCO][NO_2]}{k_1[H_2O][N_2O_4]} \quad , \text{ as } [NO_2^-]_{t=0} = 0 \text{ and } [NO_3^-]_{t=0} = 0 \quad ..(8)$$

Since N_2O_4 and NO_2 are in equilibrium (Equation 9), Equation 8 is readily transformed to Equation 10 on substituting for N_2O_4.

$$[N_2O_4] = K[NO_2]^2 \quad ..(9)$$

$$\frac{[NO_2^-]}{[NO_3^-]} = 1 + \frac{k_2[DABCO]}{k_1 K[H_2O][NO_2]} \quad ..(10)$$

Equation 10 implies a linear dependence for the $[NO_2^-]/[NO_3^-]$ ratio on substrate concentration at constant NO_2 concentration with an intercept of unity. This has been confirmed in Section 2.4.3.. Equation 10 also implies a linear dependence for the $[NO_2^-]/[NO_3^-]$ ratio on $1/[NO_2]$ with an intercept of unity. The relevant plots from the data presented in Section 2.4.4. are shown in Figures 10-16 together with further data for DABCO and 4-nitrophenol. These are linear but their intercepts are both greater than unity and dependent on the substrate . This suggests that either the model outlined in Scheme 22 is incorrect or the results are artifactual.

One potential artifact is that the gaseous NO_2 contains an NO impurity which manifests itself as excess NO_2^- on hydrolysis (Scheme 18). This would give an intercept greater than unity for the substrate dependence plots but its value would be independent of the type and concentration of the substrate. This explanation is therefore eliminated.

Another potential artifact is that dimerisation of NO_2 to N_2O_4 in solution is slow and that mass transfer is therefore important. Komiyama and Inoue[94] have shown that the absorption of NO_2 is first-order in NO_2 below 300 ppm and second-order above 800 ppm NO_2. They deduce that the absorbed species is NO_2 below 300 ppm and N_2O_4 above 800 ppm as illustrated in Scheme 23.

Figure 10. $[NO_2^-]/[NO_3^-]$ vs $1/[NO_2]$, 1.0×10^{-2}M 2,4,6-trichlorophenol in 0.1M NaOH at 25°C

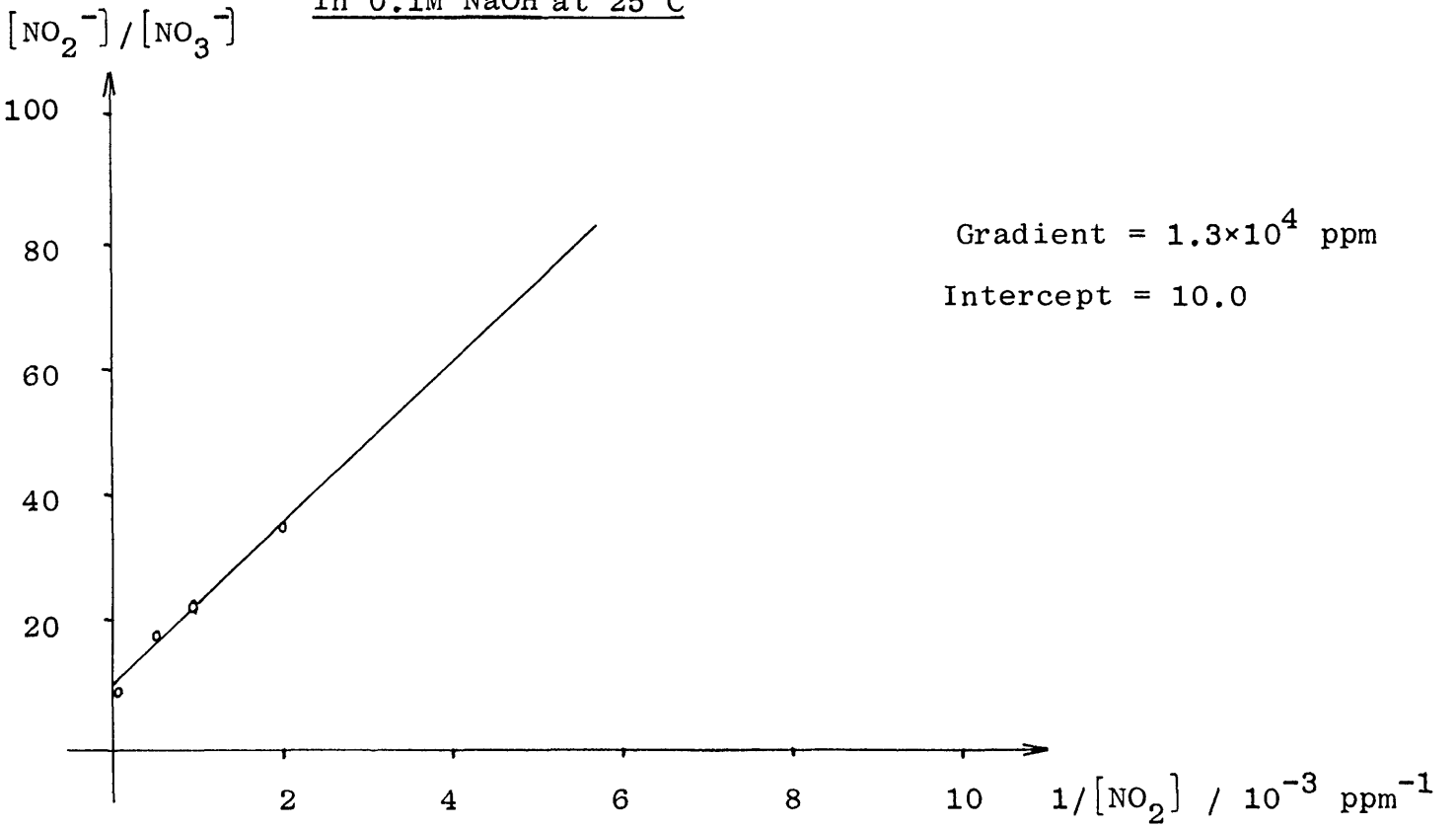


Figure 11. $[NO_2^-]/[NO_3^-]$ vs $1/[NO_2]$, 1.0×10^{-2}M DABCO in 0.1M NaOH at 25°C

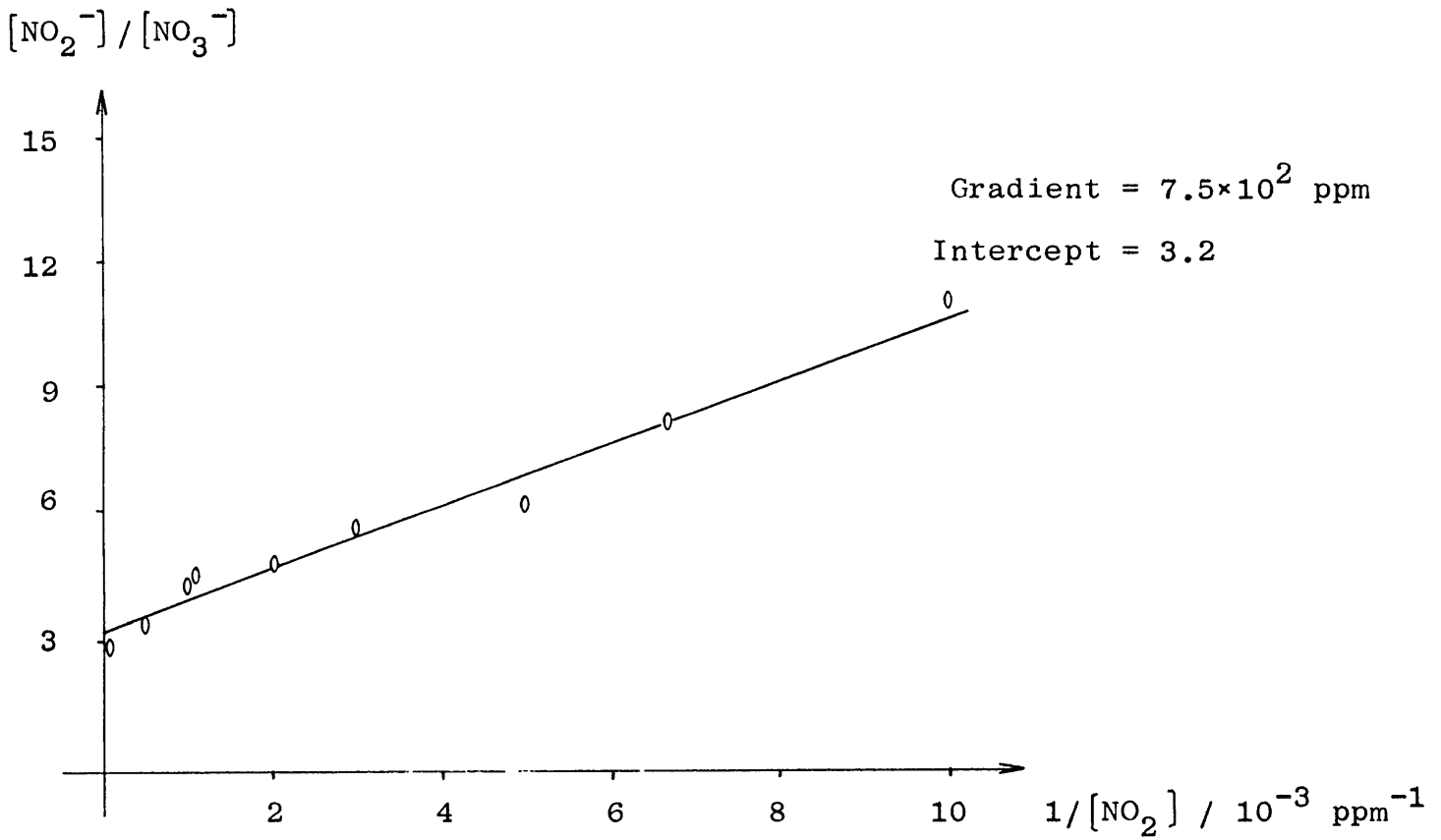


Figure 12. $[NO_2^-]/[NO_3^-]$ vs $1/[NO_2]$, 2.0×10^{-2}M DABCO in 0.1M NaOH at 25°C

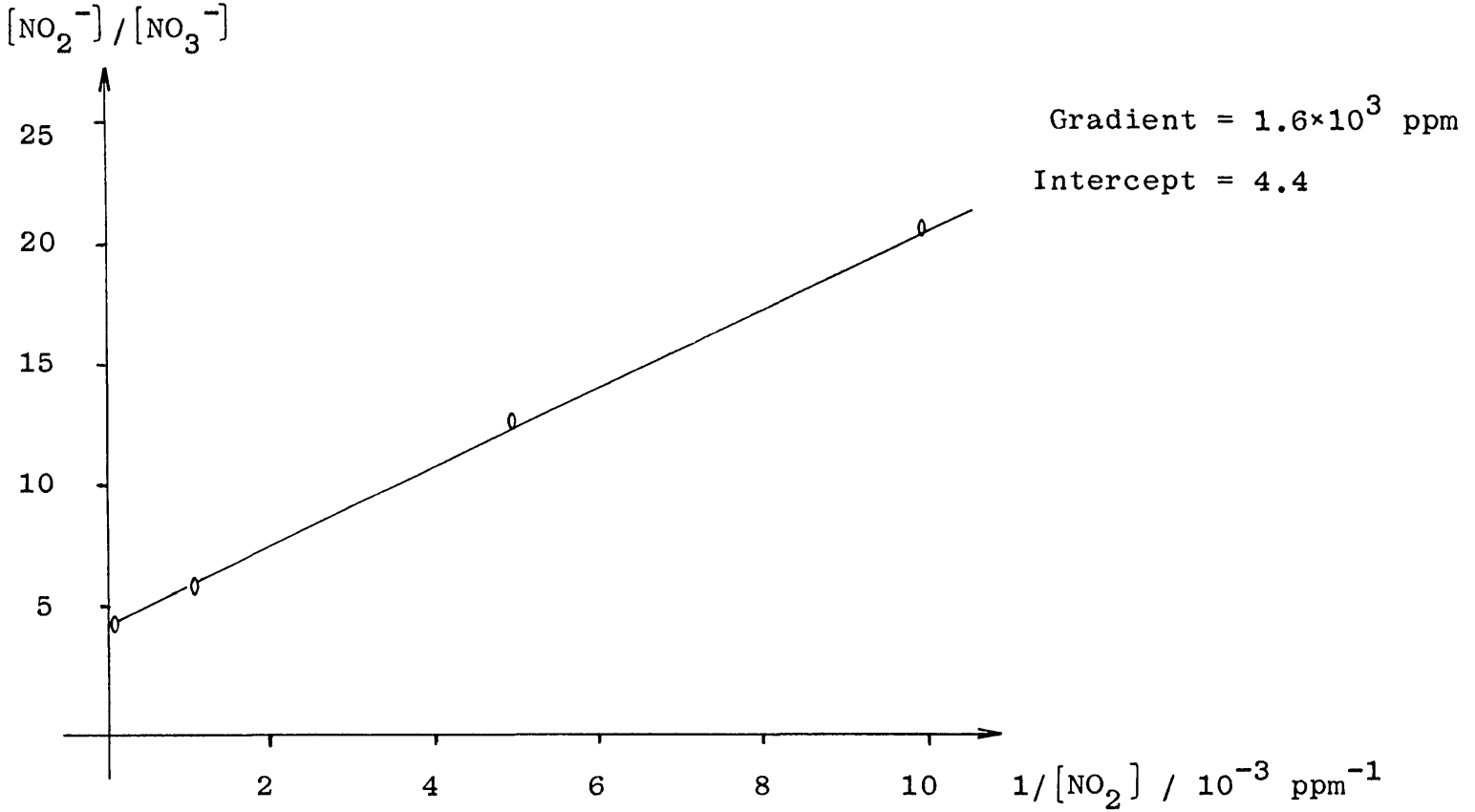


Figure 13. $[NO_2^-]/[NO_3^-]$ vs $1/[NO_2]$, 3.0×10^{-2}M DABCO in 0.1M NaOH at 25°C

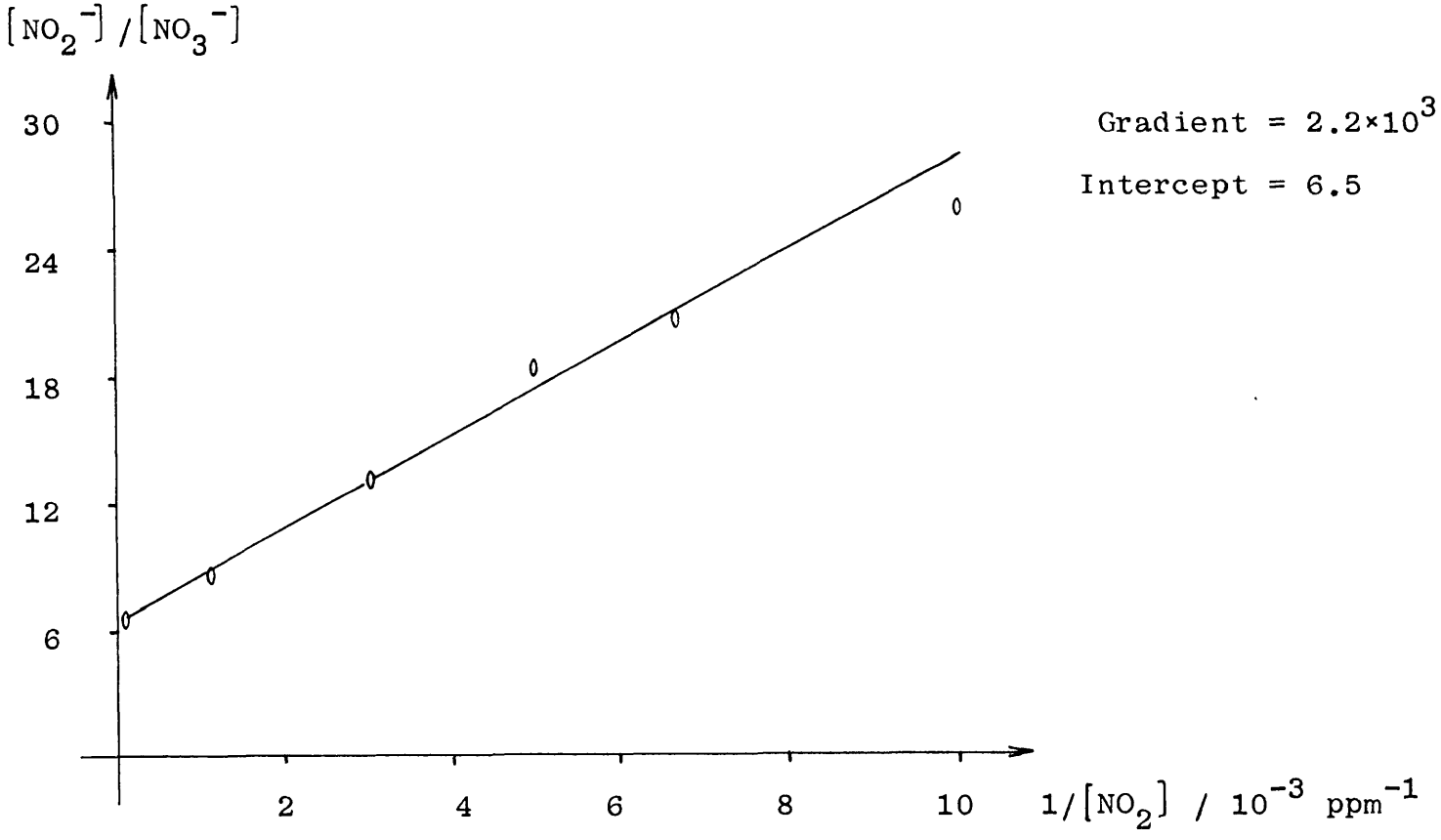


Figure 14. $[NO_2^-]/[NO_3^-]$ vs $1/[NO_2]$, 2.5×10^{-2}M 4-nitrophenol at 25°C in 0.1M NaOH

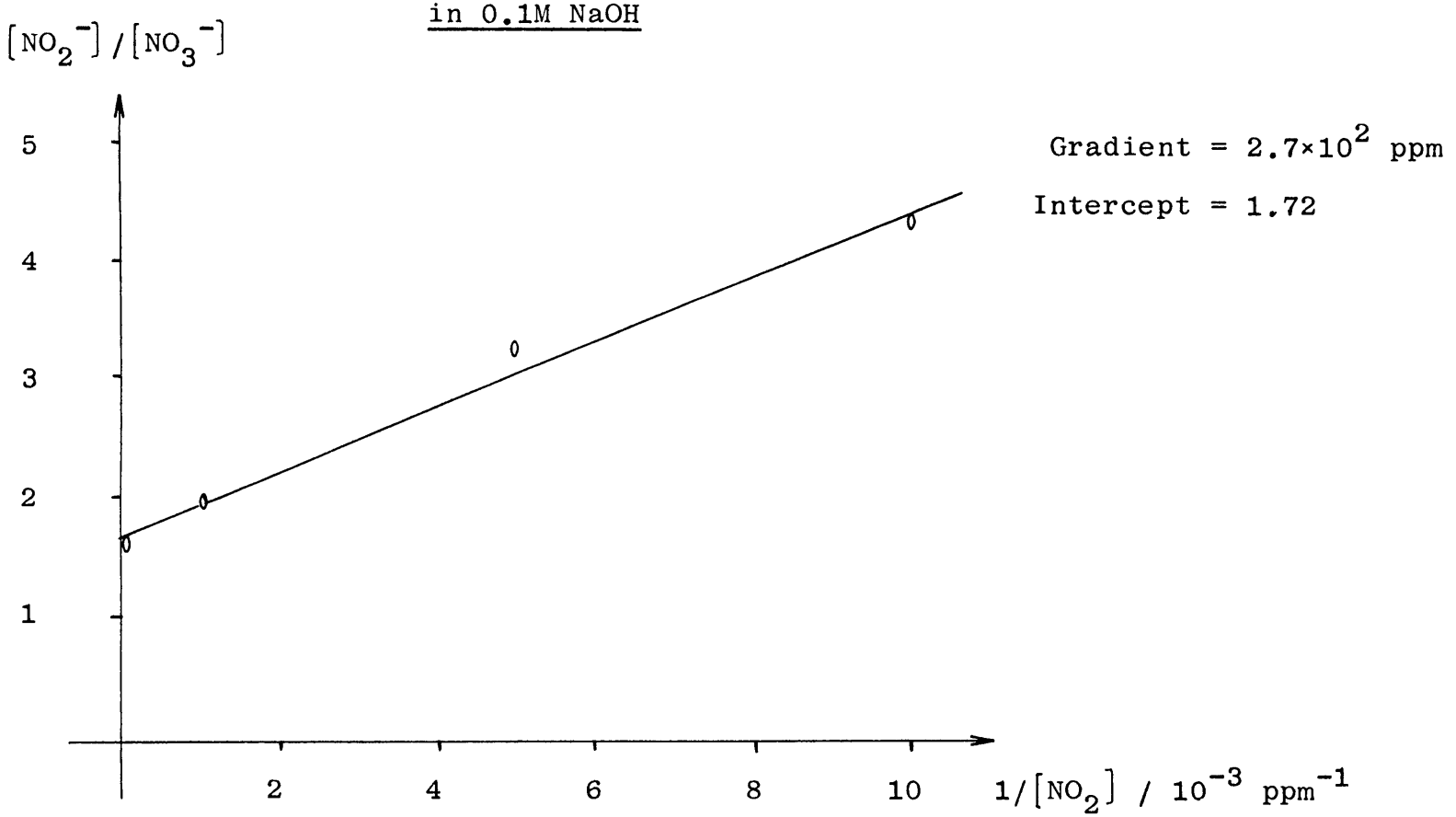


Figure 15. $[NO_2^-]/[NO_3^-]$ vs $1/[NO_2]$, 5.0×10^{-2}M 4-nitrophenol at 25°C in 0.1M NaOH

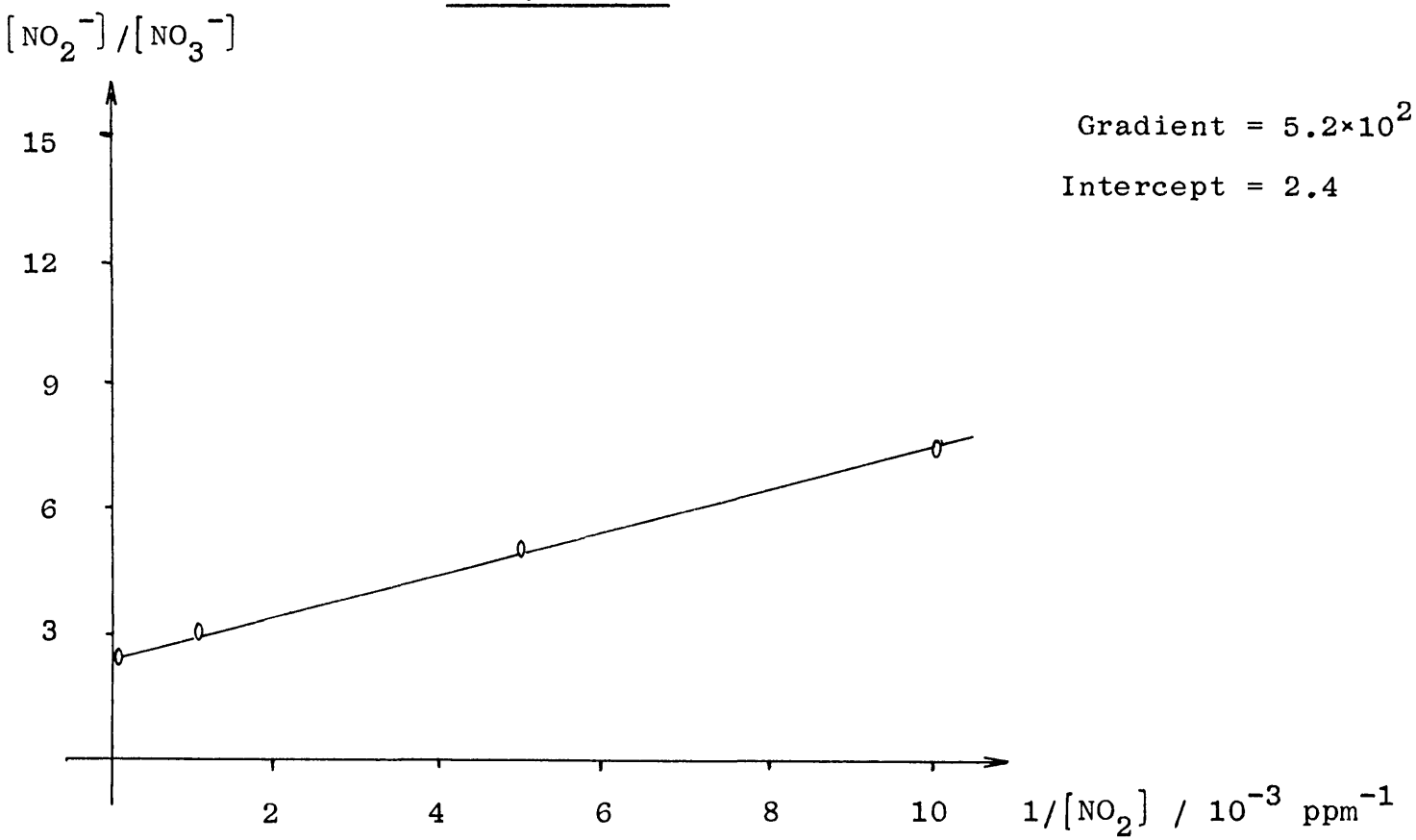
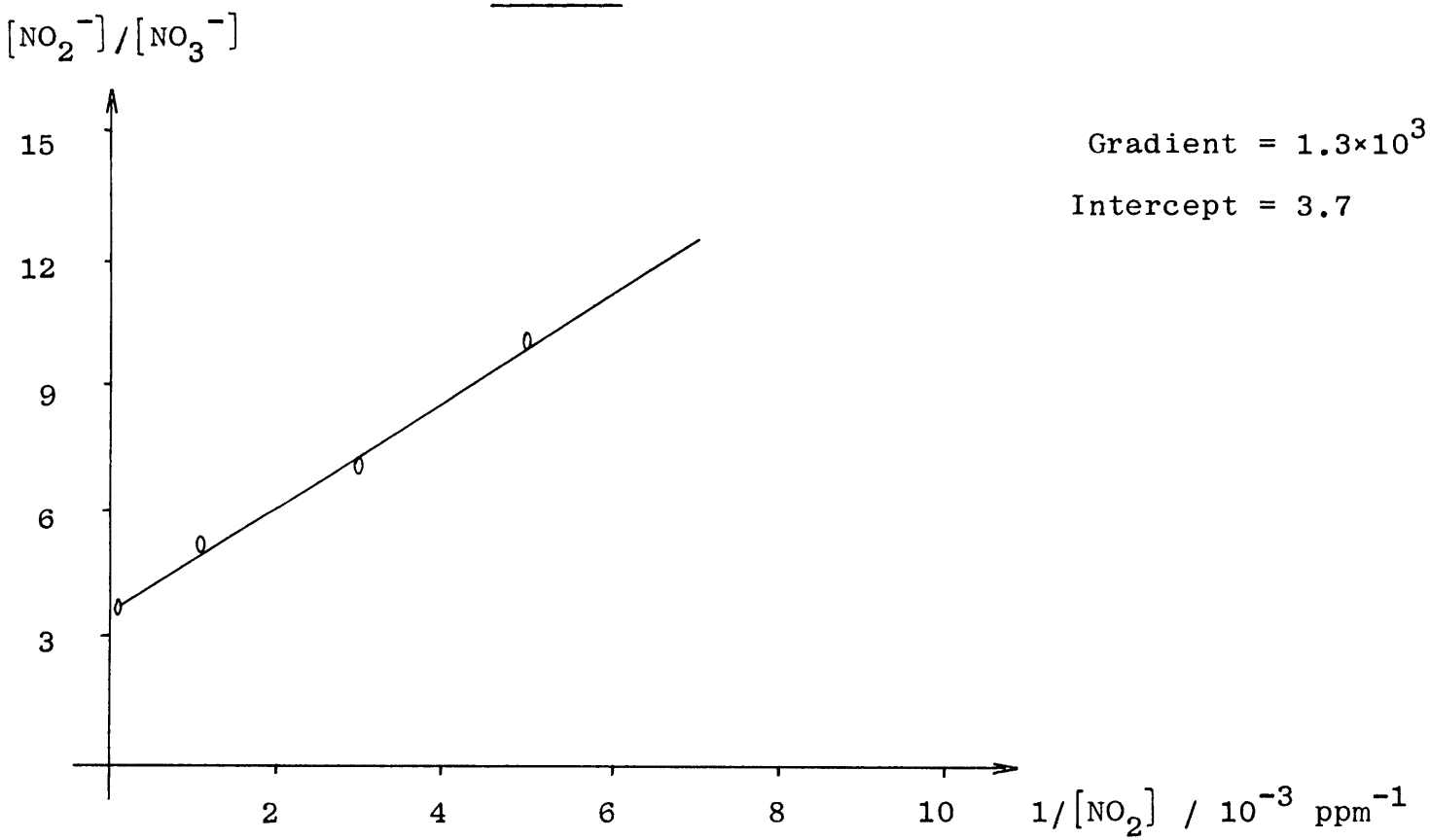


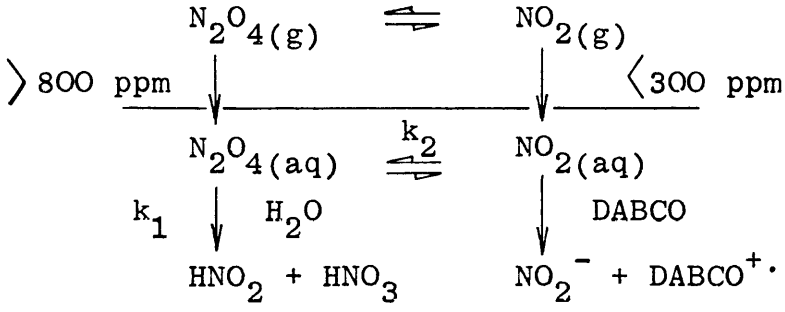
Figure 16. $[NO_2^-]/[NO_3^-]$ vs $1/NO_2$, 0.1M 4-nitrophenol in 0.1M NaOH at 25°C



Gradient = 1.3×10^3 ppm

Intercept = 3.7

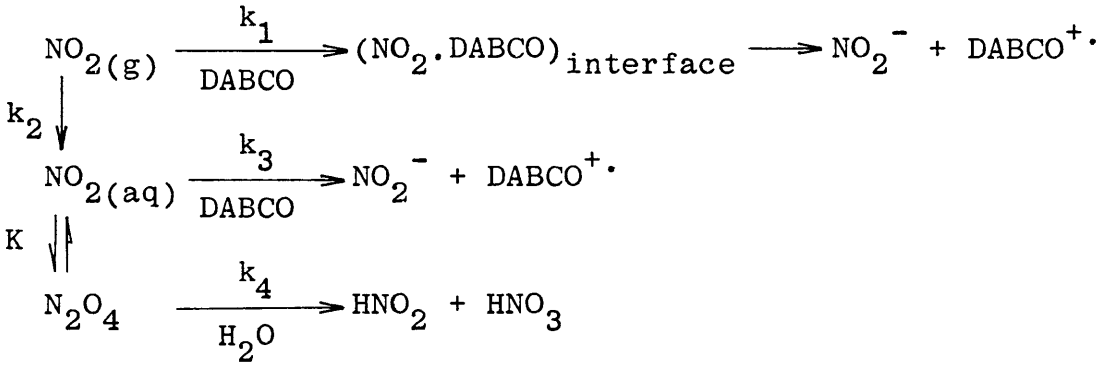
The intercepts of Figures 10-16 would be determined by Equation 11 and therefore independent of substrate concentration. This explanation can therefore be eliminated.



Scheme 23. Mass Transfer Model

$$\frac{[NO_2^-]}{[NO_3^-]} = \frac{k_1[N_2O_4][H_2O] + k_2[N_2O_4]}{k_1[N_2O_4][H_2O]} = 1 + \frac{2k_2}{k_1[H_2O]} \quad ..(11)$$

A third potential artifact is that reaction occurs between the substrate in solution and gaseous NO_2 at the interface, which increases NO_2 absorption as illustrated in Scheme 24.



Scheme 24. Heterogeneous Reaction of DABCO and NO_2

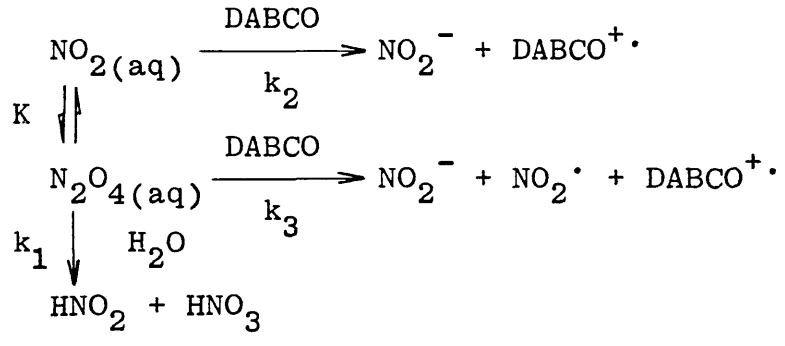
From consideration of competition for NO_2 in the gas phase between DABCO and absorption, Equation 12 is

obtained for the $[NO_2^-]/[NO_3^-]$ ratio. This contains a substrate dependent intercept for the plot of $[NO_2^-]/[NO_3^-]$ vs $1/[NO_2]$ but also an additional term bearing dependence on $[DABCO]^2$. The plots in Figures 7-8 are linear with no indication of a squared dependence. It is possible,

$$\frac{[NO_2^-]}{[NO_3^-]} = 1 + \frac{2k_1[DABCO]}{k_2} + \frac{k_3[DABCO]}{Kk_4[H_2O][NO_2]} + \frac{k_1k_3[DABCO]^2}{k_2Kk_4[NO_2]} \quad ..(12)$$

however, that the additional term makes a small contribution and is therefore undetected in Figures 7-8. It is therefore not possible to exclude the pathway in Scheme 24 on the evidence available. It seems unlikely, however, that very soluble substrates such as phenolate ions and DABCO should preferentially react with gaseous NO_2 at the interface.

An alternaive mechanistic explanation that satisfies all the experimental observations is outlined in Scheme 25. This differs from Scheme 22 in that both NO_2 and N_2O_4 are able to transfer electrons from the DABCO substrate. The kinetic analysis of Scheme 25 (outlined in Equations 13-15) leads to Equation 16 for the $[NO_2^-]/[NO_3^-]$ ratio.



Scheme 25. Electron Transfer by NO_2 and N_2O_4

$$\frac{d[NO_2^-]}{dt} = k_2[DABCO][NO_2] + k_3[DABCO][N_2O_4] + k_1[H_2O][N_2O_4] \quad ..(13)$$

but $[N_2O_4] = K[NO_2]^2$, therefore

$$\frac{d[NO_2^-]}{dt} = k_2[DABCO][NO_2] + Kk_3[DABCO][NO_2]^2 + Kk_1[H_2O][NO_2]^2 \quad ..(14)$$

$$\frac{d[NO_3^-]}{dt} = Kk_1[H_2O][NO_2]^2 \quad ..(15)$$

$$\frac{[NO_2^-]}{[NO_3^-]} = 1 + \frac{k_3[DABCO]}{k_1[H_2O]} + \frac{k_2[DABCO]}{Kk_1[H_2O][NO_2]} \quad ..(16)$$

Equation 16 requires that plots of $[NO_2^-]/[NO_3^-]$ vs [substrate] (Figures 7-8) are linear with an intercept of unity and a slope = $\frac{k_3}{k_1[H_2O]} + \frac{k_2}{Kk_1[H_2O][NO_2]}$. Further,

Equation 16 requires that plots of $[NO_2^-]/[NO_3^-]$ vs $1/[NO_2]$ (Figures 10-16) are linear with an intercept = $1 + \frac{k_3[DABCO]}{k_1[H_2O]}$ and slope = $\frac{k_2[DABCO]}{Kk_1[H_2O]}$.

Thus the mechanism of Scheme 25 explains the unusual properties of Figure 9 seen previously.

The notion that N_2O_4 as well as NO_2 engages in electron transfer from oxidisable substrates is novel. It therefore requires careful scrutiny.

From Figures 11-13 and additional data for reaction of 0.05 and 0.1M DABCO with 10,000 ppm NO_2 the relationship

between the intercept $\left(= 1 + \frac{k_3[DABCO]}{k_1[H_2O]} \right)$ and the [DABCO] was investigated in Figure 17. This plot is linear having an intercept of unity and slope = $k_3/k_1[H_2O]$. From this plot the k_3/k_1 ratio was calculated as shown below:

$$\frac{k_3}{k_1[H_2O]} = 208\ M^{-1}$$

but $[H_2O] = 55.5$ M

therefore, $\frac{k_3}{k_1} = 1.15\times10^4$

Also from Figures 11-13 and additional data for reaction in the absence of DABCO, the relationship between the slopes $\left(= \frac{k_2[DABCO]}{Kk_1[H_2O]} \right)$ and [DABCO] was investigated as shown in Figure 18. This plot is also linear with an intercept of zero and slope = $k_2/Kk_1[H_2O]$. From the slope, the value of k_2/k_1 was calculated as shown below:

$$\frac{k_2}{Kk_1[H_2O]} = 75.1\times10^3\ \text{ppm}\ M^{-1}$$

but 1 ppm = 4.46×10^{-8} M

therefore, $\frac{k_2}{Kk_1[H_2O]} = 3.35\times10^{-3}$

$[H_2O] = 55.5$ M

Figure 17. Intercepts vs [DABCO] in 0.1M NaOH at 25°C

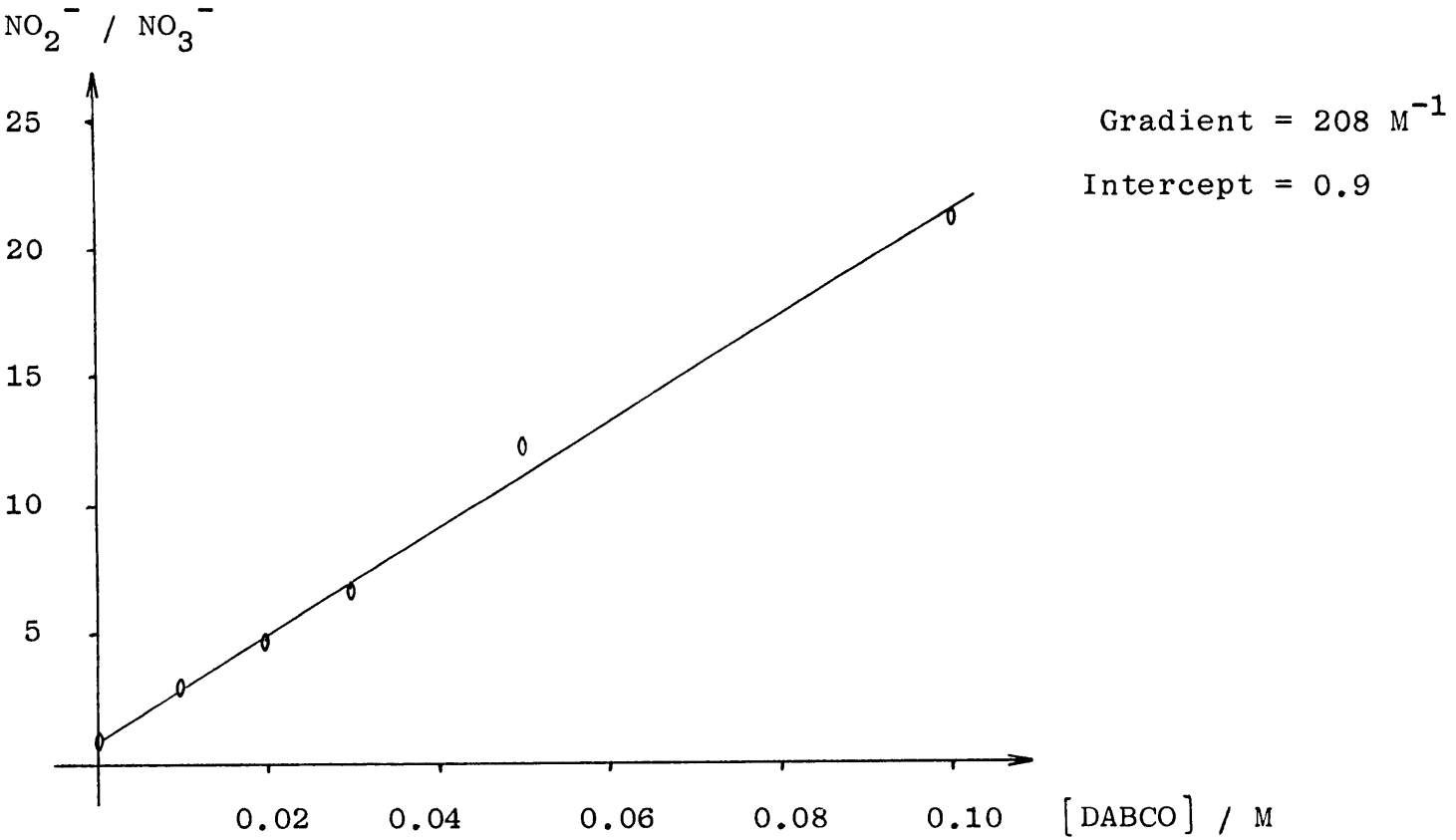
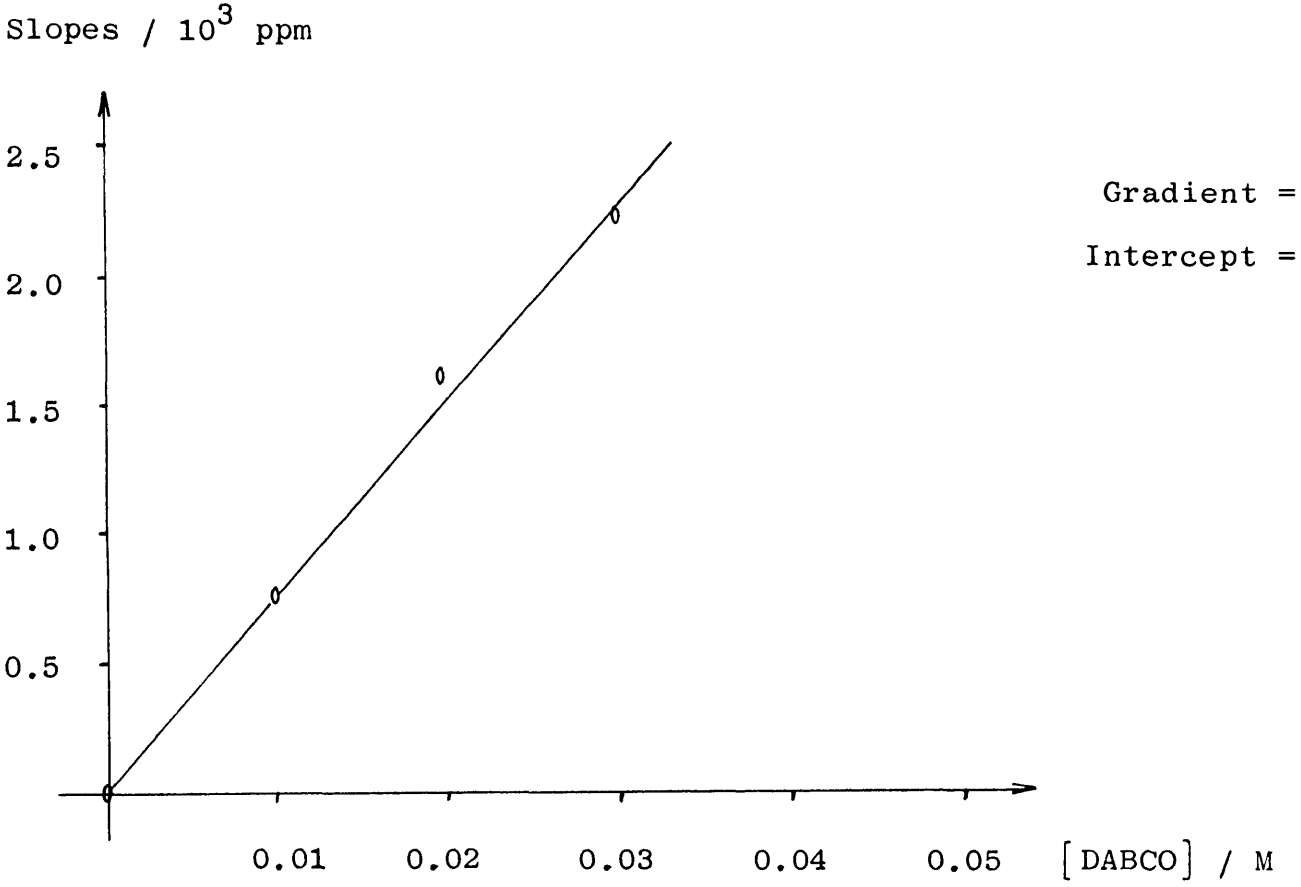


Figure 18. Slopes vs [DABCO] in 0.1M NaOH at 25°C



Gradient = 75.1×10^3 ppm M^{-1}

Intercept = 0.02×10^3 ppm

therefore, $\frac{k_2}{Kk_1}$ = 0.186 M

$[N_2O_4] = K[NO_2]^2$, and $K = 6.5\times10^4\ M^{-1}$ [10]

therefore, $\frac{k_2}{k_1} = 1.2\times10^4$

A similar analysis was applied to the data for reactions with 4-nitrophenol in 0.1M NaOH (Figures 14-16). These data gave good linear plots for both Intercept vs [4-nitrophenol] and Slope vs [4-nitrophenol] and the values for k_3/k_1 and k_2/k_1 are given in Table 7 together with those for DABCO.

Substrate	$\frac{k_3}{k_1}$	$\frac{k_2}{k_1}$
DABCO	1.15×10^4	1.2×10^4
4-Nitrophenol	1.49×10^3	2.0×10^3

Table 7. Rate Coefficient Ratios at 25°C

The numerical analysis outlined above for reaction of both DABCO and 4-nitrophenol with gaseous NO_2 suggests that the experimental results are most consistent with a mechanism in which both NO_2 and N_2O_4 act as electron transfer acceptors (Scheme 25).

2.4.6. Electron Transfer to Dinitrogen Tetraoxide

The conclusion that N_2O_4 may act as an electron transfer acceptor is novel with important structural consequences.

Five possible structures for N_2O_4 can be envisaged (Figure 19) and their possible existence has been considered from time to time. Good evidence[7,8] supports the symmetrical N-N dimer (I) as the thermodynamically stable isomer. Nitrosation studies[9] have suggested formation of the unsymmetrical molecule (III) as a kinetic isomer.

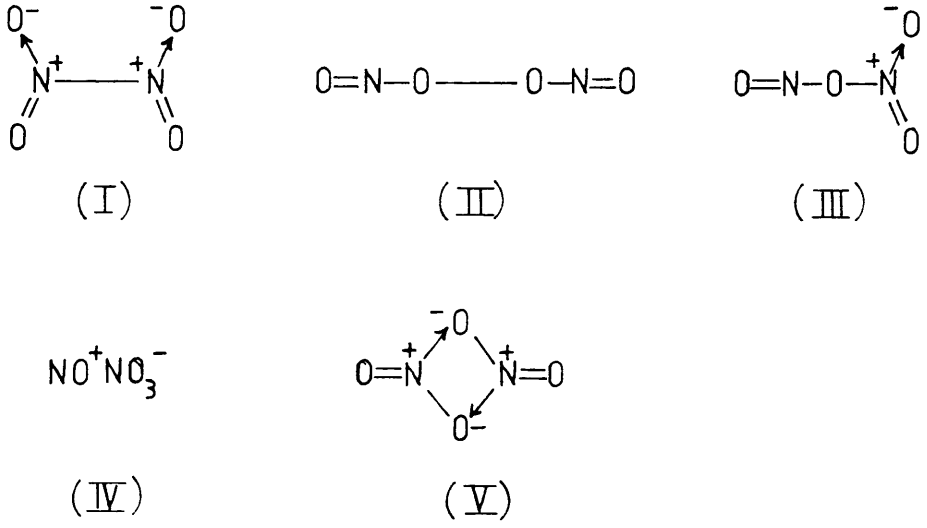
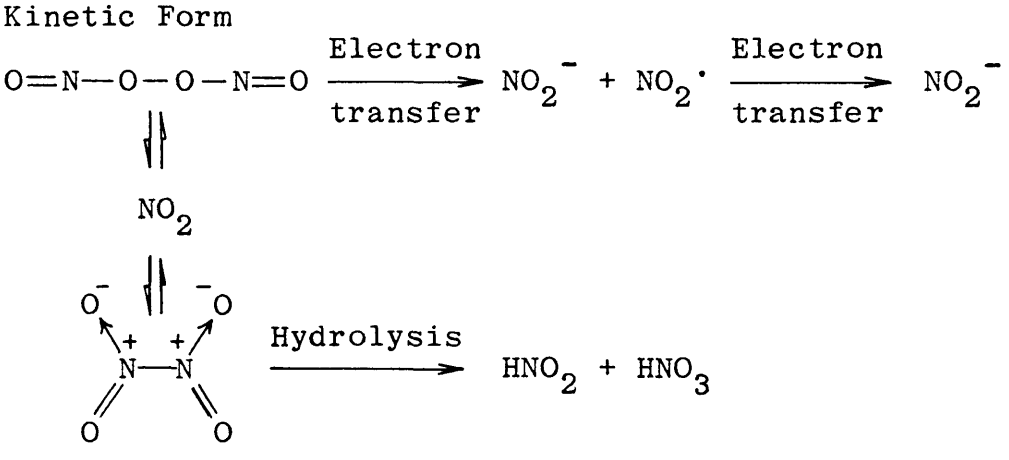


Figure 19. Possible Structures of N_2O_4

Electron transfer to (III) and (IV) should produce the more stable $NO^{\cdot}/NO_3^-$ radical-ion pair rather than the less stable $NO^-/NO_3^{\cdot}$ pair. This can be envisaged as oxidation by either NO^+ or $NO_3^{\cdot}$ The NO produced could then combine with NO_2 to produce N_2O_3 which in turn hydrolyses to NO_2^- (Scheme 18). The occurrence of this sequence would produce only a 2-fold excess of NO_2^-

over NO_3^- under our reaction conditions. Since more than a 10-fold excess of NO_2^- is observed for several of our reactions, electron transfer to either the unsymmetrical isomer (III) or the ion-pair (IV) can be excluded. The dimeric oxidant in our reactions must therefore be one of the symmetrical isomers (I) or (II). Isomer (I) as the thermodynamically stable isomer is most likely to form NO_2^- and NO_3^- on hydrolysis. Thus, isomer (II) the peroxidic form of N_2O_4 and a kinetic isomer appears to be the most likely candidate for the dimeric oxidant as illustrated in Scheme 26. Since the NO_2 produced by electron transfer can engage in further electron transfer to give NO_2^-, no upper limit applies to the magnitude of the $[NO_2^-]/[NO_3^-]$ ratio.



Scheme 26. Electron Transfer and Hydrolysis by N_2O_4

2.4.7. Rate Coefficients

Rate coefficients for the electron transfer processes in Scheme 25 can be obtained from the rate coefficient ratios on multiplication by k_1. Measurement of k_1 by pulse radiolysis[95] and NO_2 absorption[94] gives values of 18 and 10 $M^{-1}S^{-1}$ respectively. The k_2 and k_3 values calculated using the higher value of k_1[95] are shown in Table 8. The magnitudes of k_2 and k_3 are similar implying that NO_2 and N_2O_4 are similarly reactive in the one-electron oxidation of organic molecules.

Substrate	$k_3/M^{-1}s^{-1}$	$k_2/M^{-1}s^{-1}$
DABCO	2.1×10^5	2.2×10^5
4-Nitrophenol	2.7×10^4	3.6×10^4

Table 8. Absolute Rate Coefficients at 25°C

Recently rate coefficients for the one-electron transfer reactions of NO_2 with a wide variety of compounds in aqueous solution have been measured by pulse-radiolysis studies, monitoring the substrate products formed[96]. The exact nature of the oxidant was not established and it may be either NO_2 or N_2O_4. Values obtained for these rate constants are given in Table 9.

The Standard Reactivity Index (Appendix) suggests that phenolate ion is ca. 64-fold more reactive than DABCO at pH 13. From the calculated value of $k_2 = 2.2\times10^5$ $M^{-1}s^{-1}$ for DABCO (Table 8), k_2 = ca. 1.4×10^7 $M^{-1}s^{-1}$ for phenolate ion by electron transfer ~~(Table 9)~~. c.f. Table 9.

Substrate	$k/M^{-1}s^{-1}$ (pH)
phenol	8.6×10^{6} (12.1)
p-methoxyphenol	1.4×10^{8} (12)
hydroquinone	1.6×10^{8} (10.3)
N,N-dimethylaniline	2.6×10^{7} (9.2)
p-phenylenediamine	4.6×10^{7} (9.2)
ascorbate	6.4×10^{7} (9.2)
$Fe(CN)_4^-$	4.3×10^{6}
SO_3^{2-}	$\sim3.5\times10^{7}$ (12.1)

Table 9. Rate Coefficients - Pulse Radiolysis Studies[96].

2.5. Summary

Quantitation of NO_2^- and NO_3^- yields by hplc is a useful method of investigating the reactions of gaseous NO_2 in aqueous solution.

In water, hydrolysis of gaseous NO_2 produces equimolar quantities of NO_2^- and NO_3^- which are best explained as a reaction of the thermodynamically stable N_2O_4 dimer ($O_2N—NO_2$). In the presence of a wide variety of readily oxidised substrates, an excess of NO_2^- is produced. This arises from electron transfer from the substrate to NO_2 and N_2O_4 rather than hydrogen abstraction. The $[NO_2^-]/[NO_3^-]$ ratio is a simple method of detecting the occurrence of electron transfer by gaseous nitrogen dioxide.

Analysis of the data suggests that both NO_2 and a kinetically stable dimer are one-electron transfer oxidants of various substrates. The kinetically stable

dimer with oxidant capability probably has a peroxidic structure (ON—OO—NO).

The results also show that the excess NO_2^- formed in Saltzman type experiments is due to electron transfer from the organic solute to NO_2.

Chapter 3

Factors Governing Substrate Reactivity

3.1. Reduction Potentials

Results in Chapter 2 show that nitrogen dioxide and dinitrogen tetraoxide accept an electron from various organic substrates to give the nitrite ion. An important factor in these processes must be the relative redox potentials of the reactants.

The Standard Reduction Potential for the conversion of NO_2 to NO_2^- at 25°C in water has been estimated to be 1.03±0.04 V vs Normal Hydrogen Electrode (NHE)[97]. In principle, the ability of a substrate to effect the reduction of NO_2 to NO_2^- can be ascertained from its redox potential in water. Unfortunately, these data are available for few compounds. Steenken and Neta[98] have published the aqueous one-electron redox potentials of various phenols, hydroxy- and aminophenols and related compounds of biological interest. Their data is summarised in Table 10. Huie and Neta[96] have calculated the aqueous one-electron redox potentials of aniline and N,N-dimethylaniline to be 1.03 V at pH 6.9 and 0.87 V at pH 9.6.

The absolute values of the reduction potentials summarised in Tables 11-17 are not of direct utility because they refer to measurements in different solvents and with different electrodes. Further, several of the reactions are irreversible. They constitute an unreliable guide to the ease of oxidation of subtrates in water, and therefore of substrates towards oxidation by gaseous NO_2. The potentials in each Table were measured under the same conditions so comparisons within any one Table should be

Table 10. One-Electron Redox Potentials in Water at 22°C [98]

Compound	E,mV
1,2,4-trihydroxybenzene	-110
methoxyhydroquinone	- 85
ethyl gallate	- 54
duroquinone	- 54
2,5-dihydroxyphenylacetate (homogentisic acid)	- 50
quercetin	- 37
pyrogallol	- 9
ascorbate	15
DL-β-3,4-dihydroxyphenylalanine	14
	22
3-hydroxytyramine	18
3,4-dihydroxyphenylacetate	21
hydroquinone	23
2,5-dihydroxybenzoate (gentisic acid)	33
5-hydroxydopamine	42
catechol	43
DL-norepinephrine	44
L-epicatechin	48
DL-catechin	79
quinalizarin	73
3,4-dihydroxycinnamate	84
2,5-dihydroxyacetophenone	118
2,3-dihydroxybenzoate	118
3,4-dihydroxybenzoate	119
2,4,5-trihydroxypyrimidine	132
p-(N-methylamino)phenol	146
	156
	146
p-(N,N-dimethylamino)phenol (DMAP)	174
	174
adrenalone	~ 180
6-hydroxy-2,5,7,8-tetramethyl-chromone-2-	192
carboxylate (HTCC)	185
ellagic acid	187

Continued.....

Table 10, continued

Compound	E,mV
DL-5-hydroxytryptophan	208
5-hydroxyindole	216
	197
p-aminophenol	217
N,N,N',N'-tetramethyl-p-	266
phenylenediamine (TMPD)	265
7-hydroxycoumarine	315
p-phenylenediamine	309
	366
o-phenylenediamine	346
	360,420
resorcinol	392
	379
4-methoxyphenol	402
	~ 460
phenol	> 600

The potentials are given for reduction of the phenoxy type radicals vs NHE. All were measured at pH 13.5. The experimental error is ±10mV.

Table 11. Reduction Potentials, General[99]

Compound	$E_{1/2}$ (V) in Acetonitrile vs NHE
Tri-(p-tolyl)amine	0.29
1-Naphthylamine	0.34
Dimethylaniline	0.45
Diphenylamine	0.53
Tetracene	0.53
Perylene	0.55
Azulene	0.61
Aniline	0.70
3,4-Benzopyrene	0.71
9,10-Diphenylanthracene	0.75
Triethylamine	0.79
4,4'-Dimethoxybiphenyl	0.80
Phenoxanthiin	0.81
Trimethylamine	0.82
Thianthrene	0.83
Anthracene	0.84
1,12-Benzoperylene	0.90
Coronene	0.93
1,2-Benzoanthracene	0.99
Dibenzo-1,4-dioxin	1.01
Phenol	1.04
1,4-Dimethoxybenzene	1.04
4-Methoxytoluene	1.13
Hexamethylbenzene	1.20
Chrysene	1.22
2-Methylnaphthalene	1.22
Phenanthrene	1.23
1-Methylnaphthalene	1.24
Fluorene	1.25
Indene	1.25
Dimethyl sulphide	1.26
Pentamethylbenzene	1.28
1,2,4,5-Tetramethylbenzene	1.29
N-Butyl mercaptan	1.34

Continued.....

Table 11, continued

Compound	$E_{1/2}$ (V) in Acetonitrile vs NHE
Naphthalene	1.34
Durene	1.34
Triphenylene	1.35
Diethyl sulphide	1.35
Anisole	1.40
1,2,4-Trimethylbenzene	1.41
Diphenyl	1.48
Mesitylene	1.53
p-Xylene	1.54
o-Xylene	1.58
1,2,3-Trimethylbenzene	1.58
m-Xylene	1.60
1,4-Cyclohexadiene	1.60
Anisaldehyde	1.64
Thiophene	1.70
p-Bromotoluene	1.72
Dimethyl sulphoxide	1.73
Quinoline	1.73
p-Chlorotuluene	1.76
Iodobezene	1.77
Pyridine	1.82
N,N-Dimethylacetamide	1.82
2,3-Dimethyl-1,3-butadiene	1.84
N-Butylamine	1.87
2-Propylbenzene	1.88
Toluene	1.96
1-Propylbenzene	1.97
1,4-Dioxane	1.97
2-Methyl-1-butene	1.97
Bromobenzene	1.98
Cyclohexene	1.98
1,3-Butadiene	2.03
2-Iodopropane	2.04

Continued.....

Table 11, continued

Compound	$E_{1/2}$ (V) in Acetonitrile vs NHE
Benzene	2.04
Chlorobenzene	2.07
Methyl iodide	2.12
2-Butene	2.21
2-Methylpropane	2.65
1-Octene	2.70
1-Butene	2.78
Ethylene	2.90
tert-Butylalcohol	2.94
2-Methylpentane	3.01
2,2-Dimethylbutane	3.28

Table 12. Reduction Potentials, Phenols, Effect of pH[100]

Compound	Medium	$E_{1/2}$(V) vs NHE
2,4,6-Tri-tert-butylphenol	pH=5.6	0.40
"	0.01M Me_4NOH	-0.059

Conditions: Graphite Electrode

Table 13. Reduction Potentials, Phenols[101]

Phenol	$E_{1/2}$(mV)		Phenol	$E_{1/2}$(mV)	
Phenol	+1004	a	4-Phenyl-2-chloro	+560	c
1-Naphthol	740	a	2,4-Dichloro	660	c
2-Naphthol	820	a	4-Carboxy-2-chloro	920	c
2-Hydroxybiphenyl	970	a	4,6-Diphenyl-2-cyano	593	d
4-Hydroxybiphenyl	890	a	2,6-Diphenyl-4-cyano	549	d
4-Methyl	543	b	Pentaphenyl	366	d
3-Methyl	607	b	2,4,6-Triphenyl-3-cyano	433	d
2-Methyl	556	b	3-Chloro-2,4,6-triphenyl	347	d
4-Methoxy	406	b	2,3,4,6-Tetraphenyl	238	d
3-Methoxy	619	b	2,4,6-Triphenyl	211	d
2-Methoxy	456	b	4-Fluoro-2,6-diphenyl	164	d
4-Nitro	924	b	2,4,6-Tri-p-phenoxyphenyl	179	d
3-Nitro	855	b	2,4,6-Tri-p-methoxyphenyl	124	d
2-Nitro	846	b	4-t-Butyl-2,6-diphenyl	120	d
4-Chloro	653	b	6-t-Butyl-2,4-diphenyl	112	d
3-Chloro	734	b	4,6-Di-t-butyl-2-phenyl	76	d
2-Chloro	625	b	2,6-Di-t-butyl-4-phenyl	- 14	d
4-t-Butyl	578	b	2,4,6-Tri-t-butyl	- 59	d
2-t-Butyl	552	b			
4-Phenyl	534	b			

a Pt Anode, Ag/0.1N Ag^+ ref. electrode, solvent system: acetonitrile + perchlorate salt

b Graphite Anode, saturated calomel ref. electrode, aqueous buffered solution, pH 5.6

c Pt Anode, saturated calomel ref. electrode, solvent system: 0.14M aqueous LiCl

d Graphite Anode, Ag/AgCl ref. electrode, solvent system: acetonitrile-H_2O + $(CH_3)_4NOH$

Table 14. Reduction Potentials, Amines[100]

Compound	E_p (V) vs NHE
N-Propylamine	1.63
N-Butylamine	1.63
Iso-Butylamine	1.62
Tert-Butylamine	1.62
N-Pentylamine	1.69
N-Nonylamine	1.72
Di-N-Propylamine	1.26
Di-N-Butylamine	1.31
Di-Sec-Butylamine	1.40
Di-N-Pentylamine	1.35
Dibenzylamine	1.49
Trimethylamine	1.29
Triethylamine	1.19
Tri-N-Propylamine	1.02
Tri-N-Butylamine	1.02
Tribenzylamine	1.27

Conditions: CH_3CN, $NaClO_4$, Pt Anode

Table 15. Reduction Potentials, Anilines[100]

Compound	$E_{p/2}$(V) vs NHE
Aniline	0.90
N-Methylaniline	0.77
N,N-Dimethylaniline	0.74

Conditions: CH_3CN, TEAP, Pt Anode

Table 16. Reduction Potentials, Diamines[100]

Compound	$E_{1/2}$(V) vs NHE
Aniline	0.54
o-Phenylenediamine	0.06
p-Phenylenediamine	0.16

Conditions: CH_3CN, $NaClO_4$, Pt Anode

Table 17. Reduction Potentials, Diamines[100]

Compound	E_p(V) vs NHE
N,N,N',N'-Tetramethylenediamine	0.87
N,N,N',N'-Tetramethylethylenediamine	0.67
1,4-Diazabicyclo 2,2,2 octane	0.60

Conditions: CH_3CN, $NaClO_4$, Pt Anode

more reliable than those across two Tables. Unfortunately, insufficient correlations[102] are available in the literature to estimate standard one-electron reduction potentials of these compounds in aqueous solution.

As more one-electron reduction potential data becomes available for correlation with the Standard Reactivity Index (Appendix), it should be possible both to estimate the reduction potential of compounds from their reactivity towards gaseous NO_2 and to predict their ability to reduce gaseous NO_2 from reduction potential data.

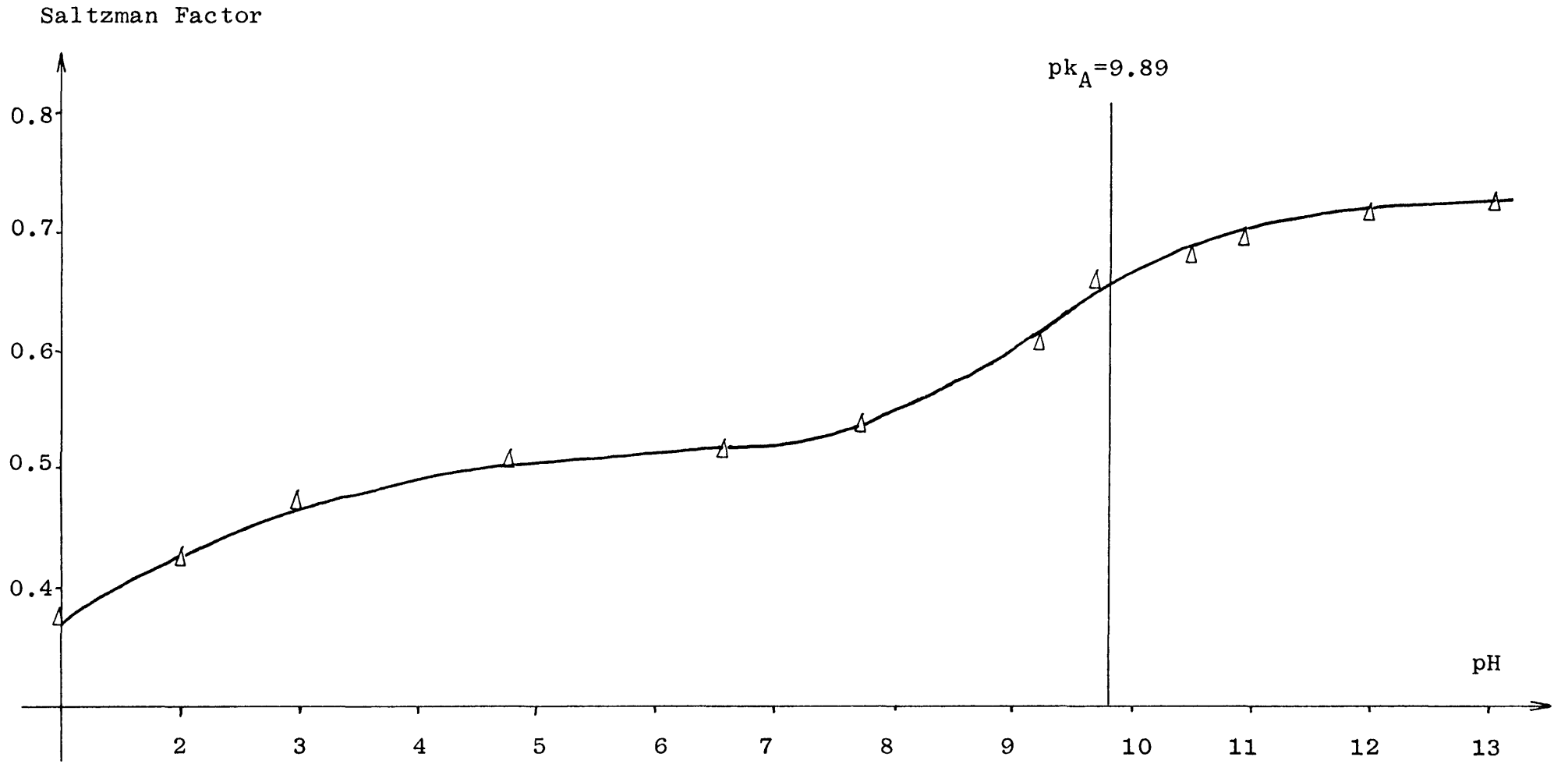
3.2. The Reactive Moiety in Solution

Results presented in Section 2.3.3. (Figure 3) showed that the Saltzman Factor for the absorption of 200 ppm gaseous NO_2 was virtually independent of pH. Similar results do not apply to absorption of gaseous NO_2 in the presence of a reductant and the pH dependency gives useful information about the reactive moiety in solution.

3.2.1. Phenol

Figure 20 shows the variation of the Saltzman Factor (SF) with pH for 200 ppm gaseous NO_2 in the presence of 10^{-4}M phenol. At pH$<$7, the plot is little different from that observed in the absence of phenol. At pH$>$7, the SF increases steadily to reach a maximum at pH$\gg$12. The change in the SF is largest in the region of pH 9.9, which is close to the pk_A for phenol.

Figure 20. pH profile for reaction of 10^{-4}M phenol with 200 ppm NO_2 at 25°C



The plot in Figure 20 is very reminiscent of the titration curve for phenol. It suggests that only the phenolate reduces gaseous NO_2 to NO_2^- and that phenol, itself, is unreactive. This is supported by 10^{-3}M Anisole giving equimolar quantities of NO_2^- and NO_3^- on reaction with 200 ppm NO_2 at pH 6.

Section 6.2. reports the products of this reaction.

3.2.2. DABCO

Figure 21 shows the SF/pH profile for 200 ppm gaseous NO_2 in the presence of 10^{-3}M DABCO. Its shape is very similar to Figure 20 with a clear transition in the SF at pH close to the pk_A for mono-protonation of DABCO at 8.7. A reasonable conclusion is that only neutral DABCO reduces gaseous NO_2. It is interesting that DABCO.H^+ is unreactive, which is evidence for transannular interaction.

The products arising from the reaction of DABCO with gaseous NO_2 were not characterised.

3.2.3. Aniline

Figure 22 shows the SF/pH profile for reaction of 10^{-3}M aniline with 900 ppm gaseous NO_2 at 25°C. Electron transfer is only apparent at pH$\rangle$4.6 where unprotonated aniline is available. Below pH 4.6, two effects come into play. Firstly, the anilinium ion is formed which does not react by electron transfer with gaseous NO_2 and secondly, aniline is diazotised[26] by nitrous acid produced by hydrolysis of the gaseous NO_2.

Figure 21. pH profile for reaction of 10^{-3}M DABCO with 200 ppm NO_2 at 25°C

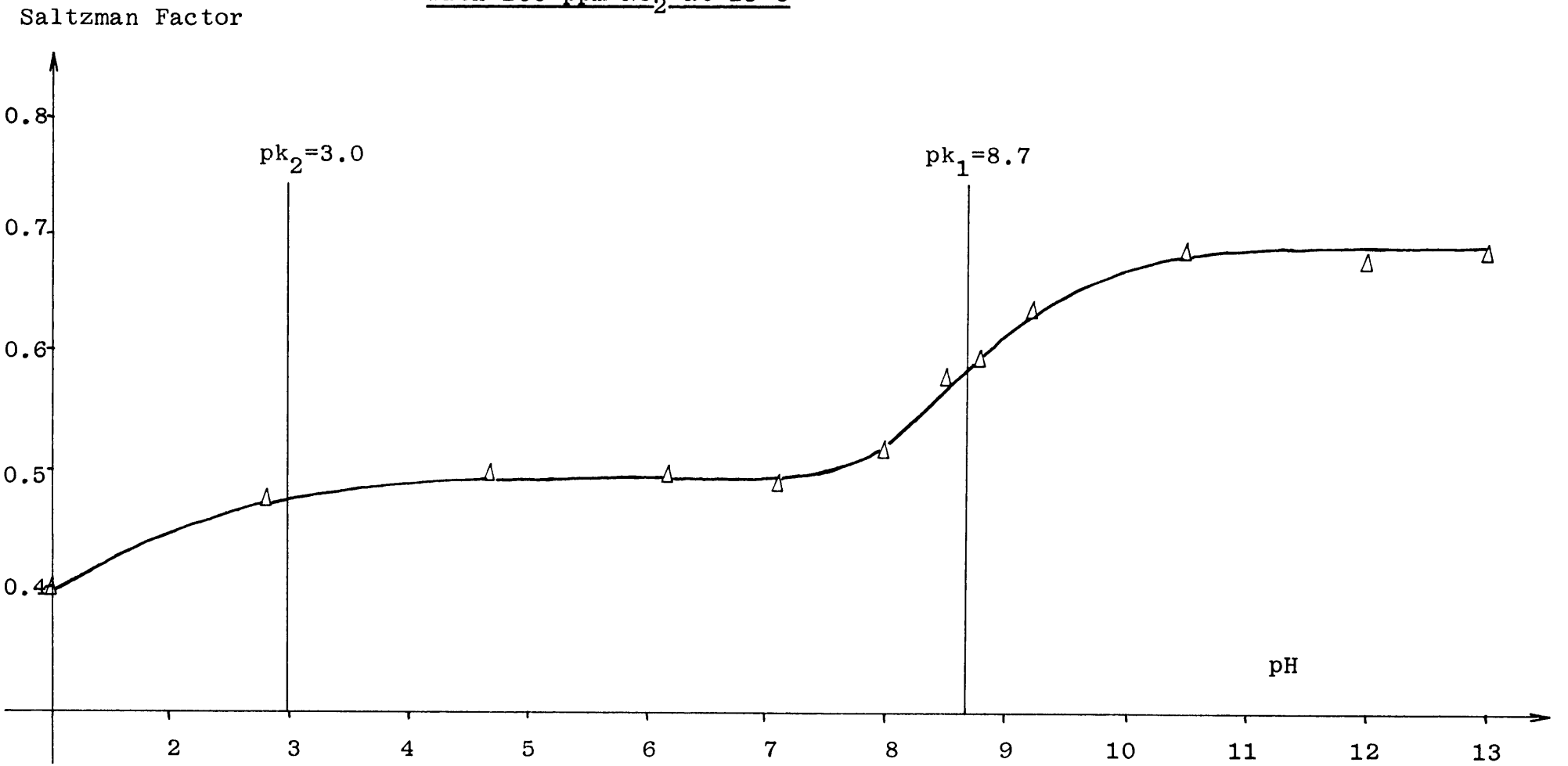
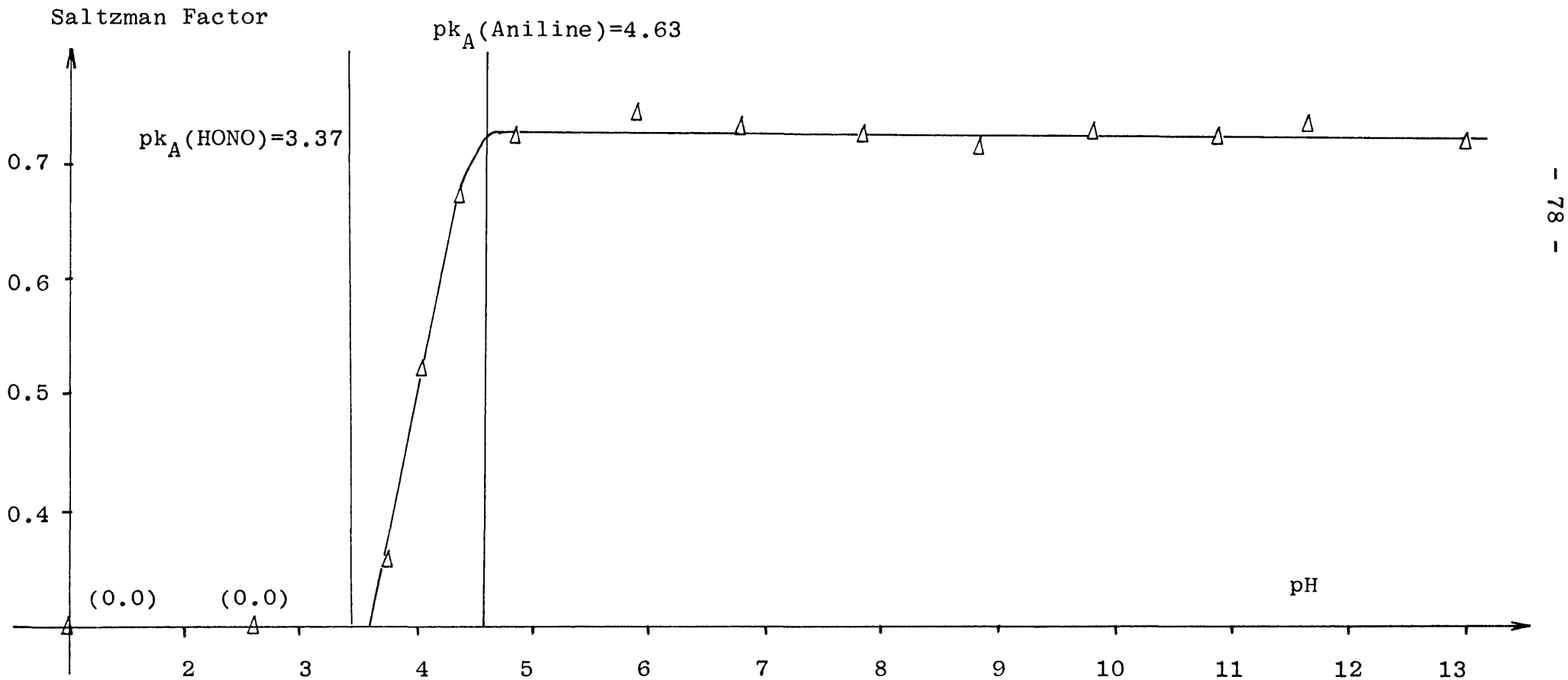


Figure 22. pH profile for reaction of 10^{-3}M aniline with 900 ppm NO_2 at 25°C

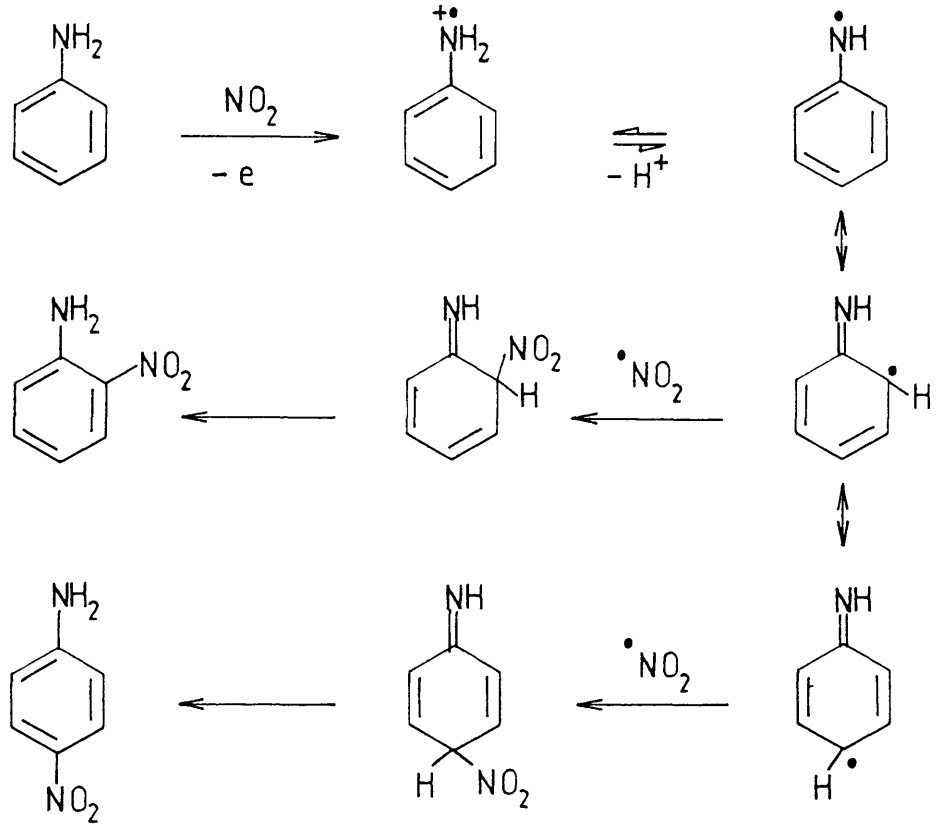


Product analysis showed that 2-nitroaniline and 4-nitroaniline are major products of the reaction at pH 13 (Table 18). A plausible mechanism for their

$[NO_2]$	Yields		Total
	2-Nitroaniline	4-Nitroaniline	
900 ppm	22.3%	24.2%	46.5%
500 ppm	22.8%	25.0%	47.8%
200 ppm	22.7%	24.4%	47.1%

Table 18. Product Analysis 10^{-3}M Aniline at pH 13

formation is shown in Scheme 27.



Scheme 27. Formation of Nitroanilines

3.2.4. Conclusion

Figures 20-22 illustrate the utility of SF/pH profiles in identifying moieties which reduce gaseous NO_2 to NO_2^- in solution. They show that only substrates with readily available electrons reduce NO_2.

3.3. Radical Cation Basicities

The oxidation of thiols by gaseous nitrogen dioxide in various solvents at room temperature to produce nearly quantitative yields of disulphides has previously been reported[103].

Reactions of dilute NO_2 with cysteine, glutathione, thiocyanate ion and thiophenol were investigated in the present study and their SF/pH profiles are shown in Figures 23-26, respectively. There are clear discontinuities at pH ca. 5.0, 4.5 and 8.5 in the SF/pH profiles for cysteine, glutathione and thiocyanate ion that are unrelated to the basicity of the thiol group. These discontinuities can be explained by the onset of reversible redox reactions in the presence of radical cations. Electron transfer reactions of radical cations are well-documented[34,104] and the observed discontinuities in the SF/pH profiles would relate to the basicities of radical cation intermediates. A possible reaction scheme accomodating this behaviour is illustrated in Scheme 28. This explanation is supported by the SF/pH profile for tryptophan (Figure 27). The tryptophan radical cation has $pk_A=4.3$[105], and the SF/pH profile drops rapidly about this pH.

Figure 23. pH profile for reaction of 5.0×10^{-4}M cysteine with 200 ppm NO_2 at 25°C

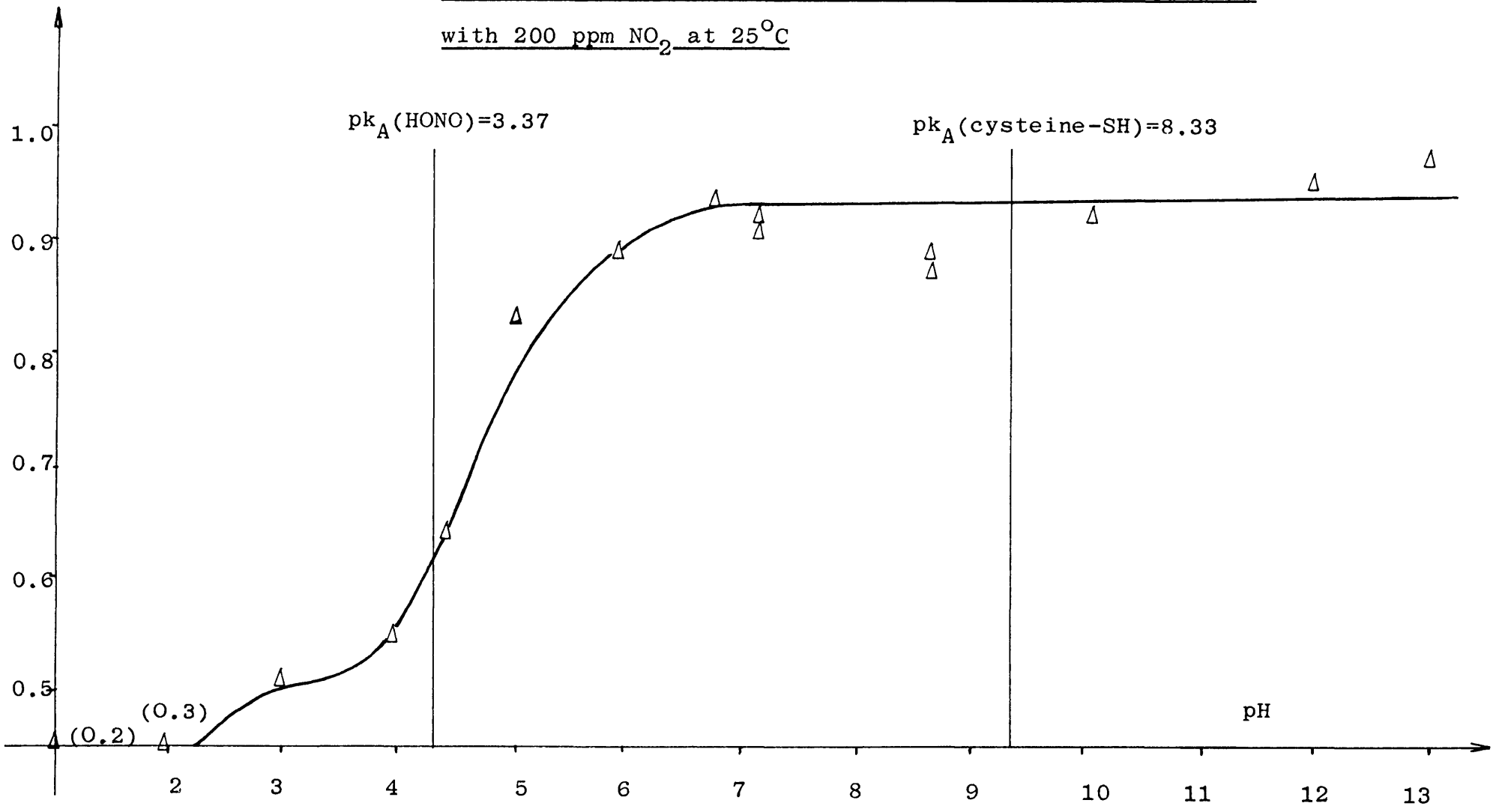


Figure 24. pH profile for reaction of 1.36×10^{-3}M glutathione with 900 ppm NO_2 at 25°C

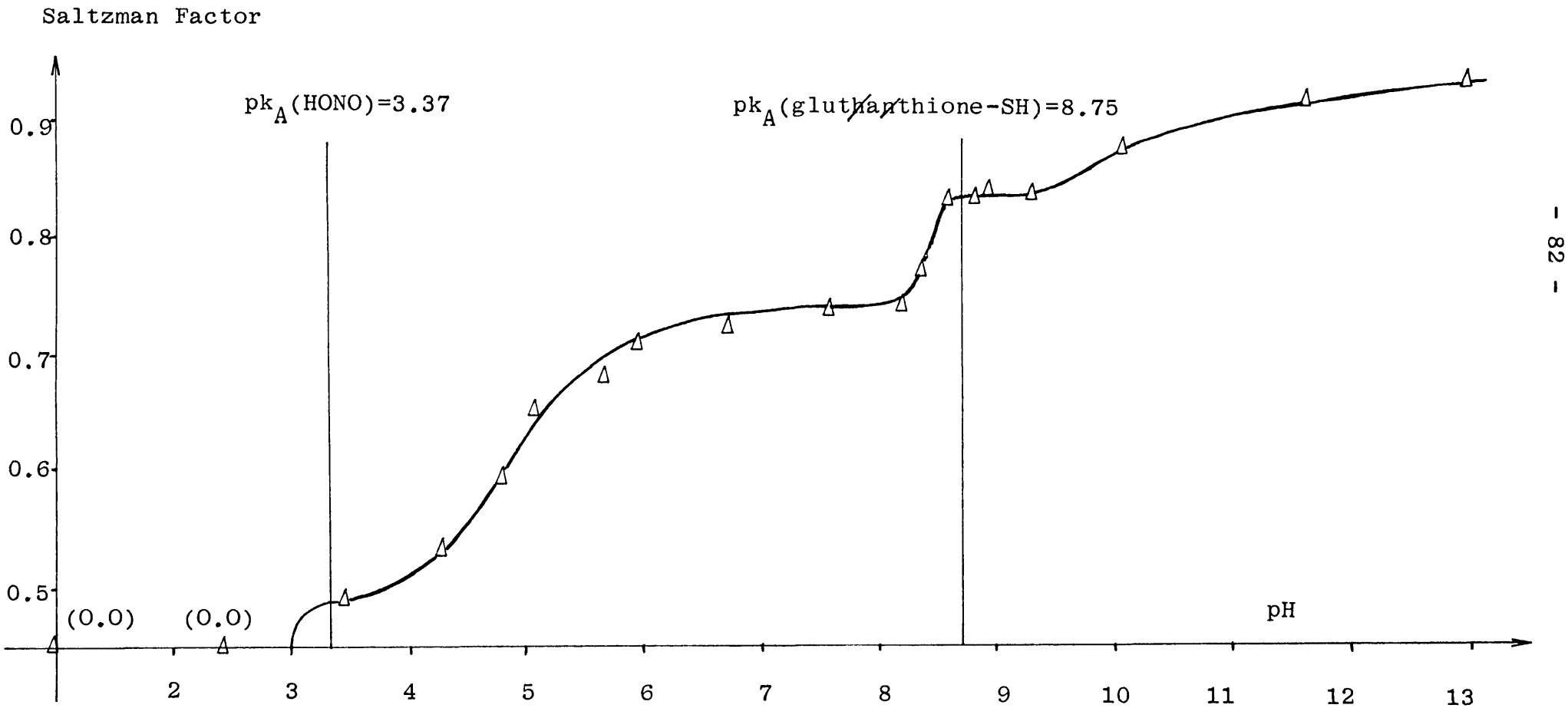
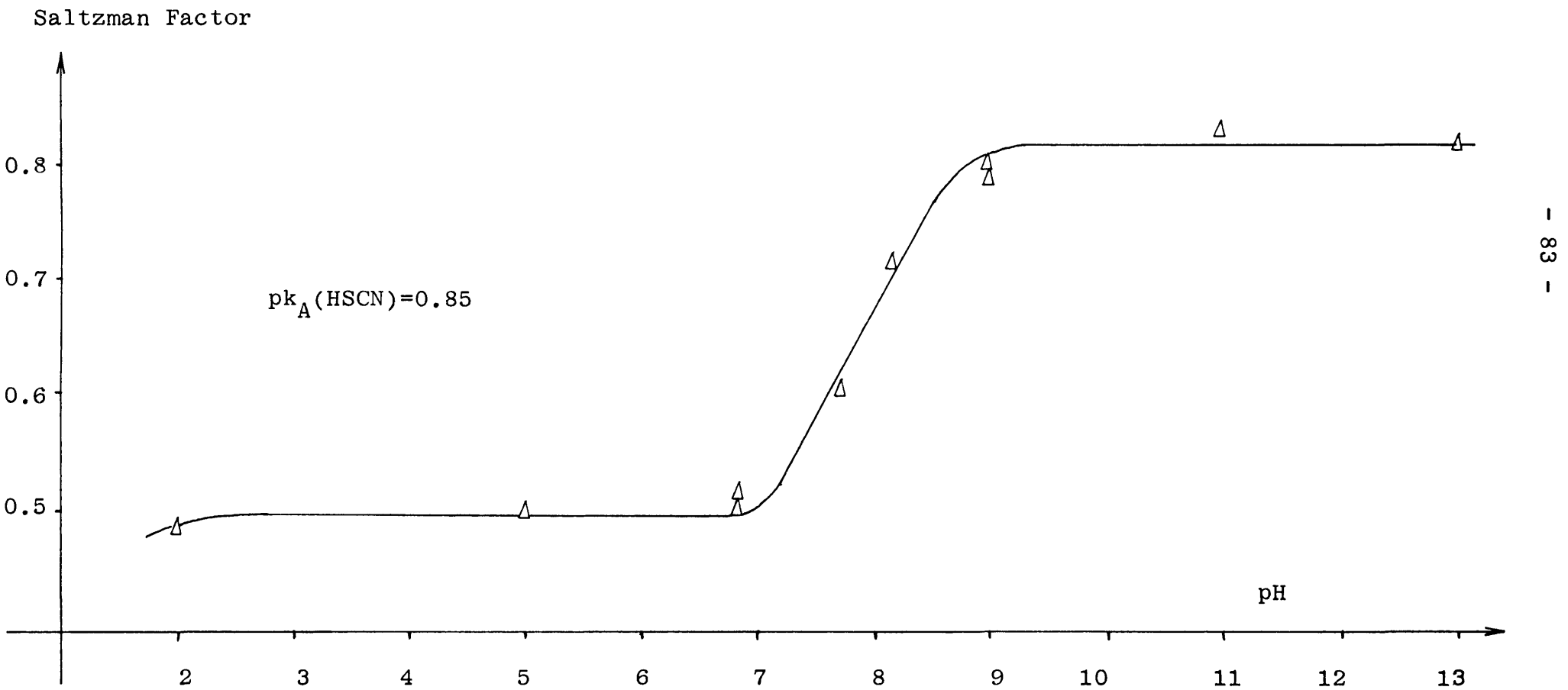


Figure 25. pH profile for reaction of 0.1M thiocyanate with 330 ppm NO_2 at 25°C



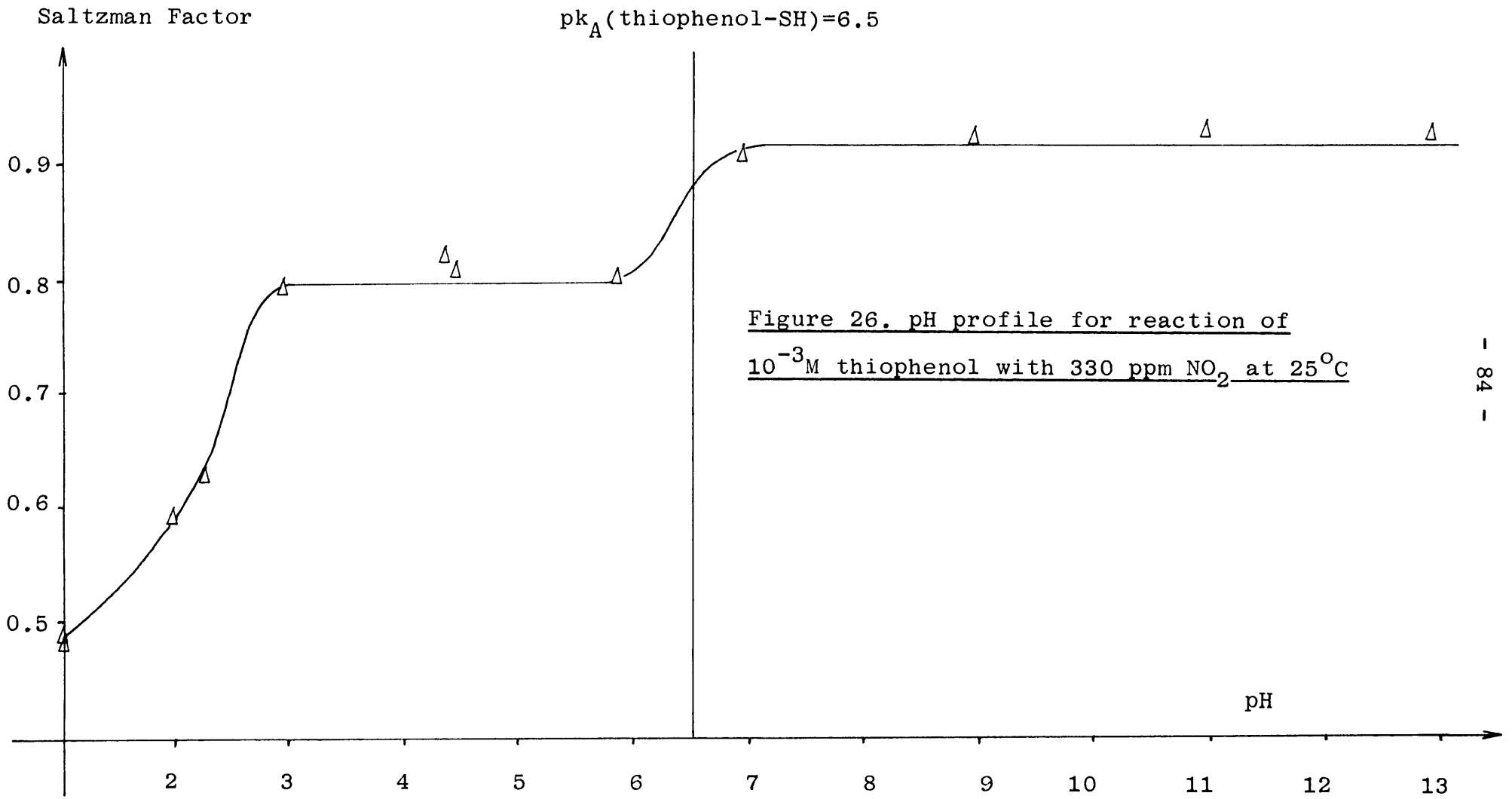


Figure 26. pH profile for reaction of 10^{-3}M thiophenol with 330 ppm NO_2 at 25°C

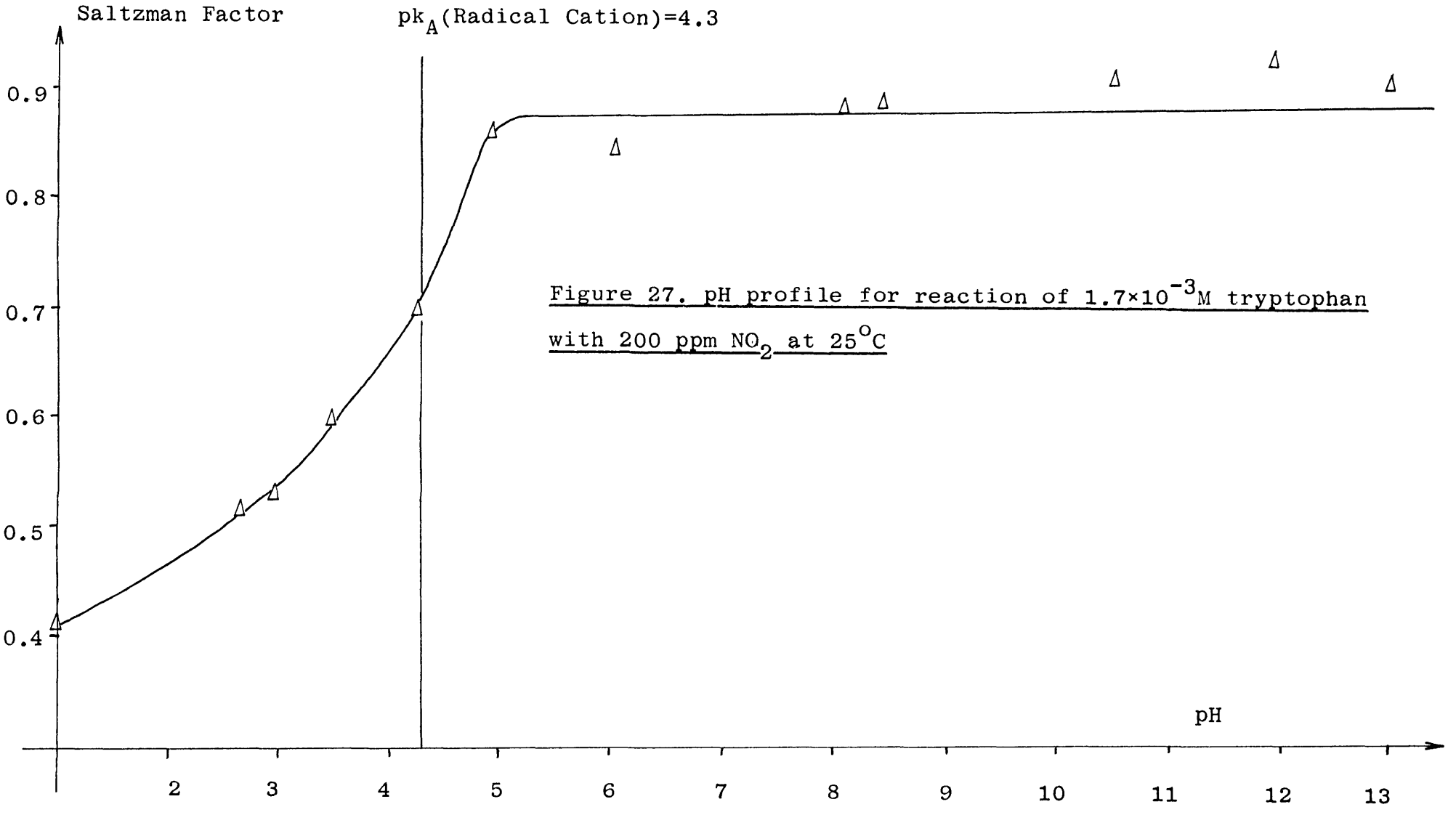
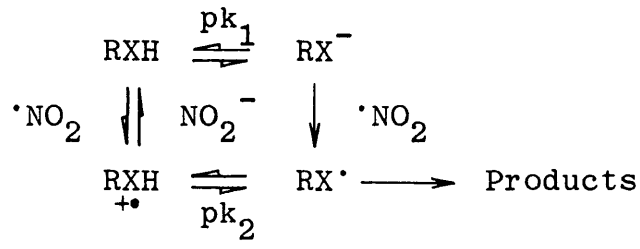


Figure 27. pH profile for reaction of 1.7×10^{-3}M tryptophan with 200 ppm NO_2 at 25°C

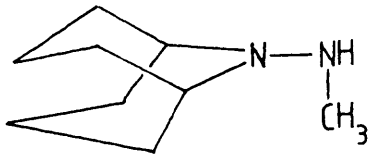


Scheme 28. Reversibility of Electron Transfer via Radical Cations

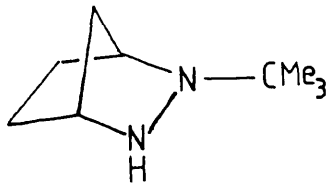
The basicities of other relevant radical cations reported in the literature are given in Table 19. The anilinium radical cation has $pk_A = 7.0$ but the SF/pH profile is without an inflection at this pH (Figure 22). This appears to contradict the above arguement, but the anilinium radical cation may delocalise and therefore be unable to oxidise nitrite.

Table 19. Known Values of pk_A for $RH^{+\cdot}$. 104

Substrate	pk_A
(10)	10.4
(11)	7.0
Dimethylamine	6.5-7.5
Aniline	7.0
o-Methylhydroxylamine	2.9
Hydroquinone	- 0.8
4-Methylphenol	- 1.6
Phenol	- 2.0
Benzene	~ - 3
Toluene	~ -11



(10)



(11)

3.3.1. Thiol Reactivity

The SF/pH proflies for cysteine, glutathione and thiophenol have been reported above. It is apparent that all three compounds react in both neutral and anionic forms. For glutathione and thiophenol electron transfer reactivity increases about pH=pk_A of the thiol group which implies the anionic form is more reactive. Glutathione also becomes significantly more effective at pH$\rangle$10.5, which may relate to further reaction of the glutathione disulphide product[103]. Evidence to this effect is given in Table 20 where the SF is significantly higher at pH$\rangle$10.5.

pH	Saltzman Factor
7.60	0.51
8.65	0.55
9.80	0.60
10.60	0.77
11.38	0.96
13.00	1.00

Table 20. Reaction of Glutathione Disulphide (10^{-2}M) with 330 ppm Gaseous NO_2 at 25°C

The SF for glutathione and cysteine at pH<3 is lower than expected, as observed previously for aniline. A possible explanation is the onset of acid catalysed nitrosation of the thiol[106] to give the thio-nitrite ester which may be stable to thermal decomposition (Equation 17) under the reaction conditions.

$$2RSNO \xrightarrow{\Delta} RSSR + 2NO \qquad ..(17)$$

S-Methylcysteine is unreactive at pH 13 (Appendix), this does not contravene the above but suggests that S-methylcysteine radical cation undergoes reverse electron transfer with nitrite.

3.4. Summary

One-electron reduction potentials from the literature have been collated together with other reduction potentials. The utility of these data in assessing the ability of substrates to reduce NO_2 is outlined.

SF/pH profiles identify the reactive moiety in solution. They show that only the phenoxide ion and unprotonated DABCO and aniline are reactive.

Inconsistancies exist in the SF/pH profiles of thiols and thiocyanate. They can be rationalised by reversible redox behaviour of radical cation intermediates but more work is required to fully understand these complex reactions.

Chapter 4

The Reaction of Gaseous Nitrogen Dioxide with Organic Substrates in Aqueous-Organic Solvent Mixtures

4.1. Introduction

In Chapter 2 it was concluded that both NO_2 and N_2O_4 effect one-electron oxidation of a variety of organic substrates in aqueous solution to produce nitrite.

An extension of these studies to aqueous-organic solvent mixtures was undertaken to accomodate water insoluble substrates. Further, the effect of solvent dielectric on the electron transfer should give further information about the processes involved.

4.2. Electron Transfer in Aqueous-Organic Solvent Mixtures

In aqueous acidic solutions, passage of gaseous NO_2 produces an excess of nitrate ion because nitrous acid either evaporates or is oxidised to nitrate ion (Section 2.3.3.). Similarly, excess nitrate ion was formed when gaseous NO_2 was bubbled through pure organic solvents (Table 21), they were analysed by hplc directly or by extraction with 0.1M NaOH. Presumeably the NO_2 is hydrolysed by a small water impurity in the solvents to give an acidic system. Acid-catalysed nitration may also occur and lead to some confusion.

Solvent	$[NO_2^-]/[NO_3^-]$
Acetonitrile	0.2
CCl_4	0.3

Table 21. Reaction of Gaseous 1000 ppm NO_2 with Pure Organic Solvents at 25°C

For the above reasons aqueous-organic solvent mixtures were chosen in which a hydroxide ion concentration of 0.1M was maintained using 0.1M NaOH (or 0.1M Bu_4NOH when the NaOH was insoluble). It is noted that interference free hplc analysis of nitrite and nitrate was made in 0.1M Bu_4NOH / aqueous-organic solvent mixtures by the same pre-dilution procedure as for 0.1M NaOH samples and direct injection into the Waters Ion Chromatography System.

The hydrolysis reaction and the reaction of 10^{-3}M phenoxide ion in the range 0-93.5% of the organic solvent have been studied using tetrahydrofuran and dioxan as the organic cosolvent. Figures 28-29 show the results obtained, in both cases the hydrolysis shows a slight excess of nitrite. This was caused by the Bu_4NOH (impurity) as 0.1M NaOH reaction solutions showed equimolar quantities of nitrite and nitrate. In both cases electron transfer is demonstrated for a known electron transfer substrate, a vast excess of nitrite is seen on phenoxide addition. This demonstrates that we can observe electron transfer reactions in aqueous-organic solvent mixtures. Table 22 details the results for 80% DMSO and MeCN and Table 23 summarises the results.

Figure 30 details the results for EtOH. Electron transfer is clearly seen but both plots deviate towards excess nitrate at high % EtOH. This is interpreted as formation of ethyl nitrite which is lost by evaporation (bp. 17°C).

Figure 28. Electron Transfer Reaction of 330 ppm Gaseous NO_2 with 10^{-3}M Phenoxide Ion in the presence of 0.1M Bu_4NOH in THF/H_2O

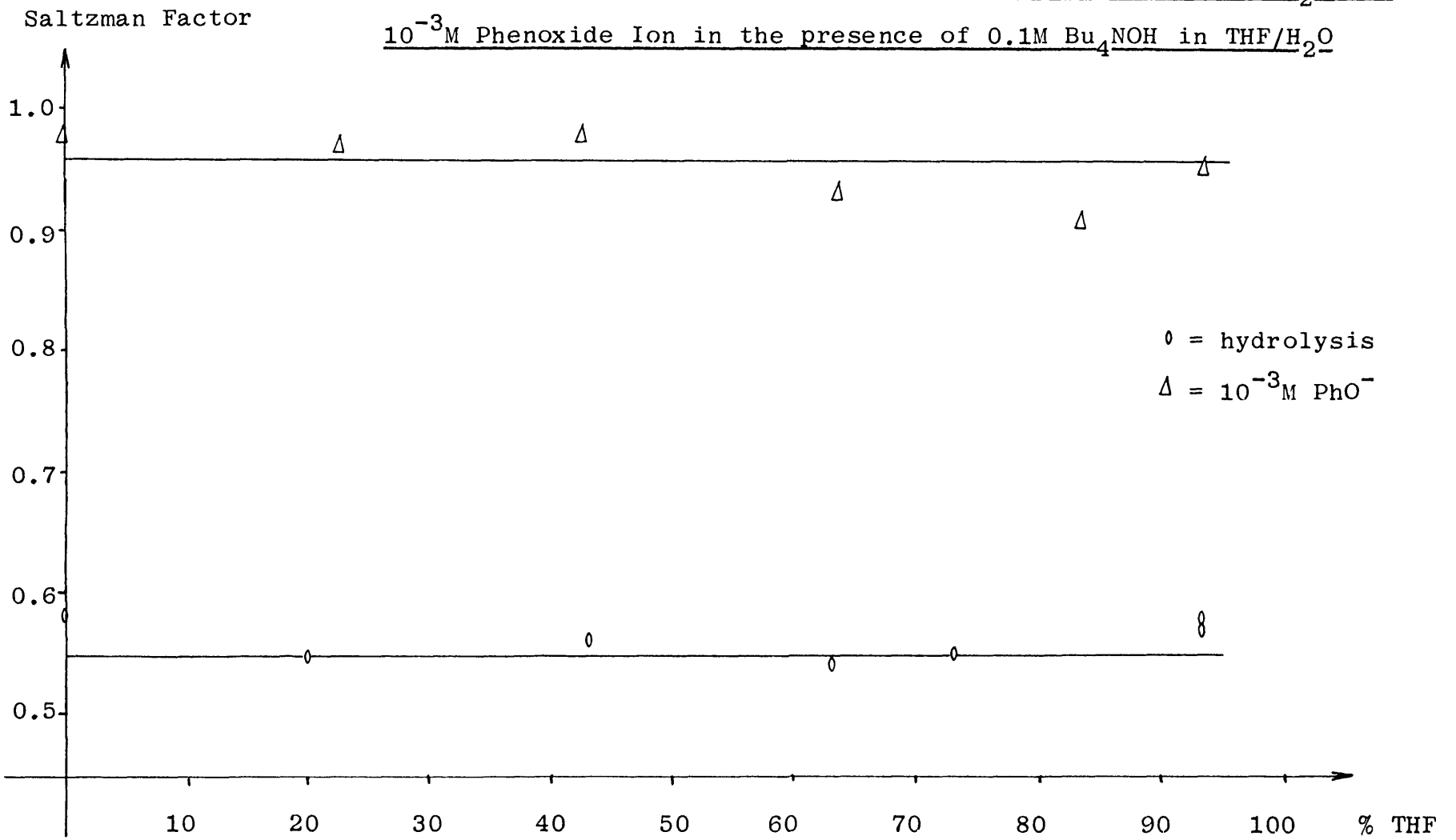
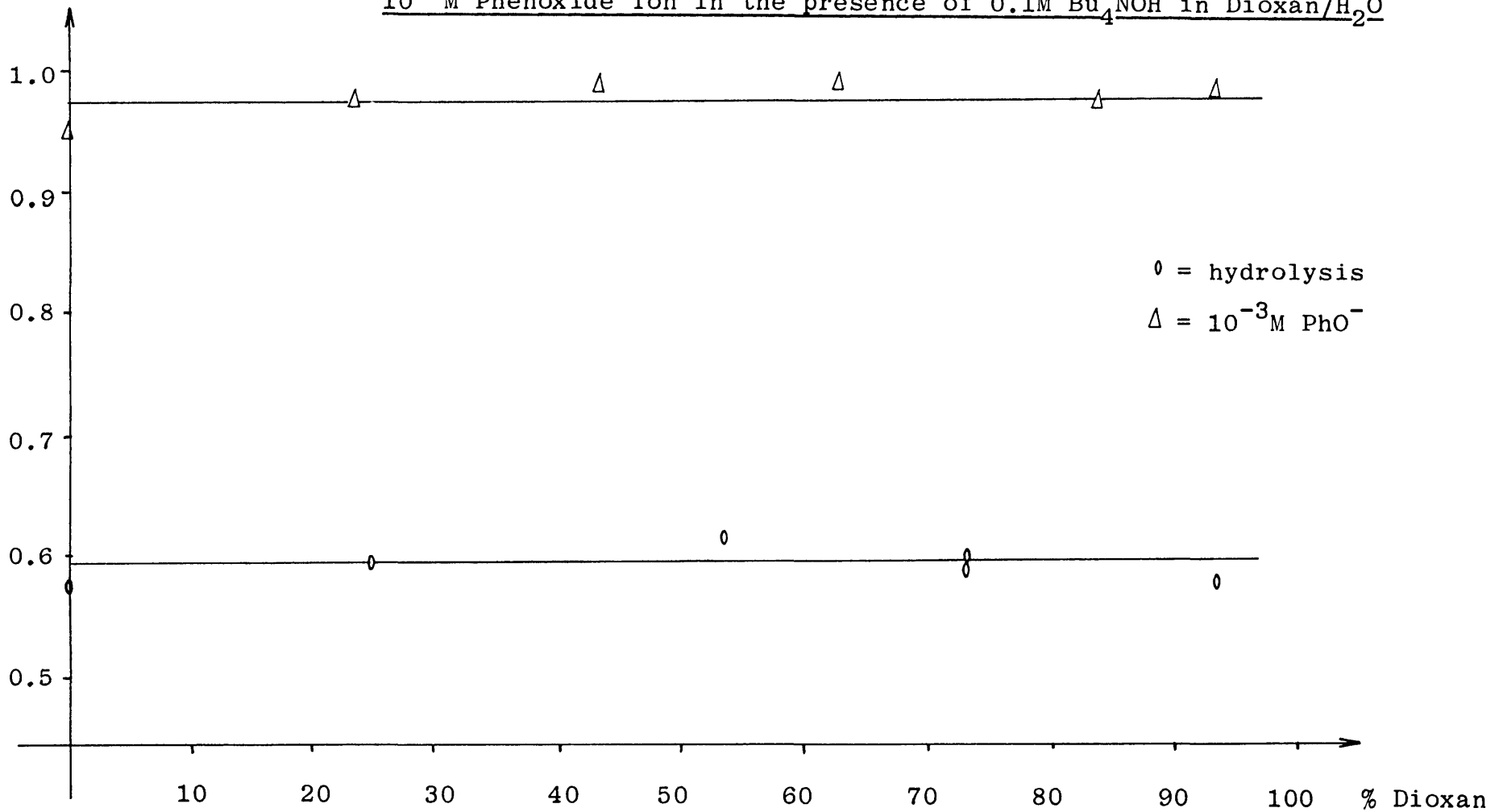


Figure 29. Electron Transfer Reaction of 330 ppm Gaseous NO_2 with 10^{-3}M Phenoxide Ion in the presence of 0.1M Bu_4NOH in Dioxan/H_2O



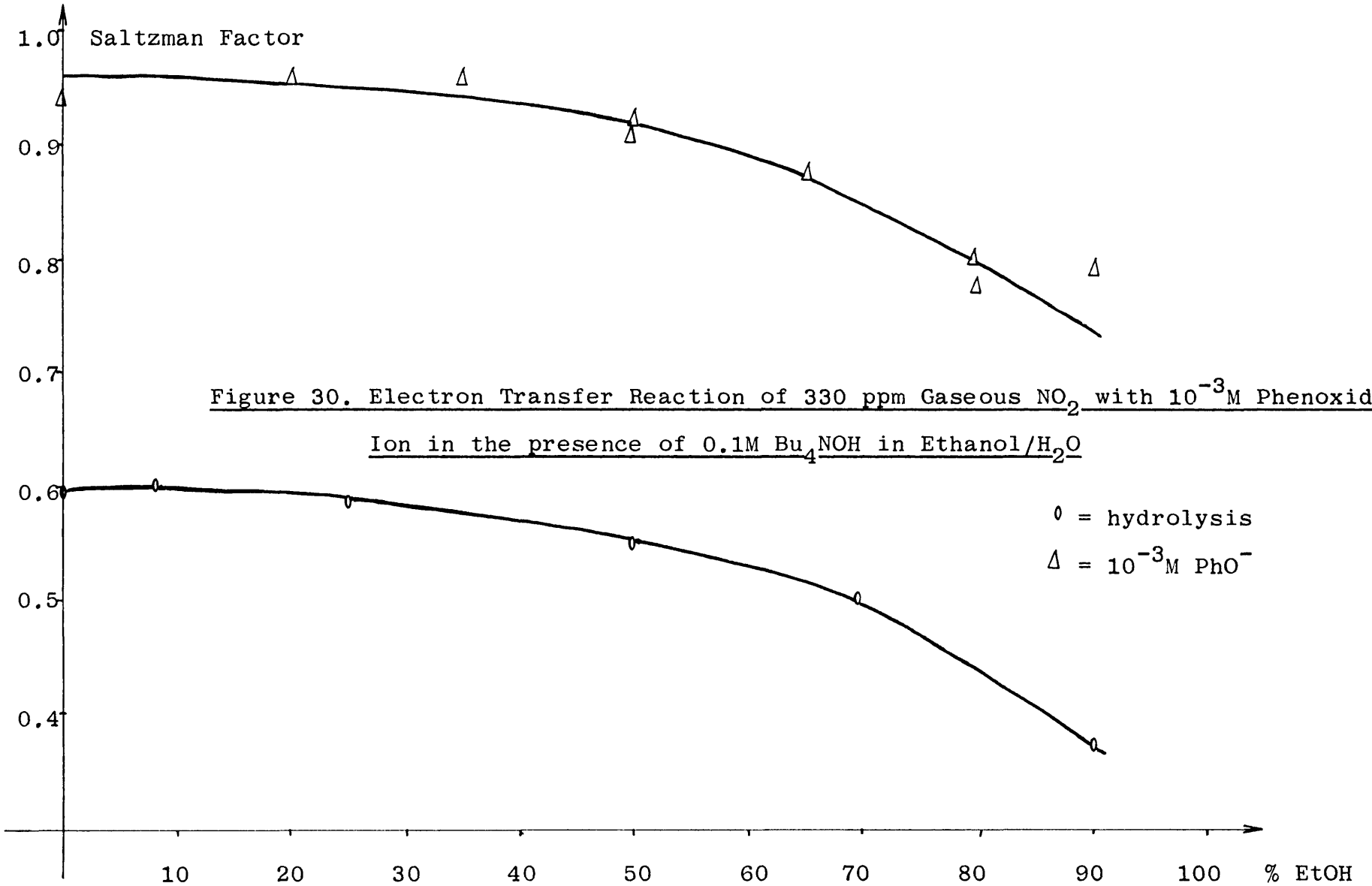


Figure 30. Electron Transfer Reaction of 330 ppm Gaseous NO_2 with 10^{-3}M Phenoxide Ion in the presence of 0.1M Bu_4NOH in Ethanol/H_2O

Solvent System	Saltzman Factor	
	Hydrolysis	10^{-3}M PhO^-
80% DMSO /0.1M Bu_4NOH	0.49	0.93
80% MeCN /0.1M Bu_4NOH	0.55	0.90

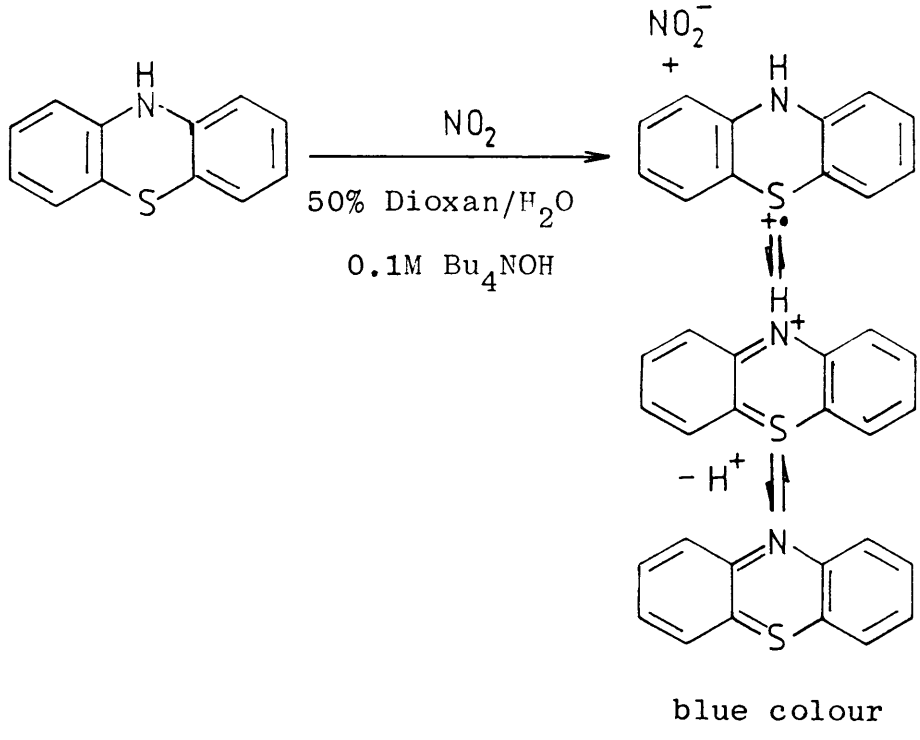
Table 22. Electron Transfer by Gaseous 330 ppm NO_2 in DMSO and MeCN Aqueous-Organic Solvent Mixtures

Solvent	ϵ	Comments
H_2O	79.5	Electron transfer demonstrated-Chapter 2
DMSO	46.7	Electron transfer demonstrated-Table 22
MeCN	36.0	Electron transfer demonstrated-Table 22
EtOH	24.0	Electron transfer demonstrated-Figure 30
THF	7.6	Electron transfer demonstrated-Figure 28
Dioxan	2.2	Electron transfer demonstrated-Figure 29

Table 23. Electron Transfer in Aqueous-Organic Solvent Mixtures

4.3. Water Insoluble Substrates

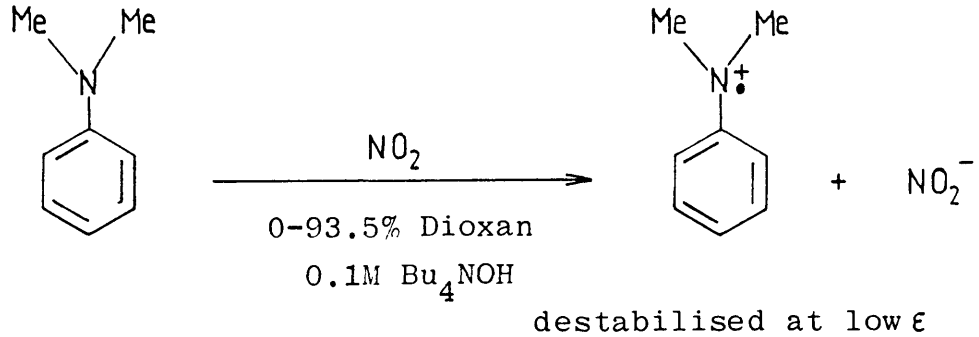
Aqueous-organic solvent systems are suitable to solubilise some compounds into basic aqueous solutions. Their reactivity towards NO_2 is given in the Standard Reactivity Index (Appendix). These compounds include indole, 2-(2'-chlorophenoxy)phenol, dibenzo[1,4]dioxin, 1-naphthylamine, N-(1-naphthyl)ethylenediamine dihydrochloride (NED) and phenothiazine. NED is a powerful electron transfer substrate and was used by Saltzman[37] and others in their absorbing solutions, it is therefore likely that they were observing this electron transfer reaction. Phenothiazine reacts with gaseous NO_2 to give a deep blue solution which is characteristic of its radical cation as indicated in Scheme 29. This lends further support to our electron transfer mechanism.



Scheme 29. The Reaction of Phenothiazine with Gaseous NO_2

4.4. Solvent Effects

An interesting solvent effect is illustrated in Figure 31 in the reaction of N,N-dimethylaniline with gaseous NO_2 in 0-93.5% dioxan. A significant decrease in the SF is seen with increasing % dioxan. These results support the electron transfer mechanism to produce a radical cation which will be destabilised as the dielectric constant of the solvent decreases (Scheme 30).



Scheme 30. Solvent Effect for Reaction of N,N-Dimethylaniline with Gaseous NO_2

Figure 32 shows the opposite solvent effect in the reaction of 4-nitrophenol with gaseous NO_2 in 0-93.5% MeCN. Above 70% MeCN a significant increase in reactivity is seen. These results support the formation of a neutral radical which is stabilised as the dielectric constant of the solvent decreases (Scheme 31). In Figure 32 it is noted that there is an equimolar quantity of nitrite and nitrate in the range 0-70% MeCN rather than a slight excess of nitrite, a purer batch of Bu_4NOH was used in this work.

Figure 31. Solvent Effect for Reaction of 10^{-2}M N,N-Dimethylaniline with 330 ppm Gaseous NO_2 in the presence of 0.1M Bu_4NOH at 25°C

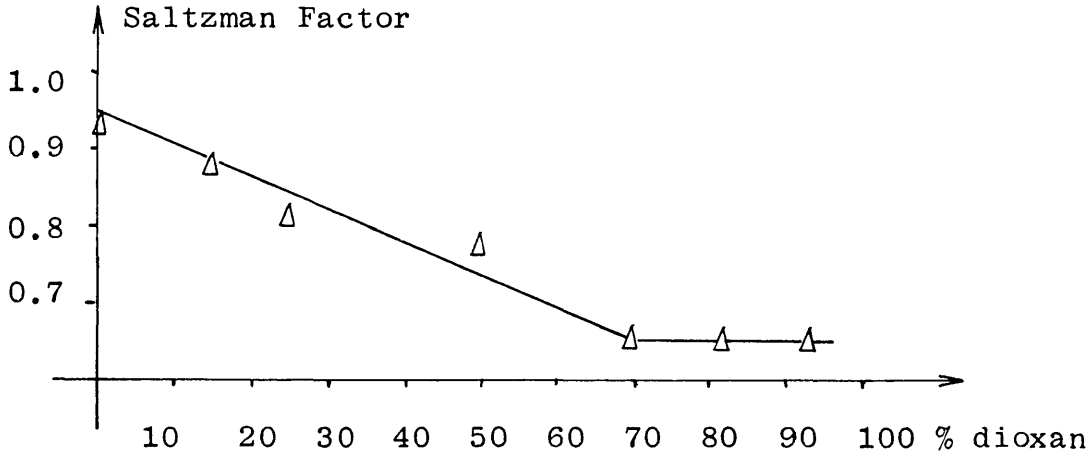
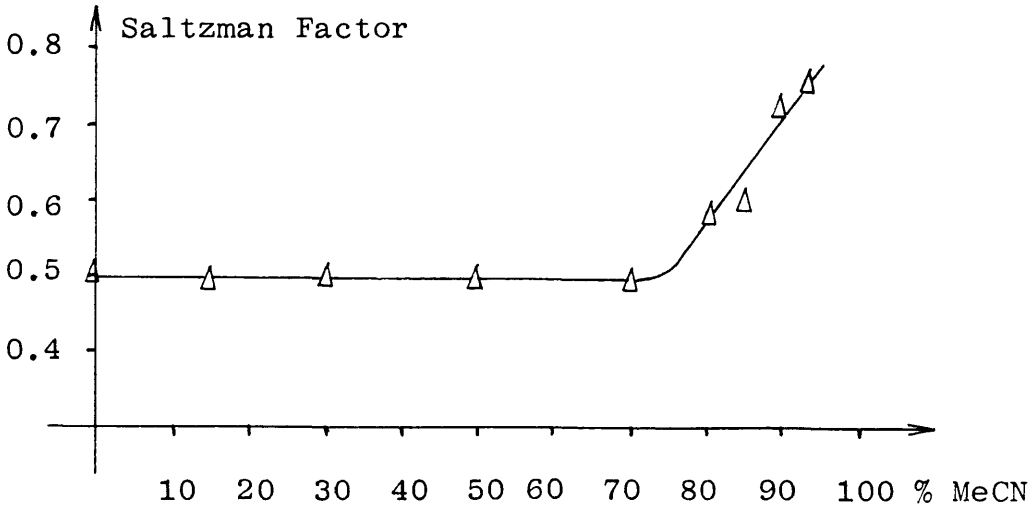
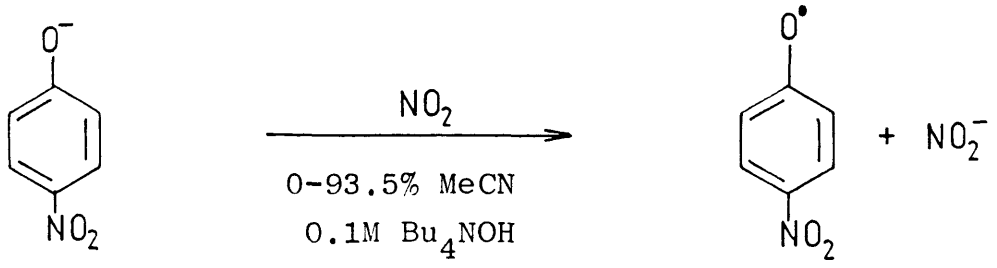


Figure 32. Solvent Effect for Reaction of 10^{-2}M 4-Nitrophenol with 900 ppm Gaseous NO_2 in the presence of 0.1M Bu_4NOH at 25°C





Scheme 31. Solvent Effect for Reaction of 4-Nitrophenol with Gaseous NO_2

4.5. Micelles

Another methodolgy to study the reaction of water insoluble compounds with NO_2 in aqueous solution utilises micelles[107-108]. The study of micellular solutions with relevance to this reaction is considered important in three respects;

i) the importance of micelles in biological systems

ii) their ability to solubilise organic compounds in aqueous systems,

iii) their possible influence on the reaction (i.e. an anionic surfactant may promote electron transfer from an anionic species to NO_2).

This work is directed towards solubilising biologically important compounds. Sodium lauryl sulphate (SDS), an anionic surfactant was used. The hydrolysis reaction was initially explored using 0.1M SDS, 0.1M NaOH and 900 ppm NO_2. It was found that a silicone polymer (Antifoam A concentrate, Sigma) had to be added to the reaction solution to prevent foaming. When the normal pre-dilution procedure was followed for hplc analysis of

0.1M NaOH samples the SDS precipitated and was removed by filtration (0.45μm) prior to injection. Studies showed equimolar quantities of nitrite and nitrate suggesting no interference by SDS or the silicone polymer in electron transfer reactions.

It was then shown that the solubility of 2,6-ditertbutylphenol is enhanced by the above micellular system over 0.1M NaOH solutions. This is illustrated in Table 24.

Conditions	[2,6-Ditertbutylphenol] (determined by uv)	$[NO_2^-]/[NO_3^-]$
0.1M SDS / 0.1M NaOH	2.5×10^{-3}M	9.8
0.1M NaOH	3.2×10^{-4}M	2.2

Table 24. Micellular Solubilisation and Reaction of 2,6-Ditertbutylphenol with 900 ppm Gaseous NO_2 in the presence of a Silicone Polymer at 25^{o}C

Studies in Chapter 5 relevant to biological systems utilise micelles.

4.6. Summary

Work reported in this chapter demonstrates the use of aqueous-organic solvent mixtures in demonstrating electron transfer reactions, solubilising new substrates and showing interesting solvent effects.

Solvent effects for the reaction of N,N-dimethylaniline and 4-nitrophenol with gaseous NO_2 support the electron transfer mechanism proposed (Section 2.4.2.).

Initial studies on the use of micelles to solubilise substrates are reported.

Chapter 5

Biological Substrates

5.1. Introduction

NO_2 is an environmental pollutant and its fate on inhalation is physiologically interesting. Little is known about the interaction of NO_2 with blood and cellular constituents (Section 1.3.3.). The reaction of NO_2 with serum was investigated.

5.2. The Reaction of Nitrogen Dioxide with Serum

The reaction of nitrogen dioxide with human serum was performed at a variety of nitrogen dioxide concentrations. The results are shown in Table 25. Serum is clearly seen to react by electron transfer with NO_2 to produce NO_2^-. The nitrite to nitrate ratio is seen to increase with decreasing NO_2 concentration (Section 2.4.4.). The final entry indicates that the electron transfer reaction capability is limited. This was investigated further.

$[NO_2]$ /ppm	Flow Rate /ml/min	Reaction Time /mins	Concentrations		$\frac{[NO_2^-]}{[NO_3^-]}$
			$[NO_2^-]$ /M	$[NO_3^-]$ /M	
50	80	60	3.15×10^{-3}	2.38×10^{-4}	13.2
100	80	30	7.40×10^{-3}	8.45×10^{-5}	8.8
200	69	15	9.84×10^{-4}	1.51×10^{-4}	6.5
900	80	4	1.21×10^{-3}	2.90×10^{-4}	4.2
1000	69	15	5.26×10^{-3}	2.86×10^{-3}	1.8

Table 25. The Reaction of Gaseous Nitrogen Dioxide with Serum at 25°C

5.2.1. Antioxidant Capability

The total electron transfer capability of human serum was investigated by the reaction of serum with 900 ppm NO_2 for 30 minutes, analysing for nitrite and nitrate at regular intervals.

Figure 33 shows the results of two of these studies and shows the serum to display approximately $2.5\times10^{-3}M$ of electron transfer capability ($=[NO_2^-]-[NO_3^-]$) under these conditions.

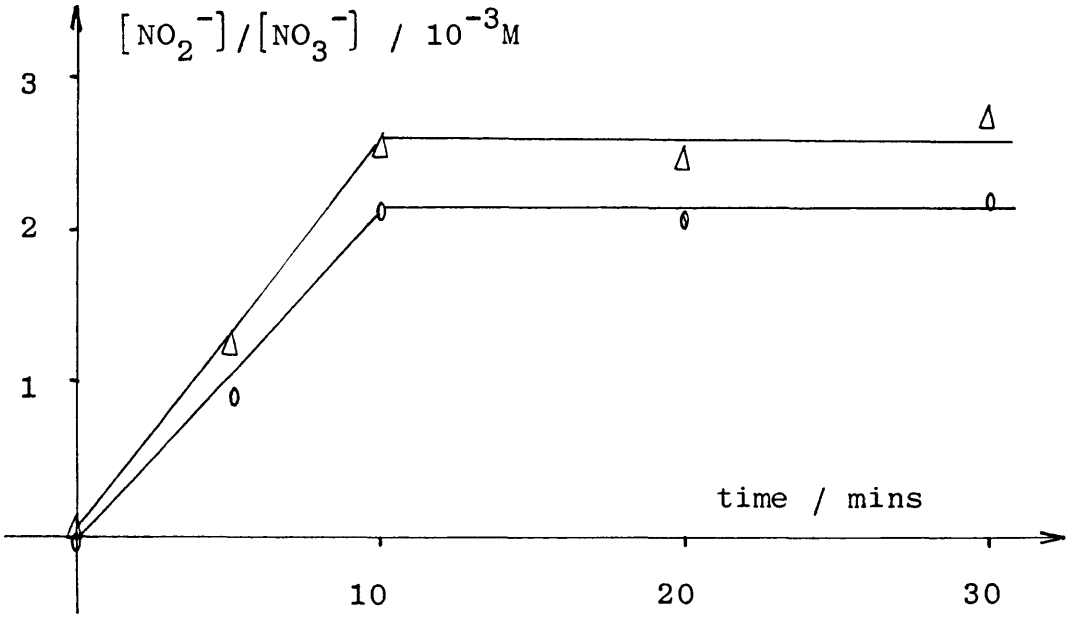


Figure 33. Electron Transfer Capability of Serum on Reaction with Gaseous NO_2 at 80 ml/min at 25°C

Ascorbic acid (vitamin C), ∝-tocopherol (vitamin E), glutathione and uric acid are known to be biological antioxidants[109]. All these compound were found to react by electron transfer with gaseous NO_2 at pH 13 (Appendix). Glutathione is not present in serum[109] so the reactivity and stiochiometry of the three remaining compounds were

examined in 0.05M tris(hydroxymethyl)aminomethane at pH 7.9 (the pH of serum) by reaction with 900 ppm NO_2. The results are presented in Table 26. The mean concentrations

Compound	Concentration	$[NO_2^-]/[NO_3^-]$	Stiochiometric Factor
∝-Tocopherol	5.0×10^{-5}M	1.06×10^{-4}M	2.1
Ascorbic Acid	2.0×10^{-4}M	4.71×10^{-4}M	2.4
Ascorbic Acid	5.0×10^{-5}M	1.14×10^{-4}M	2.3
Uric Acid	2.3×10^{-4}M	4.13×10^{-4}M	1.8

Table 26. Antioxidant Reactivities and Stiochiometric Factors at pH 7.9 and 25°C

of these compounds in serum are shown in Table 27[109] together with the concentrations of other compounds that are oxidised when determining glucose[109]. Creatine, creatinine and glucose do not react with gaseous NO_2 by electron transfer (Appendix).

Calculation of the expected electron transfer capability due to ascorbic acid, uric acid and ∝-tocopherol in serum can be made from their concentrations and stiochiometric factors. 7.0×10^{-4}M capability would be expected against 2.5×10^{-3}M observed, clearly other compounds are reacting in addition.

Ingold and co-workers[110] have recently measured the total peroxyl radical-trapping antioxidant capability of human blood plasma by controlled peroxidation. They found

Compound	Mean Concentration in Serum[109]
Ascorbic Acid	5.1×10^{-5}M
Uric Acid	2.9×10^{-4}M
∝-Tocopherol	2.5×10^{-5}M
Creatine	6.0×10^{-5}M
Creatinine	1.1×10^{-4}M
Glucose	5.0×10^{-3}M

Table 27. Antioxidant Concentration in Serum

that simple antioxidants still left 57-73% of the total antioxidant capability unaccounted for, although they determined the stiochiometric factors for uric acid and ascorbic acid to be only 0.8 and 0.7 respectively. By gel-filtration studies they suggest that plasma proteins account for the remaining reactivity.

The possibility remained that our serum contained higher than normal amounts of uric acid. The measured amount of uric acid in our serum was 2.3×10^{-4}M (RPIC,PRP-1 system), this possibility is therefore eliminated.

5.2.2. Serum Proteins

Serum proteins may react with gaseous NO_2 by electron transfer and this may reflect the reactivity of their constituent amino-acids. Table 28 details the serum protein fractions of adults[109] and Table 29 gives the

	Absolute Values (g/l serum) 30 subjects	
	Mean	Extreme Range
Total Protein	73	68 -82
Albumin	46.2	42.2-53.9
Globulin	26.8	22.5-31.0
α -Globulin	6.8	5.1- 9.8
α_1-Globulin	-	-
α_2-Globulin	-	-
β -Globulin	8.2	5.5-10.1
γ -Globulin	11.6	8.8-15.0
Fibrinogen	-	-

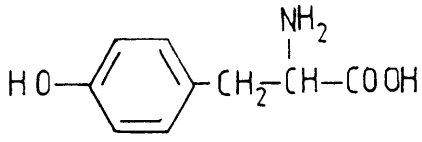
Table 28. Serum Protein Fractions of Adults[109]

amino-acid composition of albumin and γG-globulin[109]. The reactivity of all the available amino-acids was examined under standard conditions at pH 13 (Appendix).

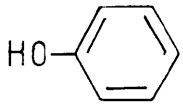
Four amino-acids are seen to be very reactive, they are L-histidine, L-proline, L-tyrosine and L-tryptophan. L-Cystine is much less reactive (L-cysteine is very reactive but not present in human serum proteins[109]). Figure 34 presents these amino-acids together with related compounds and pk_A data[111]. The dependence of the electron transfer reactivity of these amino-acids with pH for reaction with gaseous NO_2 is reported in Table 30.

	Albumin	γG-Globulin
Lysine	10.95	6.96
Histidine	3.17	2.28
Ammonia	0.94	1.46
Arginine	5.38	4.02
Aspartic Acid	9.05	7.69
Threonine	4.31	7.18
Serine	3.15	9.69
Glutamic Acid	15.85	11.26
Proline	3.65	6.05
Glycine	1.05	3.35
Alanine	6.67	3.18
Cystine ½	5.09	2.20
Valine	6.17	8.10
Methionine	1.08	0.85
Isoleucine	1.31	2.14
Leucine	10.30	7.21
Tyrosine	4.03	5.97
Phenylalanine	6.74	4.29
Tryptophan	0.13	3.83
Sum	99.02	97.71

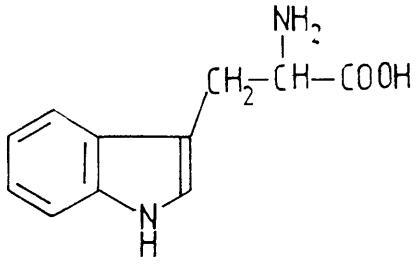
Table 29. Amino-Acid Composition of Human Serum Proteins (g/100g protein)[109]



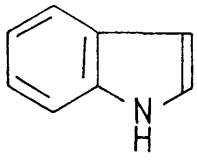
Tyrosine pk_A's=10.07,2.20,9.11



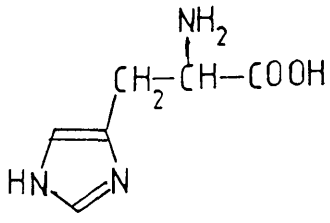
Phenol pk_A=9.89



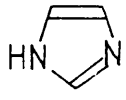
Tryptophan pk_A's=2.38,9.39



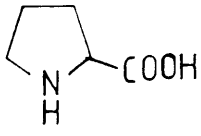
Indole pk_A=-2.4



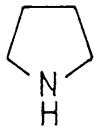
Histidine pk_A's=6.0,1.82,9.17



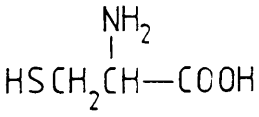
Imidazole pk_A's=7.05, 14.52



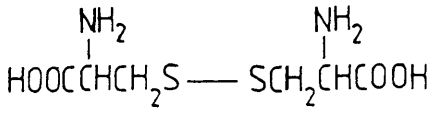
Proline pk_A's=1.99,10.60



Pyrrolidine pk_A=11.27



Cysteine pk_A's=10.78,1.71,8.33



Cystine pk_A's=1.65, 7.85

Figure 34. Selected Amino-Acids, Related Compounds and pk_A Data

Amino-Acid	Concentration	pH	$[NO_2^-]/[NO_3^-]$
L-Tryptophan	1.7×10^{-3}M	13.0	9.2
		9.0	9.0
		6.0	7.0
L-Histidine	1.7×10^{-3}M	13.0	15.8
		9.0	0.95
		6.0	0.95
L-Proline	1.0×10^{-3}M	13.0	1.8
		9.0	1.2
		6.0	1.0
L-Tyrosine	1.1×10^{-3}M	13.0	30
		9.1	20
		6.0	0.9

Table 30. Variation of Selected Amino-Acid Reactivities with pH on Reaction with 200 ppm Gaseous NO_2 at 25°C

The reactivities of L-tyrosine, L-proline and L-histidine diminish rapidly with decreasing pH, whereas L-tryptophan remains reactive down to pH 4.3 (Figure 27-Section 3.3.). A plausible explanation is that the reactivities of L-tyrosine, L-proline, L-histidine and L-tryptophan are due to the phenoxide ion, pyrrolidine neutral molecule, imidazole anion and indole neutral molecule, and that protonation of the three former species below their pk_A's of 10.07, 10.60 and 14.52 renders them unreactive. Indeed, phenol, pyrrolidine, imidazole and

indole are reactive species (Appendix) and N-methylimidazole is unreactive[112] at pH 13. L-Tryptophan is therefore the most reactive amino-acid electron transfer reductant of gaseous NO_2 at physiological pH.

5.2.3. Reactions in Serum

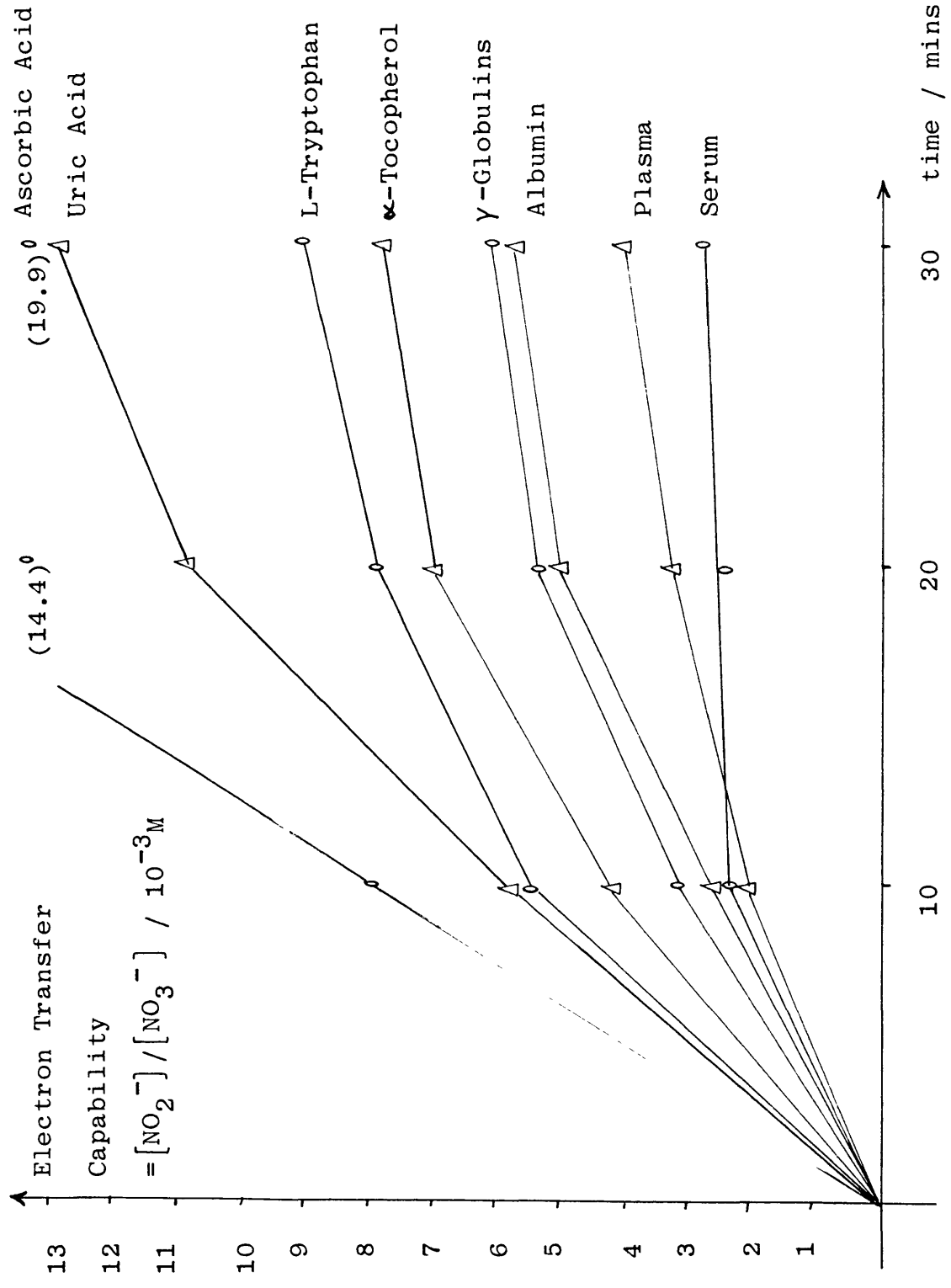
In Section 5.2.1. ascorbic acid, uric acid and α-tocopherol have been shown to be reactive reductants of gaseous NO_2 at pH 7.9, and in Section 5.2.2. serum proteins have been thought to be reactive due to their content of selected amino-acids of which L-tryptophan is expected to be the most important at physiological pH. The reactivity of all these compounds with gaseous NO_2 in serum was examined by looking for an increase in electron transfer capability due to the compound added. The results are presented in Figure 35.

Ascorbic acid, uric acid, α-tocopherol and L-tryptophan are all reactive reductants of gaseous NO_2 in serum, they increase the amount of electron transfer observed.

Addition of double the concentrations of albumin and globulin (added as γ-globulins) found normally in serum[109] are equally effective in increasing the amount of electron transfer observed. Table 31 shows the concentrations of protein tyrosine and tryptophan in the serum before and after these additions.

Comparison of Table 31 with Figure 35 suggests that both tyrosine and tryptophan are reactive in serum. However, double the concentration of albumin normally in serum is relatively unreactive in a micellular solution

Figure 35. Electron Transfer Capability of 10^{-2}M Substrates (except Albumin=92.4g/l and γ-Globulins=53.6g/l) with 900 ppm Gaseous NO_2 at 69ml/min in Serum at 25°C



Protein Added	[Tyrosine]	[Tryptophan]
None	1.74×10^{-2}M	4.60×10^{-3}M
Albumin	3.78×10^{-2}M	5.18×10^{-3}M
γ-Globulins	3.21×10^{-2}M	1.32×10^{-2}M

Table 31. Tyrosine and Tryptophan Concentrations in Serum before and after Proteins added

at pH 7.9, only 8.0×10^{-4}M of electron transfer capability is seen after 30 minutes under identical conditions to Figure 35, against an increase of ca. 3×10^{-3}M when added to serum. In the micellular solution 2.04×10^{-2}M and 5.80×10^{-4}M of tyrosine and tryptophan are present. This suggests tyrosine to be relatively unreactive. High concentrations of tyrosine are insoluble in neutral solutions as were all the tyrosine containing peptides obtained. Therefore this conclusion could not be confirmed.

Serum proteins albumin and globulin are therefore effective reductants of gaseous NO_2, but the reactivity of their constituent amino-acids tyrosine and tryptophan is not fully understood.

5.2.4. Synergistic Effect

A recent communication reports the reversibility of charge transfer between tryptophan and tyrosine[105]. It is shown that tryptophan radicals oxidise tyrosine over a wide range of pH, but that the reverse reaction proceeds in strongly acidic and alkaline solutions. These data are

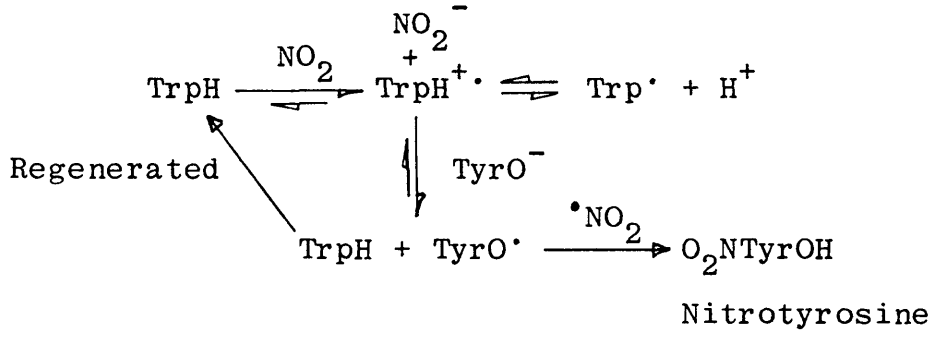
interpreted as showing the variation of the one electron reduction potentials of the corresponding radicals with pH. The data are better re-interpreted as showing that there is a reversible redox reaction between the tryptophan radical cation and the phenoxide ion of tyrosine (Equation 18).

$$TrpH^{+\cdot} + TyrO^{-} \rightleftharpoons TyrO^{\cdot} + TrpH \qquad ..(18)$$

It can be rationalised that between pH 4.3 and 10 the forward reaction dominates and any increase in $TyrO^{-}$ concentration with increasing pH is offset by decreasing $TrpH^{+\cdot}$ concentration. Above pH 10 (tyrosine phenoxide pk_A[111]) $TrpH^{+\cdot}$ continues to decrease in concentration but $[TyrO^{-}]$ does not increase, and below pH 4.3 (tryptophan radical cation pk_A[105]) $[TyrO^{-}]$ decreases but $[TrpH^{+\cdot}]$ does not increase. In both of these regions the above equilibrium is shifted to the left-hand side causing the reverse reaction to dominate as reported[105].

Further evidence for the forward reaction that is dominant at physiological pH is the emergence of a 420 nm peak in the reaction between 10^{-3}M L-tyrosine and 10^{-3}M L-tryptophan at pH 6.2 with 900 ppm gaseous NO_2 in aqueous solution. This is interpreted as the formation of nitrotyrosine as a product of the forward reaction in Equation 18. The yield was quantified as 5% at 900 ppm and 15% at 5000 ppm NO_2 using the same extinction coefficient as 2-nitro-4-methylphenol[113]. Neither substrate separately on reaction gave this absorbance. All reaction periods were 30 minutes.

It is concluded that there is a synergistic effect between tryptophan and tyrosine in which the tryptophan is regenerated. The overall reaction is illustrated in Scheme 32. All the observations of the reactions reported



Scheme 32. Synergistic Effect between Tyrosine and Tryptophan

above of tryptophan, tyrosine, albumin and γ-globulins reacting with gaseous NO_2 can be rationalised via this mechanism. It is suggested that this is the mechanism that accounts for the difference in the electron transfer capability observed in serum and that already accounted for by the reaction of the antioxidants; uric acid, ascorbic acid and ∝-tocopherol.

5.2.5. Plasma

Figure 35 shows that plasma displays a higher electron transfer capability than serum. The plasma and serum used were from the same source. This gives further support to the electron transfer reaction of proteins with gaseous NO_2 and suggests that fibrinogen[109] is a reactive protein.

5.2.6. Biological Effects of Gaseous Nitrogen Dioxide

From the above reactions of serum and plasma with gaseous NO_2 quantitative production of NO_2^- can be envisaged from inhaled gaseous NO_2 by electron transfer.

NO_2^- reacts with oxyhaemoglobin to give methaemoglobin (Equation 2 - Section 1.3.3.) which may be toxic by decreasing the oxygen transporting capability of blood[67]. Nitrite in blood is thus oxidised to nitrate with $t_{1/2}$ 10 mins[72]. This is sufficient time for its circulation around the body and the formation of possibly mutagenic diazopeptides[29] and nitrosopeptides[27] should acidic conditions be encountered. Diazopeptides may also be formed directly from N_2O_4[29].

This may account for the adverse physiological effects observed on gaseous NO_2 exposure[64].

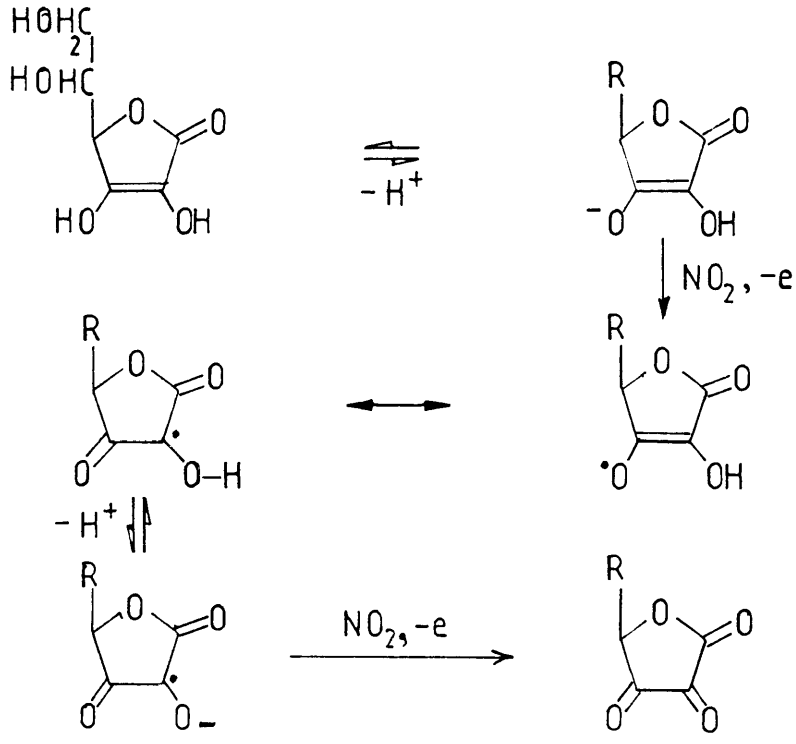
5.3. Product Analyses

The product analyses of the oxidation of the compounds that have been determined to be reactive towards gaseous NO_2 in serum (Section 5.2.) have been examined in detail in the literature except for L-tryptophan.

The oxidation reactions of phenols have been reviewed (Section 1.4.) and the products of the reaction of a number of phenols with gaseous NO_2 have been studied (Chapter 6).

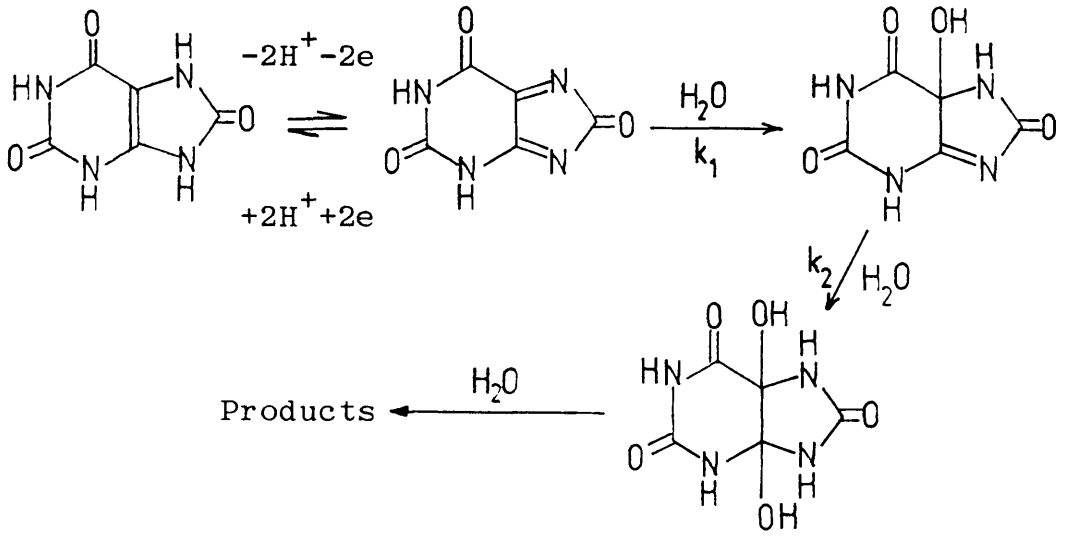
The oxidation product of ascorbic acid is dehydroascorbic acid. This can be considered to be formed by two consecutive one electron oxidations[109] as illustrated in Scheme 33 for the reaction with NO_2. This

supports the stiochiometric factor of two already measured (Section 5.2.1.).

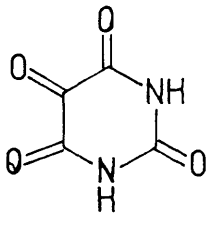


Scheme 33. Oxidation of Ascorbic Acid by NO_2 in Alkali

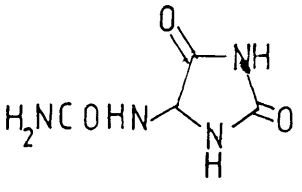
Marsh and Dryhurst[114] studied the enzymic and electrochemical oxidation of uric acid. From their results they propose the mechanism shown in Scheme 34. It is seen that two one electron oxidations are required in agreement with our stiochiometric factor (Section 5.2.1.). The ultimate products are alloxan (12), urea and CO_2 at low pH and allantoin (13), urea and CO_2 at pH 7-9[114]. Elegant earlier labelling studies have shown the oxidation to proceed via open chain intermediates[115].



Scheme 34. Oxidation of Uric Acid[114]



(12)



(13)

3-Methylindole and tryptophan give the corresponding oxindole on oxidation with hydrogen peroxide, but not in high yield[116]. 6-Bromo-3-methyloxindole and 5-bromo-3-methyloxindole are formed on oxidation of 3-methylindole with N-bromophthalimide and N-bromosuccinimide respectively[116].

5.3.1. 3-Methylindole - GC/MS Studies

The product analysis from the reaction of 10^{-2}M 3-methylindole (as a model for tryptophan) with 900 ppm gaseous NO_2 at pH 9.4 was studied by GC/MS on a BP1 capillary phase after acidification and ether extraction. Table 32 shows the intensities of the eight most abundant

Compound	m/z (Intensity)
P1	120(100%),135(58),92(39),163(M^+,36),65(24),43(15),148(14),77(11)
P2	147(M^+,100%),119(78),118(49),132(25),91(20),77(20),51(19),121(16)
P3	120(100%),135(56),163(M^+,48),92(31),65(26),43(24),148(18),77(13)
P4	245(100%),260(M^+,98),232(50),259(26),246(21),261(21),77(19),130(16)
P5	129(100%),159(62),176(M^+,57),130(34),77(24),103(19),128(16),102(16)
P6	176(M^+,100%),130(56),129(26),103(25),77(24),146(19),175(18),128(14),118(13)
P7	233(100%),276(M^+,98),261(66),232(34),247(33),102(32),77(30),130(29)
3-Methyloxindole[117]	147(M^+,100%),119(56),118(52),132(28),117(16),104(16),146(8)

Table 32. Mass Spectral Data - Eight Most Abundant Peaks of GC/MS Products and 3-Methyloxindole (Product P1 least retained)

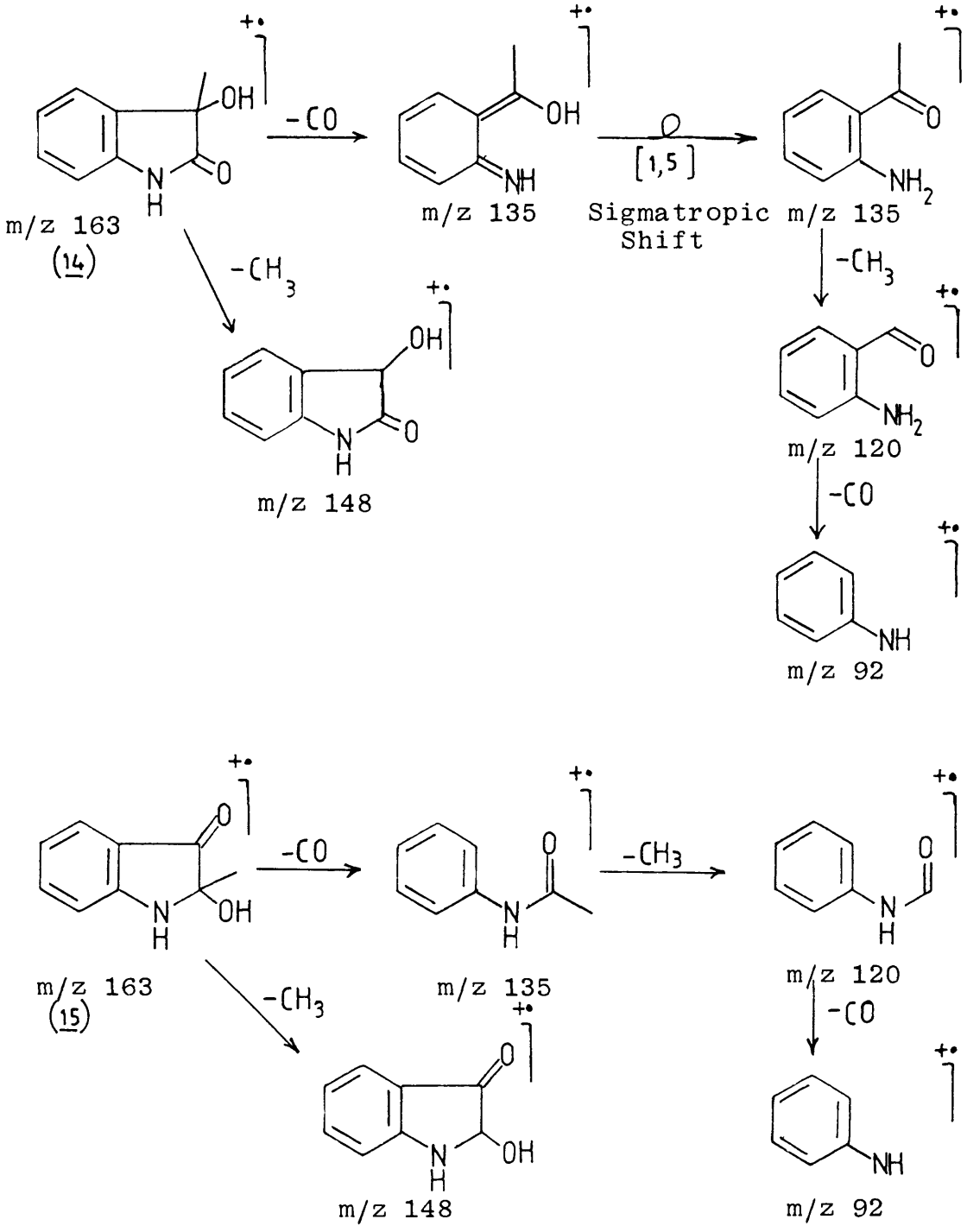
ions of the seven products (P1-P7) observed, in their elution order, together with the corresponding data for 3-methyloxindole[117]. Possible product structures and their mechanism of formation are subsequently discussed.

By comparison of the mass spectral data it is proposed that product P2 is 3-methyloxindole. The major fragmentation observed is CO loss (M-28).

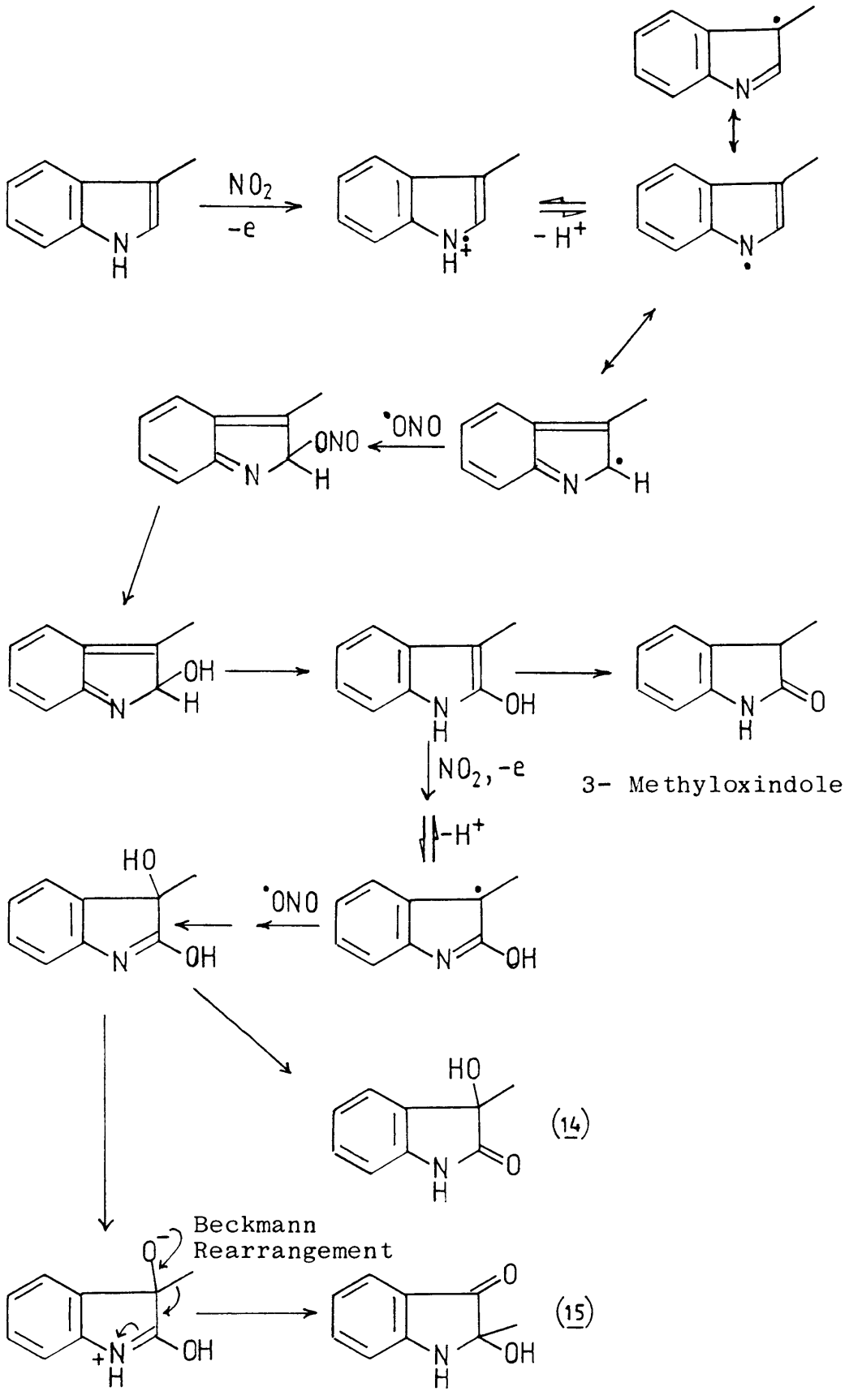
The two most abundant products are P1 and P3. The mass spectra of both products are similar and unusual compared to the other products in that they show a m/z 92 fragment, an anilino species. The proposed isomeric structures for P1 and P3 together with their fragmentation routes are shown in Scheme 35. P1 and P3 are not aromatic hydroxy compounds as although CO is a common loss from these compounds[118] the anilino species would not be observed.

Scheme 36 shows the proposed mechanism of formation of products P1, P3 and 3-methyloxindole. An interesting methyl migration (Beckmann Rearrangement) is seen to produce (15). The key intermediate in this scheme is the 3-methylindole radical, further supporting our electron transfer mechanism. Product (15) could also arise from a 2-methylindole impurity in the starting material without the need for a methyl migration. The integrity of the starting material was checked and found to contain $<$ 0.5% 2-methylindole by GC, making this possibility unlikely.

Product P6 is proposed to be an aromatic nitro derivative (16) and shows distinctive mass spectral features[118]. A strong molecular ion is observed and the two main fragmentations involve the nitro group. Loss of

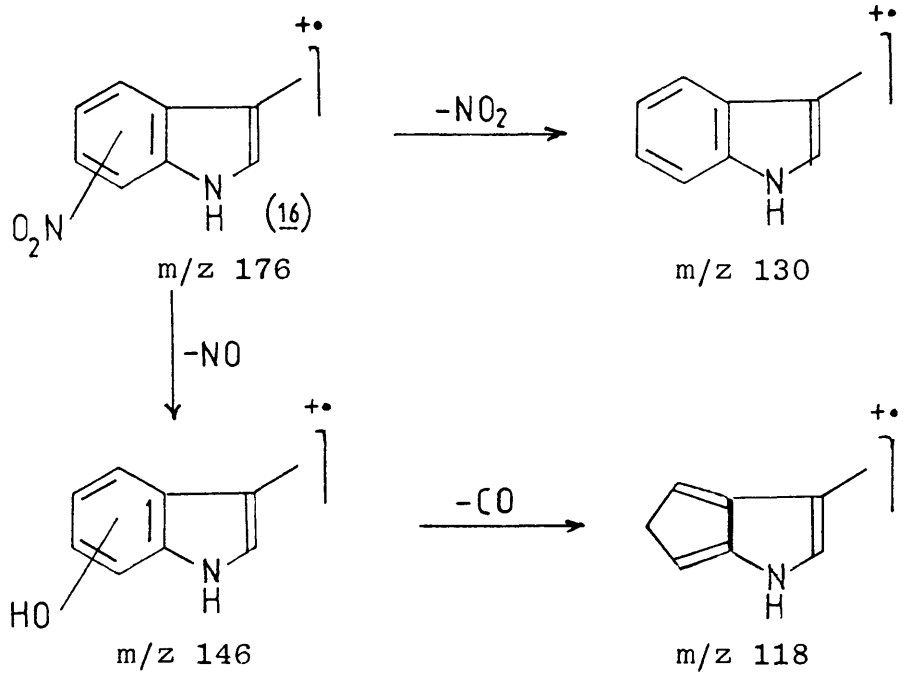


Scheme 35. Proposed Structures and Mass Spectral Fragmentation for P1 and P3

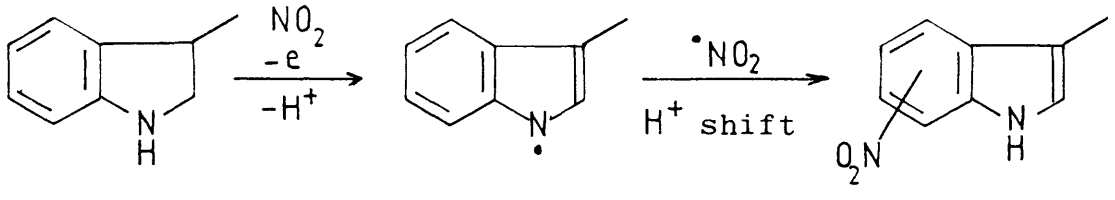


Scheme 36. Mechanism of Formation of Products P1, P3 and 3-Methyloxindole

NO_2 (M-46) is prominant together with loss of NO (M-30) and the subsequent loss of CO (M-28) from the phenol formed as illustrated in Scheme 37. The nitro derivative is easily formed by radical coupling of the 3-methylindole radical and NO_2 as illustrated in Scheme 38.

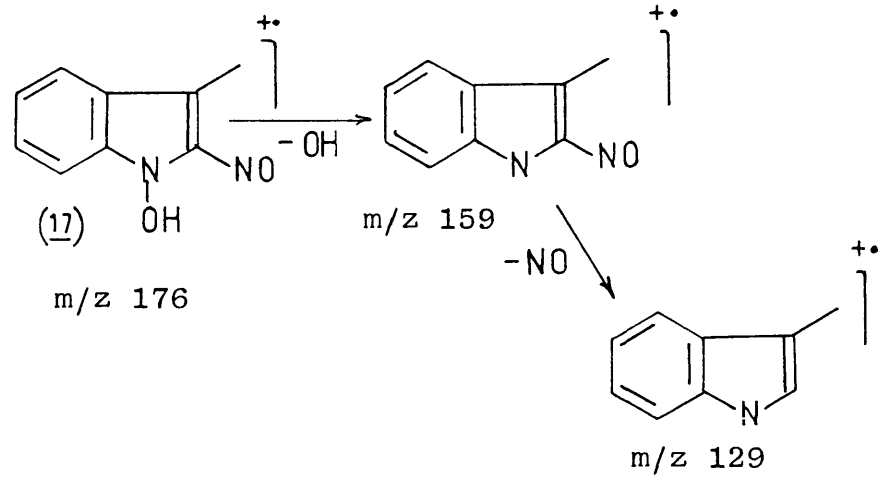


Scheme 37. Fragmentation of the Nitroindole Product

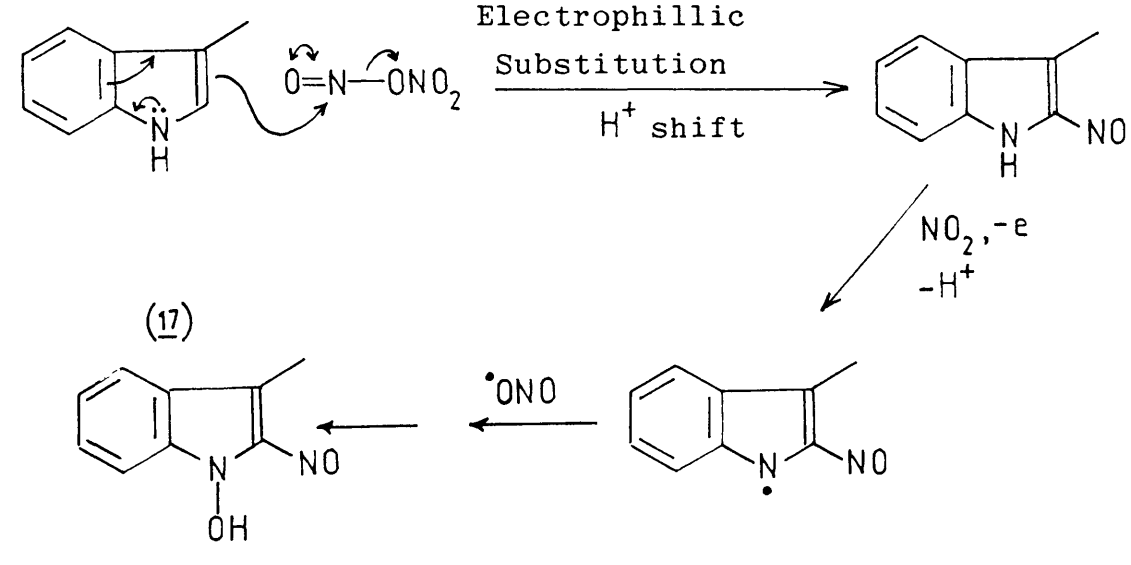


Scheme 38. Formation of the Nitroindole Product

Product P5 may be an ∝-nitroso-N-hydroxy compound (17) whose main fragmentation can be rationalised by Scheme 39. This product may be formed via an electrophillic substitution pathway and subsequent oxidation of the indole formed (Scheme 40). Alternative structures for this product have been considered, however, an N-hydroxy compound is the only isomer that will give an M-17 fragmentation. The nitroso group may be on the benzene ring.

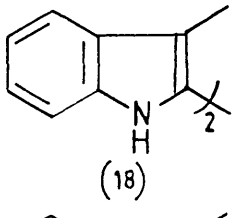


Scheme 39. Structure and Fragmentation of Product P5

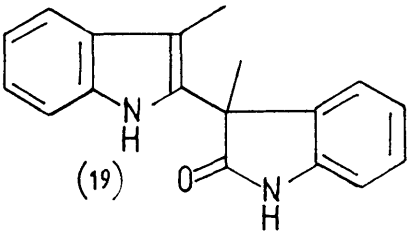


Scheme 40. Formation of Product P5

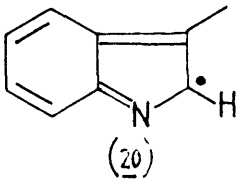
The remaining products P4 and P7 are thought to be the dimeric species (18) and (19) formed by radical coupling of (20), and (20) and (21) respectively. The fragmentations observed are consistent with these structures.



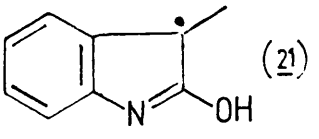
(18)



(19)

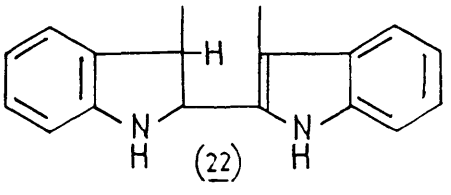


(20)



(21)

Indoles are known to dimerise and trimerise in acid[116] and it was thought that these products may be a result of the acidic work-up. The mechanism of acidic dimerisation is electrophillic substitution initiated by 3-protonation, but the dimer formed in acid from 3-methylindole (22) results from electrophillic substitution at the 2-position and has a higher molecular weight than the product P4 observed.



(22) M.W.=262

Table 33 summarises the proposed identities of the products formed in the reaction between 3-methylindole and gaseous nitrogen dioxide, deduced from the GC/MS data. Some novel products are seen, all resulting from oxidation by NO_2 in addition to the previously observed oxidation product 3-methyloxindole. This therefore presents an interesting area for future studies as elevated levels of

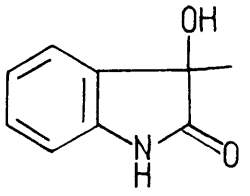
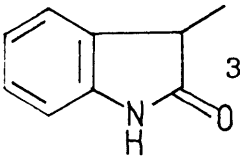
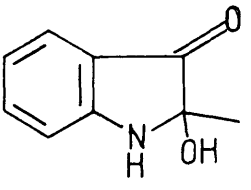
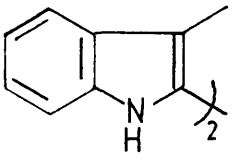
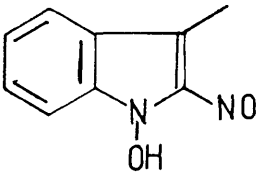
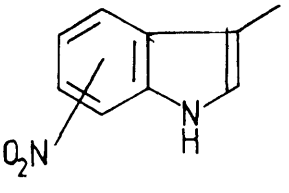
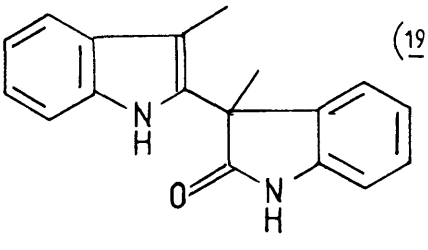
Product	Proposed Structure
P1	 (or P3) (14)
P2	 3-Methyloxindole
P3	 (or P1) (15)
P4	 (18)
P5	 (17)
P6	 (16)
P7	 (19)

Table 33. Proposed Product Structures

methylindoles in saliva are known to result from cigarette smoking[119].

The above oxidation products are consistant with 3-methylindole exhibiting an excess of NO_2^- on reaction with gaseous NO_2 (Appendix).

5.4. Summary

The reaction of nitrogen dioxide with serum is examined. Nitrogen dioxide reacts by electron transfer but only a proportion of the reactivity observed can be accounted for by the reaction of the simple antioxidants; uric acid, ascorbic acid and ∝-tocopherol.

Serum proteins are reactive towards NO_2 by electron transfer. Their reactivity results from their amino-acid content. L-Tyrosine, L-tryptophan, L-histidine and L-proline are reactive amino-acids at pH 13 but only L-tryptophan is reactive at physiological pH. However, both tryptophan and tyrosine are important in the reactivity of serum proteins. A synergistic effect operates where the tyrosine phenolate regenerates tryptophan by an electron transfer reaction with the tryptophan radical cation. Serum proteins are therefore thought to account for the remainder of the NO_2 reactivity with serum.

The product analysis of the reaction of 3-methylindole with gaseous NO_2 has been studied by GC/MS and the product structures assigned based on their mass spectral fragmentation. Interesting oxidation products derived from the 3-methylindole radical are deduced which are consistent therefore with gaseous NO_2 acting as a one electron oxidant.

Chapter 6

Phenol Oxidations

6.1. Introduction

Phenol oxidations have been the subject of many reviews. There have been a wide variety of oxidising agents used, substrates studied and products observed (Section 1.4.). We have seen in Chapter 5 that tyrosine plays an important role in the fate of inhaled nitrogen dioxide. The product analyses of the reactions of a number of phenols with gaseous NO_2 in aqueous solution have been studied.

6.2. The Reaction of Gaseous Nitrogen Dioxide with Phenol

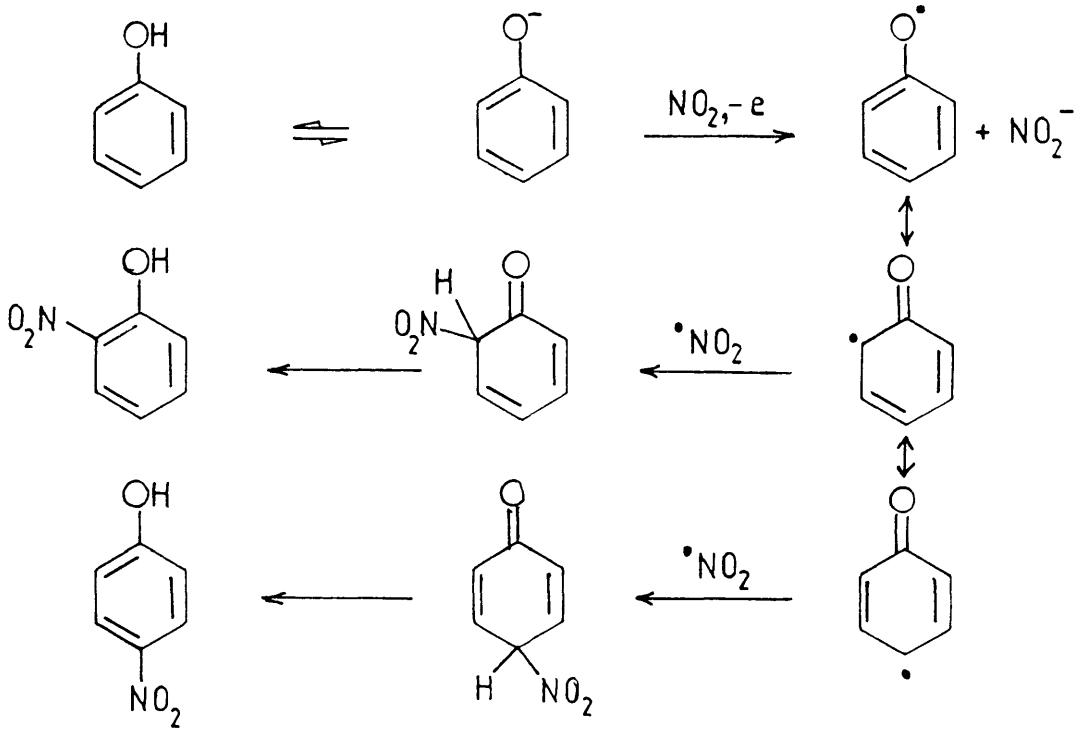
In our initial studies on the reaction of gaseous NO_2 with organic substrates phenol was observed to be very reactive (Section 2.4.1.). Its pH profile (Section 3.2.1.) shows that only the phenoxide ion is reactive. The product analysis of the reaction between phenol and gaseous NO_2 at pH 13 has been studied. Initial GC studies showed only 2- and 4-nitrophenol as products, there was no trace of 3-nitrophenol or 4-nitrosophenol. Table 34 presents the results of later hplc analyses at a range of [phenol] and $[NO_2]$.

2- and 4-Nitrophenol are therefore established as the major products of the reaction at high $[NO_2]$. It is proposed that they are formed by direct coupling of the phenoxy radical with NO_2 as illustrated in Scheme 41.

[Phenol] /M	$[NO_2]$ /ppm	Yields / % consumed (based on phenol)		Total /%
		2-Nitrophenol	4-Nitrophenol	
10^{-2}	5000	37	37	74
	1650	27	33	60
	900	18.9	10.5	29.4
	500	15.3	8.2	23.5
	200	10.8	5.4	16.2
10^{-3}	900	44.7	30.0	74.7
	500	40.3	28.5	68.8
	200	34.8	24.2	59.0
10^{-4}	900	51.2	33.8	85.0
	500	51.2	31.4	82.6
	200	51.2	27.1	78.8
	20	30.3	19.2	49.5
	2	16.3	8.2	24.5

Table 34. Nitrophenol Yields from Phenol Oxidation by Gaseous NO_2 in 0.1M NaOH at $25^{o}C$

Note:- Equimolar quantity of NO_2 passed in all the above reactions.



Scheme 41. Mechanism of Nitrophenol Formation

This mechanism is supported by a recent paper by Ridd[35]. He details kinetic evidence to show that the nitrous acid catalysed nitration of p-nitrophenol in aqueous nitric acid proceeds *via* the p-nitrophenoxy radical.

Table 34 clearly indicates that the nitrophenol yields increase with increasing $[NO_2]$ and decreasing [phenol]. These effects are easily explained by Scheme 41, an increasing $[NO_2]$ increases the efficiency of the radical trapping of the phenoxy radical by NO_2 and a decreasing [phenol] has the same effect by reducing the possibility of coupling reactions between the phenoxy radicals themselves (presumeably the product balance is not monomeric in phenol (Section 6.5.)).

From the above mechanism a 2:1 ratio of 2- to 4-nitrophenol might be expected. Both nitrophenol isomers are far less reactive than phenol but 2-nitrophenol shows some electron transfer reactivity with gaseous NO_2 (Appendix) therefore the observed ratio is lower than expected, although no dinitrophenol products were observed by GC studies.

Table 35 presents the nitrophenol yields of the reaction of 10^{-2}M phenol, 2-chlorophenol and 2-(2'-chlorophenoxy)phenol with 1650 ppm gaseous NO_2. The products of the reaction of 2-chlorophenol were identified by GC/MS, synthesised[18,120] and quantified by GC studies. The products from 2-(2'-chlorophenoxy)phenol were determined by hplc studies using synthesised[18] authentics. Nitrophenols are seen to be the major products of these reactions.

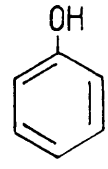
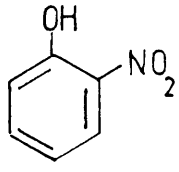
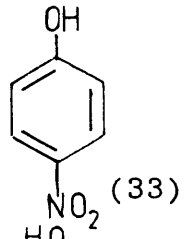
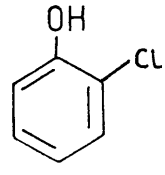
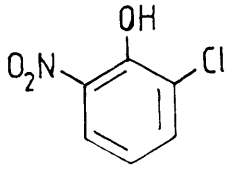
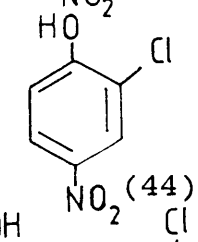
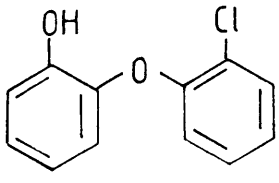
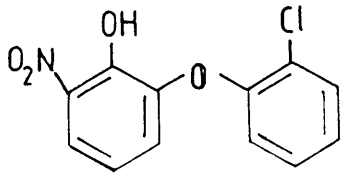
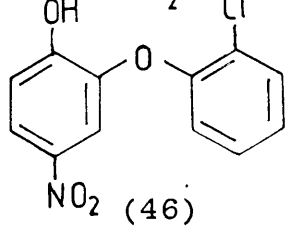
Substrate	Product (% Yield)		Total
	 (27)	 (33)	60%
	 (35)	 (44)	79%
	 (35)	 (46)	81%

Table 35. Nitrophenol Yields from Reaction of 10^{-2}M Substrate with 1650 ppm Gaseous NO_2 in 0.1M NaOH at 25°C

6.3. The Reaction of Gaseous Nitrogen Dioxide with 2,4,6-Trimethylphenol

The product analysis of the reaction between 1650 ppm gaseous NO_2 and 10^{-2}M 2,4,6-trimethylphenol was studied. A number of peaks were seen by GC examination of an ether extraction after sample acidification of the 0.1M NaOH reaction solution. Six products in addition to the starting material were observed by GC/MS studies. Table 36 details the mass spectra observed together with the product structures in order of increasing retention time.

2,6-Dimethylbenzoquinone was identified by having identical mass spectral behaviour to the literature[117]. The corresponding hydroquinone is thought to form in the mass spectrometer, otherwise its retention time would be much longer.

2-Hydroxy-2,4,6-trimethyl-3,5-cyclohexadien-1-one (23) and 4-hydroxy-2,4,6-trimethyl-2,5-cyclohexadien-1-one (24) were shown to be products after they were synthesised by the periodic acid oxidation of 2,4,6-trimethylphenol[121] (Scheme 42).

The major products observed by GC/MS were 3,5-dimethyl-4-hydroxybenzaldehyde which was synthesised, characterised and isolated from the oxidation of 2,4,6-trimethylphenol with iodine[122] (Scheme 43), and 2,6-dimethyl-4-nitrophenol obtained commercially.

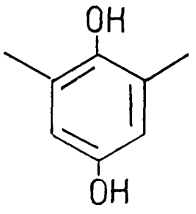
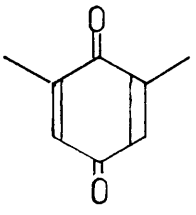
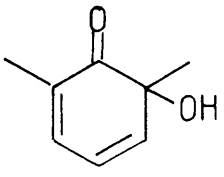
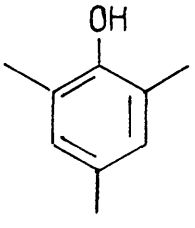
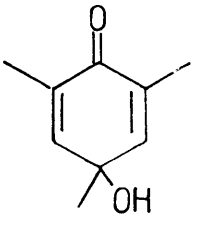
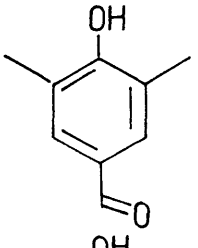
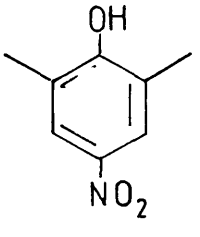
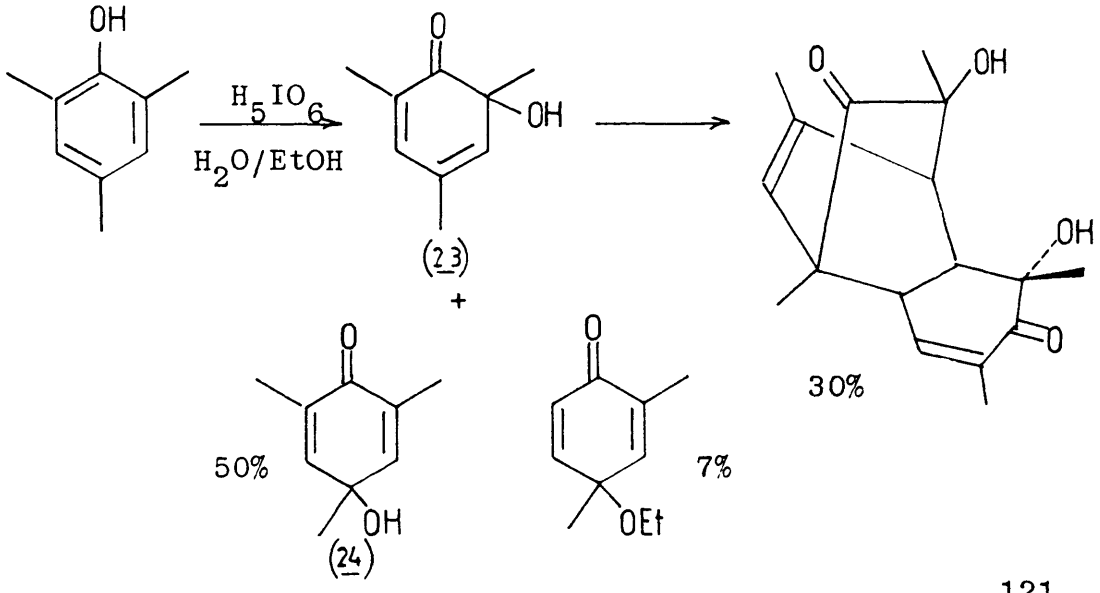
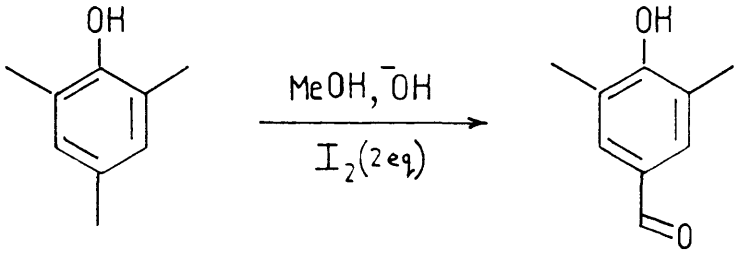
Product Structure	m/z (Intensity)
	123(100%),138(M^+,44),28(32),43(25), 41(16),109(14),39(14),124(13)
	68(100%),136(M^+,96),39(77),40(46), 108(40),79(40),96(28),38(19)
	43(100%),109(84),110(79),152(M^+,58), 28(36),95(25),39(23),81(20)
	136(M^+,100%),121(92),135(33),91(17), 39(15),77(13),137(10),41(9)
	137(100%),152(M^+,57),109(49),43(44), 39(25),41(19),81(17),91(16)
	149(100%),150(M^+,68),77(25),91(18), 121(16),51(11),65(9),53(9)
	167(M^+,100%),28(66),77(39),91(28), 39(14),32(13),121(12),137(12)

Table 36. Products seen by GC/MS from Reaction of 10^{-2}M 2,4,6-Trimethylphenol and 1650 ppm Gaseous NO_2

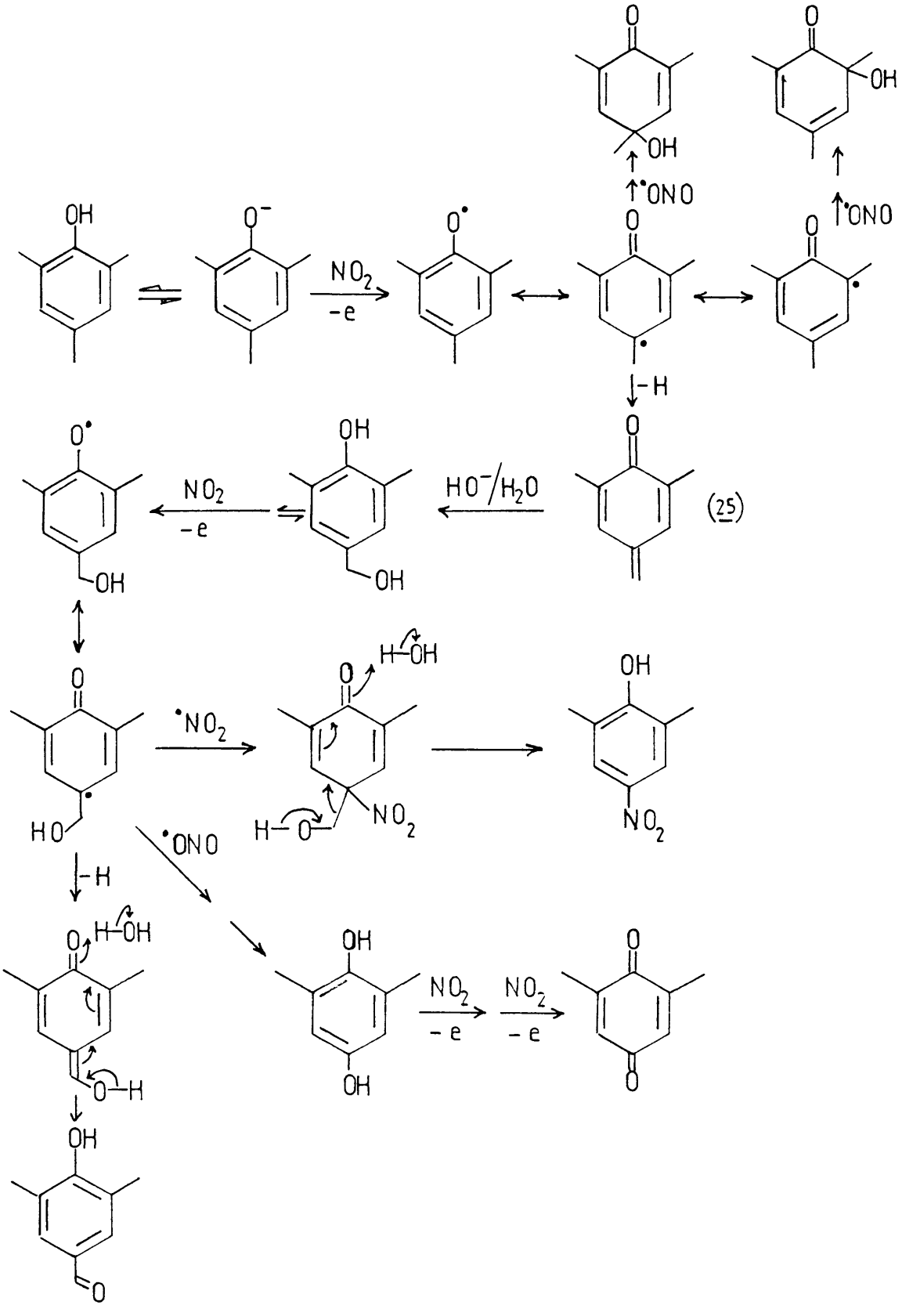


Scheme 42. Literature Synthesis of Cyclohexadieneones[121]



Scheme 43. The Preparation of 3,5-Dimethyl-4-hydroxy-benzaldehyde[122]

Formation of all these products can be rationalised by the initial product of oxidation being the 2,4,6-trimethylphenoxy radical (Scheme 44). Noteable key parts of this scheme are the formation of quinone methide intermediates, ipso attack and the reaction of NO_2 as an oxygen or nitrogen centred radical.



Scheme 44. Formation of Products from 2,4,6-Trimethylphenol and Gaseous NO_2

It was established that the 2,4,6-trimethylphenol did not have any observable 2,6-dimethylphenol impurity by capillary GC and GC/MS, as this would invalidate parts of the mechanism proposed.

Efforts were then made to quantify the yields. In 0.1M NaOH with 10^{-2}M substrate and 1650 ppm gaseous NO_2 the yields of the two major observed GC/MS products, 2,6-dimethyl-4-nitrophenol and 3,5-dimethyl-4-hydroxybenzaldehyde, were established by capillary GC as being 3% and 1% based on consumed starting material respectively. The yield of the former product was found to increase to 7.5% in 1M NaOH presumeably reflecting the increased trapping of the first quinone methide intermediate (25) with greater hydroxide ion concentration. The products seen and characterised by GC/MS are therefore not the major products of this reaction (Section 6.5.).

6.4. The Reaction of Gaseous Nitrogen Dioxide with 2,4,6-Trichlorophenol

From the ether extraction after acidification of the reaction between 1650 ppm gaseous NO_2 and 10^{-2}M 2,4,6-trichlorophenol trace amounts of products giving GC/MS data consistant with them being 2,6-dichloro-4-nitrophenol and 2,6-dichlorohydrobenzoquinone were seen. 92% of the starting material was consumed yet no major products were isolated (Section 6.5.).

6.4.1. Halide Displacement

Several reaction solutions of halophenol compounds in 0.1M NaOH after reaction with gaseous NO_2 were tested for halide displacement by acidification with nitric acid and addition of silver nitrate solution. All the precipitates disappeared on addition of ammonia solution. The results are presented in Table 37.

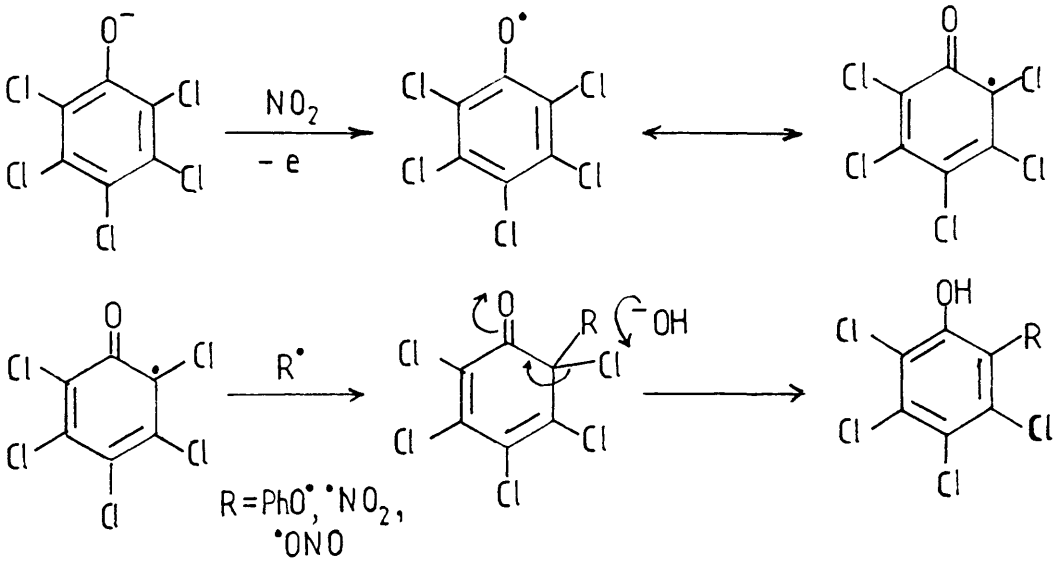
Substrate	Precipitate
4-chlorophenol	No
2,6-dichlorophenol	No
2-(2'-chlorophenoxy)phenol	No
2,4,6-trichlorophenol	White(AgCl)
pentachlorophenol	White(AgCl)
2,4,6-triiodophenol	Yellow(AgI)

Table 37. Qualitative Test for Halide by $AgNO_3$ addition after acidification of 10^{-2}M Reactions with 900 ppm Gaseous NO_2 in 0.1M NaOH at 25°C

Only halophenols where the 2-, 4- and 6- positions are all substituted show halide displacement. Simple radical couplings are therefore more favourable and O—O coupling does not lead to stable products.

Chloride was subsequently confirmed and quantified by Dionex Ion Chromatography for pentachlorophenol. In a

10^{-2}M solution 1.2×10^{-2}M electron transfer was determined and 1.6×10^{-2}M chloride was seen. Scheme 45 rationalises these observations. Formation of chloride via NO_2Cl is eliminated as only 1.9×10^{-3}M nitrate was formed. From this Scheme 4.4×10^{-2}M phenol oxidation would be expected from the 10^{-2}M solution. This suggests multiple reactions and hence polymer formation (Section 6.5.).



$$HO^- + Cl^+ \rightleftharpoons HOCl \rightleftharpoons H^+ + {}^-OCl$$

$$ClO^- + H_2O + 2PhO^- \longrightarrow Cl^- + 2HO^- + 2PhO^\bullet$$

Scheme 45. Mechanism of Chloride Formation from Pentachlorophenol and Gaseous NO_2

6.5. Polymer Formation

6.5.1. Crystallisation of Dimers and Trimers

Dimers and trimers have previously been crystallised from phenol oxidation reactions[77,81,123-124]. All the procedures used were repeated on neutralised freeze-dried reaction solutions of 10^{-2}M 2,4,6-trichlorophenol and 1650 ppm gaseous NO_2 in 0.1M NaOH (Section 6.4.) without success.

6.5.2. Gel-Permeation Chromatography (GPC) Studies

Figure 36 shows a GPC trace of the reaction between 50 ppm gaseous NO_2 and 10^{-2}M 2,4,6-trichlorophenol in 0.1M NaOH after neutralisation, freeze-drying and dissolution in THF. An approximate calibration based on polystyrene standards is shown. Clearly polymers are formed. Similar traces with similar molecular weight distributions have been observed for phenol, 2-chlorophenol, 2-(2'-chlorophenoxy)phenol, 2,4,6-trimethylphenol, 2,4,6-trichlorophenol, 2,4,6-triiodophenol and pentachlorophenol reactions with gaseous NO_2. The variation in molecular weight distribution with [phenol], $[NO_2]$ and pH has been studied. Evidence for a lower molecular weight distribution is only seen when a large excess of starting material is present, implying the polymers to be more reactive than the starting material. Fractions have been collected by semi-preparative use of the GPC system. Each fraction gave a positive ferric chloride test for phenol but no mass spectral information due to the low amount of material present.

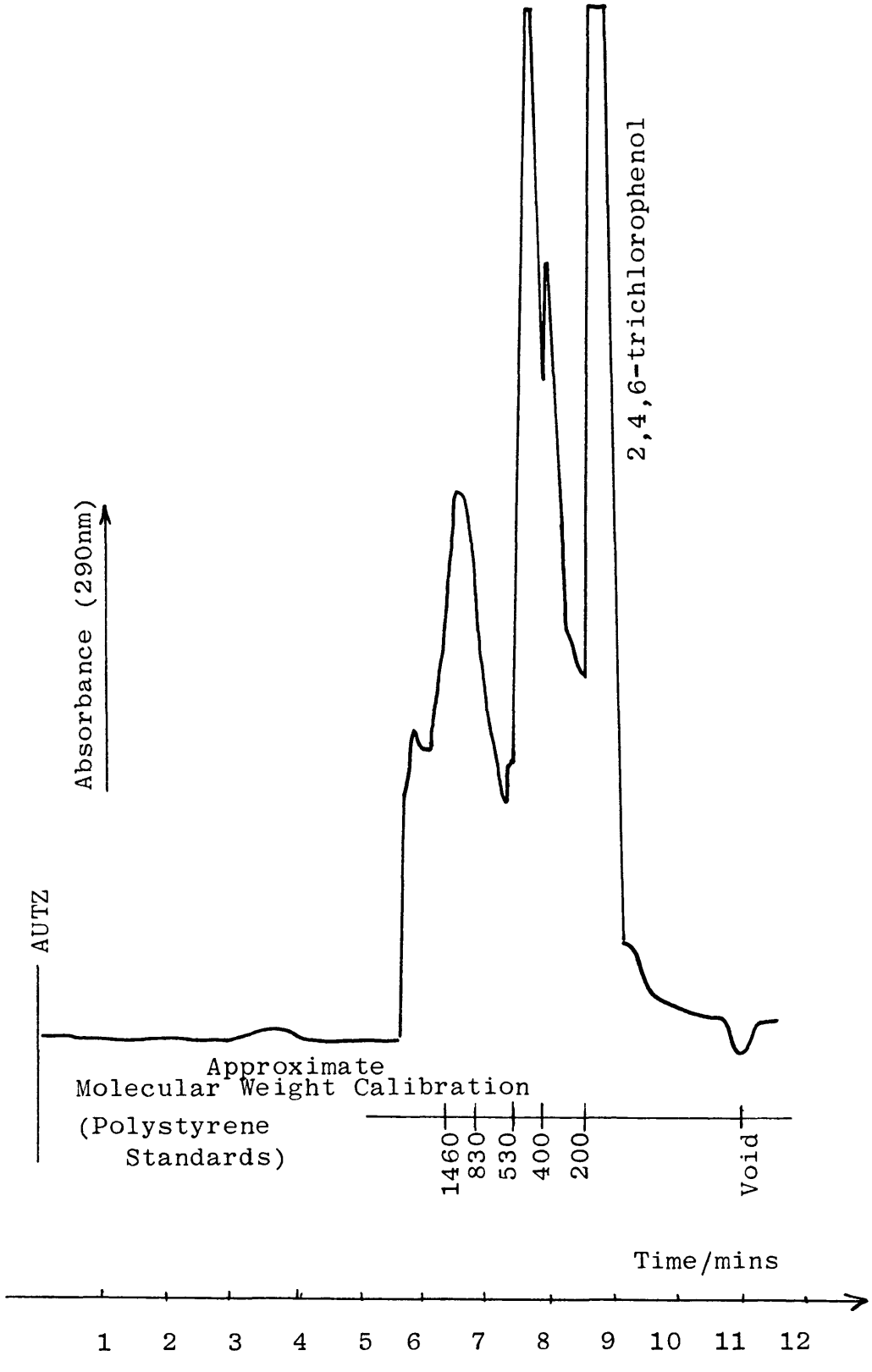


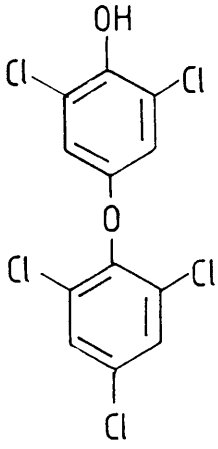
Figure 36. Typical GPC Chromatogram (of a Reaction Mixture of 10^{-2}M 2,4,6-Trichlorophenol and 50 ppm Gaseous NO_2)

It is thought that polymer formation accounts for the material imbalance observed on oxidation of phenol (Section 6.2.) and that it is especially pronounced for 2,4,6-trisubstituted phenols where simple radical coupling leading the nitration products is not possible (Sections 6.3.-6.4.).

6.5.2. Observation of Oligomers

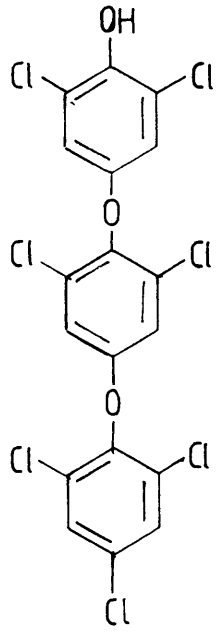
Further experiments were undertaken to elucidate the structure of the oligomeric/polymeric products indicated by GPC studies (Section 6.5.1.). In these reactions a large excess of starting material was present in order to minimise reactions of products (Section 6.5.1.). 0.1M Solutions of substrate in 0.1M NaOH were reacted with 900 ppm gaseous NO_2 at a flow rate of 140 ml/min for 5 hours. The solutions were then acidified and extracted into ether. 2,4,6-Trichlorophenol was initially studied and molecular ions corresponding to dimeric (26), trimeric (27), and tetrameric species (28) were seen. Subsequent GC/MS on a BP 1 capillary column gave some separation of these species. GC/MS analysis of a 2,4,6-trimethylphenol reaction mixture showed the presence of two dimeric species (29) and (30).

Observation of these oligomers lends support to the conclusions drawn about polymer formation as a result of the GPC studies (Section 6.5.1.) and the experimental procedure used may provide a route for quantitative studies.



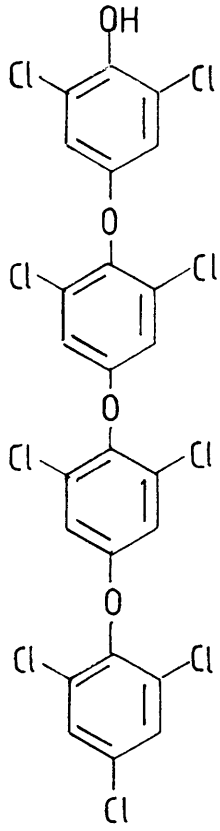
(26)

m/z 356 etc.



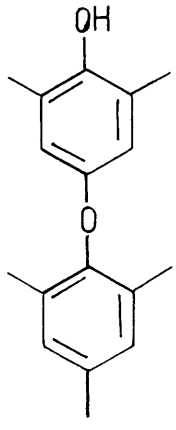
(27)

m/z 516 etc.



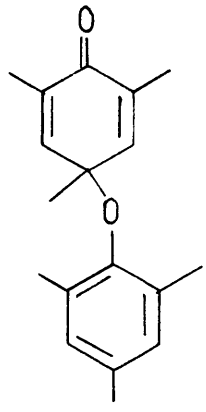
(28)

m/z 676 etc.



(29)

m/z 270

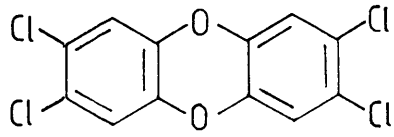


(30)

m/z 256

6.6. Dioxin Formation

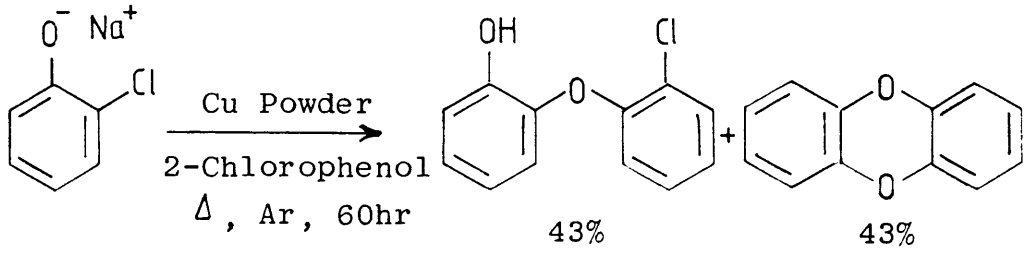
Considerable interest continues in the formation of chlorodioxins since the accident in Seveso in 1976 and subsequent environmental damage due to the tetrachlorodioxin (31) produced.



(31)

6.6.1. Synthesis of 2-(2'-Chlorophenoxy)phenol

2-(2'-Chlorophenoxy)phenol, a possible dioxin precursor (Section 6.6.2.) was synthesised by the Ullmann Ether Synthesis[125] (Scheme 46). The proposed mechanisms of this reaction involve a Cu(I) species initiating a template effect[126], or activation of the aromatic ring towards nucleophillic aromatic substitution[127].



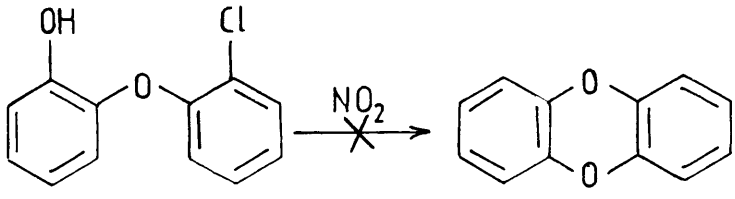
Scheme 46. Synthesis of 2-(2'-Chlorophenoxy)phenol

6.6.2. The Reaction of 2-(2'-Chlorophenoxy)phenol with Gaseous NO_2

This reaction has been shown to produce excellent yields of nitrophenols (Section 6.2.) but no halide

displacement (Section 6.4.1.).

The reaction of 900 ppm gaseous NO_2 with 10^{-2}M 2-(2'-chlorophenoxy)phenol was examined by GC analysis (Section 8.2.2.2.) in water, ethanol, THF and benzene, in acidic,neutral and alkaline conditions in each solvent. No evidence of intramolecular cyclisation to dibenzo[1,4]-dioxin (Equation 19) was found. The detection limit for the product was 0.4%. This leads to the suggestion that this cyclisation cannot be achieved via a radical pathway for this compound.



..(19)

However, free radical aromatic substitution has literature precedence in the Pschorr Cyclisation[128] and the homolytic substitution reactions of perfluoroaromatic compounds[129], therefore, bromo or iodo phenols may be better substrates for producing dioxins (Equation 19).

6.7. Summary

The oxidation of phenoxide by gaseous NO_2 is a very facile process. For simple unsubstituted phenols 2- and 4- nitration occurs via radical coupling in high yield. When this is not possible due to 2,4,6-substitution low yields of interesting oxidised monomeric products are obtained. Polymeric products are formed with all substrates and are presumed the major products of 2,4,6-substituted

phenols. The presence of a dimer, trimer, and tetramer from 2,4,6-trichlorophenol is shown by mass spectrometry.

Halide formation is seen only for 2,4,6-trihalophenals and a mechanism for its formation *via* hypohalous acid is proposed.

No evidence of the cyclisation of 2-(2'-chlorophenoxy)phenol to dibenzo[1,4]dioxin on reaction with gaseous NO_2 has been found.

The electron transfer reactivity with gaseous NO_2 of a range of phenols is reported in the Appendix.

Chapter 7

Concluding Remarks

This Thesis describes the mechanism and relevance of nitrogen dioxide oxidations. The systematic study of the reactions of gaseous NO_2 with aqueous solutions using the $[NO_2^-]/[NO_3^-]$ ratio to determine electron transfer from readily oxidised substrates has led to the following conclusions.

NO_2 and N_2O_4 are both electron transfer oxidants. The existence of a peroxidic form of N_2O_4 (ON-OO-NO) as a kinetically stable isomer able to oxidise substrates is suggested.

Electron transfer to NO_2 and N_2O_4 accounts for the varied Saltzman Factors previously observed in the measurement of ambient NO_2.

Electron transfer from biological antioxidants and serum proteins to NO_2 and N_2O_4 explains why NO_2^- is exclusively produced when gaseous NO_2 reacts with blood[71]. The physiological importance of oxidation by NO_2 and N_2O_4 is therefore established.

Reaction by substrates without active hydrogen atoms, estimates of the rate coefficients of reaction, and the product analyses of 3-methylindole, phenol, and 2,4,6-trimethylphenol on reaction with gaseous NO_2, all support NO_2 and N_2O_4 as one electron oxidants.

Chapter 8

Experimental

8.1. Reactions with NO_2

N_2O_4 (Matheson 99%) was purified by trap-to-trap distillation.

8.1.1. Gas Circulation Apparatus

Purified N_2O_4 was stored in the reservoir shown in Figure 37. The reservoir supplies a constant level of NO_2, at the temperature required, and tap (B) enables one to equilibrate the pressure to atmospheric pressure on taking a sample. A sample of NO_2 of the required volume is thus transfered via a lockable gas syringe to the Gas Circulation Apparatus (Figure 38) to achieve the concentration sought. After five minutes mixing using the peristaltic pump the reaction sample is then added. This period was found to be essential for adequate mixing of the NO_2. The system is that of an Exponential Dilution Flask[130] in that the NO_2 is not recirculated but is destroyed by the drying train after the reaction. This was necessary to keep the system dry and stop water vapour from the reaction flask condensing throughout the system, and leading to unreliable NO_2 concentrations through unwanted hydrolysis.

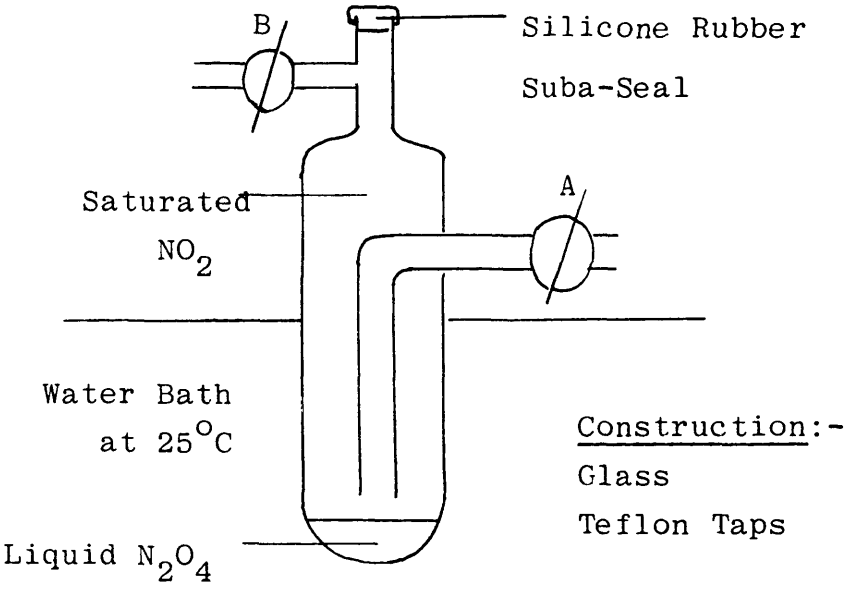


Figure 37. NO_2 Reservoir

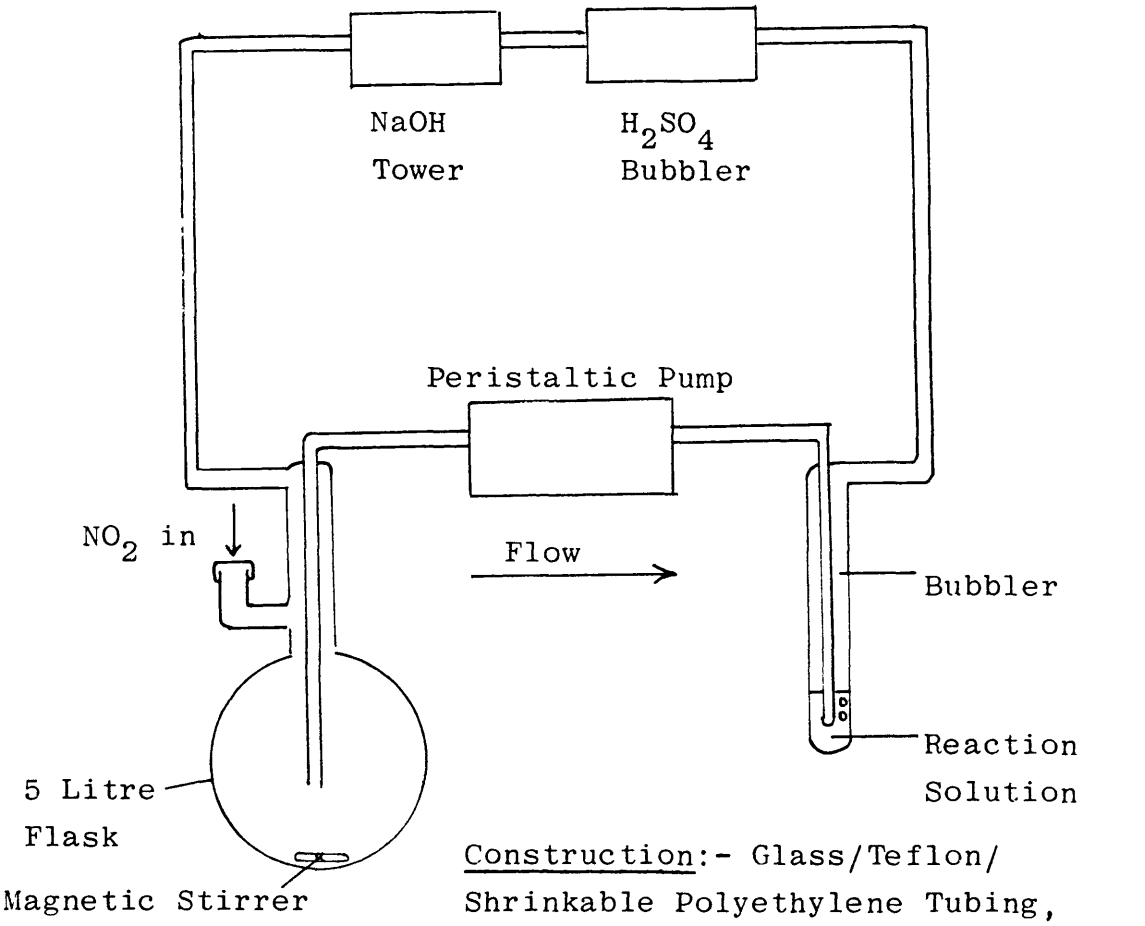
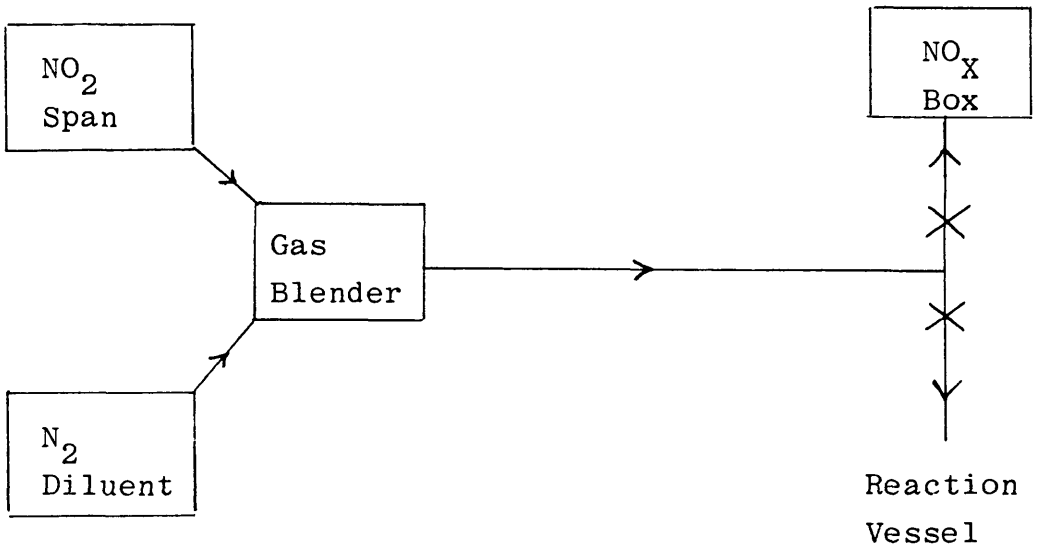


Figure 38. Gas Circulation Apparatus

8.1.2. NO_2 Line

Early studies of the reactions of NO_2 were made using the Gas Circulation System (Section 8.1.1.). However to obtain a more reliable, unlimited, controlable and measureable supply of dilute NO_2 an NO_2 line shown in Figure 39 was constructed.



Construction:-

NO_2 clyinder, 900Vpm (British Oxygen Company)
N_2 clyinder, white-spot oxygen free (British Oxygen Company)
Signal Series 850 Gas Blender (Signal Instrument Company, Camberley, Surrey)
Chemiluminescent NO-NO_2-NO_X Analyser, Model 14A (Thermo Electron Corporation, Environmental Instruments Division, Massachussetts, USA)
Inert Teflon Tubing and Stainless-Steel T-Piece and Needle Valves

Figure 39. NO_2 Line Schematic

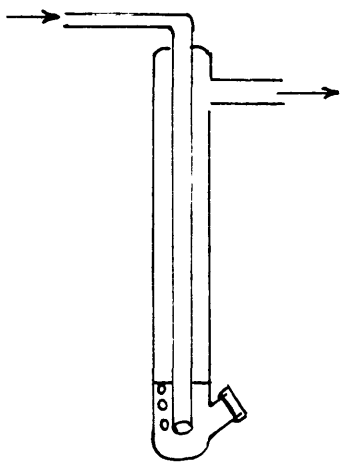
Nitrogen was chosen as the diluent as absorption of CO_2 from an air diluent was found to cause signigicant pH changes during long runs at low ppm NO_2.

A 5% CO_2 in nitrogen diluent (Btitish Oxygen Company) was used for the reactions in serum and plasma to maintain the pH at 7.4.

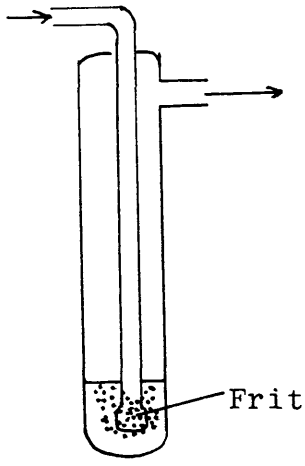
A primary standard of 900 Vpm NO_2 in air was chosen to give a versatile dynamic range of the Gas Blender (1-900 ppm) which enabled us to access environmental levels. This primary standard was also used to calibrate the Chemiluminescent NO_X Analyser so that the operation of the Gas Blender and the Gas Circulation System could be checked.

8.1.3. Bubbler Design

Two bubbler designs were used (Figure 40). The ordinary bubbler was used in early work and in work in serum and plasma. Most of the work reported used the fritted-glass bubbler. The bubblers had no effect on the electron transfer capability of the compounds studied but the fritted-glass bubbler was twice as efficient at absorbing NO_2.



Ordinary Bubbler



Fritted-Glass Bubbler

Construction:- Glass , Sample Volumes = 10 ml

Figure 40. Bubbler Design

8.1.4. Typical Reaction Conditions

Comparable reaction conditions were used for both systems (i.e. flow rate, bubbler design, temperature and reaction volume).

A typical experiment to examine for any electron transfer capability of a compound involved passing 200 ppm gaseous NO_2 through a 10^{-2}M solution of the compound in 0.1M NaOH for 10 minutes using the fritted-glass bubbler on the NO_2 line with a nitrogen diluent. The bubbler was maintained at 25°C using a thermostatted water bath. The reaction solution was then analysed for nitrite and nitrate by hplc.

The Appendix details the reactivity of all the

compounds studied using this methodology and constitutes a Standard Reactivity Index.

8.2. Analytical Protocol

8.2.1. HPLC Analysis

8.2.1.1. General and Instrumentation

HPLC analyses were performed either on a LDC/Milton Roy modular system (Constametric III dual-piston pump, Spectrometric III variable wavelength detector, Rheodyne 7125 injection valve, CI-10B Computing Integrator and Thermal Printer) or on a composite laboratory system (Altex 110A single piston pump, Cecil CE 599 Variable Wavelength Detector, Rheodyne 7120 injection valve, LDC/Milton Roy CI-10B Computing Integrator and Thermal Printer). Injection volumes were generally 20 μl.

Concentrations were calculated using peak areas and calibrated against a range of gravimetrically prepared solutions of the authentic material in the same solvent used for the analysis. Peak areas were reproducible to $\pm$5% or better and reported values are typically the average of 3 injections.

All buffer solutions were prepared from analytical grade reagents and solvents where possible. Exceptions to this were the deionised water (Elgastat B.102 deioniser, input distilled water), acetonitrile (distilled off calcium hydride) and tetra-n-butylammonium hydroxide (40% solution in H_2O, BDH General Purpose Reagent).

All buffers were degassed by bubbling helium (British Oxygen Company) through the solutions for fifteen minutes prior to use.

8.2.1.2. Nitrite and Nitrate Ion Analysis

We have used four systems for the HPLC analysis of NO_2^- and NO_3^-, details of the columns and eluents used are given in Table 38.

Figure 1 (Chapter 2) shows chromatograms for NO_2^- and NO_3^- on all these systems. The Ion Chromatography system was the preferred system due to its high resolution and low analysis time. When interferences due to substrates were found the Hamilton PRP-1 RPIC system was used, this was the preferred system for all serum and plasma analyses.

It was found that sample preparation was critical to accurate quantitative analyses. The analysis of 0.1M NaOH solutions was particularly difficult due to the low buffer capacity of the buffers used. A six-fold dilution of the sample with 0.116M KH_2PO_4 prior to injection led to interference free, accurate and reproducible results. The same methodology was used for 0.1M HCl reaction solutions. Reaction solutions in the pH range 2-12 were accurately analysed by direct injection.

The eluent in all cases except the Dionex system was monitored at 214 nm where both NO_2^- and NO_3^- show approximately equal extinction.

The Dionex system uses a conductivity detector made more efficient by a suppressor system that neutralises

Separation Mechanism	Pre-Column	Column	Eluent	pH
Strong Anion eXchange (SAX)	Partisil 10μm SAX (60×4.5mm i.d.)	Partisil 10μm SAX (250×4.5mm i.d.)	0.04M KH_2PO_4	3.0
Reversed-Phase Ion Chromatography (RPIC) a)	Pellicular ODS (60×4.5mm i.d.)	Spherical 10μm ODS (250×4.5mm i.d.)	0.05M KH_2PO_4, 0.0025M Bu_4NOH	6.0
b)	Hamilton PRP-1 (60×4.5mm i.d.)	Hamilton PRP-1 (250×4.5mm i.d.)	0.05M borax, 0.0077M Bu_4NOH, 7.5% MeCN	9.0
Ion Chromatography	Waters Guard-PAK module p/n 088141	Waters IC-PAK p/n 07355	0.05M KH_2PO_4	6.0
Suppressed Ion Chromatography (Dionex)	Guard Column	HPIC AS4A Analytical Column (p/n 037041)	0.75mM $NaHCO_3$/ 2.0mM Na_2CO_3	10.75

Table 38. Nitrite and Nitrate Ion HPLC Analysis Systems

the ions in the buffer thereby reducing the background level of ions. This enabled us to confirm the analyses of our RPIC ODS system (Ralph Cochrane, Dionex (UK) Ltd., Farnborough), and to simultaneously analyse for chloride, nitrite and nitrate ions (Dr. Michael Spiro, John Hooper, Chemistry Department, Imperial College). In these cases only 0.1M NaOH samples were analysed and sample preparation simply involved 100-fold dilution with deionised water.

8.2.1.3. Nitrophenols

Nitrophenol standards can be separated with ease by reversed-phase methodology. Analysis of real reaction mixtures causes the retention times of the compounds to vary due to the added salts present in the injected samples.

A system is described to analyse 0.1M NaOH reaction mixtures. Reliable quantitative analysis is achieved on a Spherical 10 μm ODS column and pellicular ODS pre-column with 0.05M KH_2PO_4, 5×10^{-3}M NaOH, 30% MeCN eluent monitoring the uv at 280 nm. Using a flow rate of 3.0 ml/min the retention times are 2.5 and 3.7 min for 4-nitrophenol and 2-nitrophenol respectively. The 0.1M NaOH samples are pre-diluted by 6-fold with 0.116M KH_2PO_4 prior to injection. Normally a 20μl injection loop is used but using a 500μl loop analysis down to 2.0×10^{-6}M (injected) in each nitrophenol is quantitative.

The nitration products of 2-(2'-chlorophenoxy)phenol were quantified in a similar manner using 0.05M KH_2PO_4, 40% MeCN as eluent, monitoring at 350 nm. The retention

times were 3.0 and 4.4 mins for the 4- and 2- nitro isomers respectively.

8.2.1.4. Nitroanilines

Quantitative analysis for nitroanilines in 0.1M NaOH followed a similar protocol to the analysis of nitrophenols (Section 8.2.1.3.). The experimental details are shown in Table 39.

Column	Spherical 10μ ODS
Pre-Column	Pellicular ODS
Eluent	0.05M KH_2PO_4, 25% MeCN
Flow	3.0 ml/min
Monitoring Wavelength	230 nm
Retention Times	4-Nitroaniline=2.5 mins
	2-Nitroaniline=4.1 mins

Table 39. Analysis of Nitroanilines

8.2.2. GC Analysis

8.2.2.1. General and Instrumentation

Capillary GC

All capillary GC analyses were performed using a Carlo-Erba 4160 HRGC, a BP05 12 metre capillary column with on-column injection and flame-ionisation detection (FID). Injection volumes were of the order of 0.3μl and

the gas pressures were typically 0.5, 0.7 and 1.1 kg/cm^2 for helium, hydrogen and air respectively.

Concentrations were calculated by calibration against gravimetrically prepared solutions of the authentic material in the same solvent used for the analysis. The peaks were generally sharp and had little tailing and peak heights were used to calculate concentrations. Peak heights were reproducible to within ±10% and the average value of 2 or 3 repeated injections was taken. Table 40 gives the experimental conditions and retention times of compounds analysed by capillary GC.

2-Methylindole/3-Methylindole Analysis

Separation of 2- and 3- methylindole was achieved using a Perkin-Elmer F11 GC with FID detection on a 1/8 inch stainless steel 4m column packed with 3% silicone OV-225 on Chromosorb W.HP. 100-120 mesh. The gas pressures were; N_2 50psi, H_2 30psi and Air 16psi. The injection port setting was 10 and the oven temperature 200°C. 2- and 3- Methylindole had retention times of 7.4 and 6.5 minutes and it was possible to observe a 0.5% 2-methylindole spiked impurity in 3-methylindole. No peak for 2-methylindole was seen in the 3-methylindole used subsequently. The injection volumes on this packed column system were 1.0µl.

Compound	Oven Temp /°C	Detector Temp /°C	Retention Time/mins
Phenol	100	150	0.7
2,4,6-Trichlorophenol	150	200	2.1
2,4,6-Trimethylphenol	150	200	1.1
2-Chlorophenol	150	200	0.7
2-Nitrophenol	100	150	1.1
3-Nitrophenol	100	150	8.6
4-Nitrophenol	100	150	12.4
2-(2'-Chlorophenoxy) phenol	150	200	8.5
Dibenzo 1,4 dioxin	150	200	5.0
2,6-Dimethyl-4-nitrophenol	150	200	5.7
3,5-Dimethyl-4-hydroxybenzaldehyde	150	200	3.1
2-Chloro-4-nitrophenol	150	200	2.6
2-Chloro-6-nitrophenol	150	200	1.8
4-Nitrosophenol	100	150	3.8

Table 40. Compounds Analysed by Capillary GC on a BP05 Column

8.2.2.2. Work-up Procedures

Phenol Product Analysis

0.1M NaOH reaction solutions (10ml) for solvent extraction were first acidified with 0.1M HCl (20ml) and then extracted with the required organic solvent (2×20ml). These extracts were then analysed by tlc, GC and mass spectrometry after sample concentration.

0.1M NaOH reaction solutions (10ml) for freeze-drying were neutralised with 0.1M HCl (10ml) and then freeze-dried. The organic residue was then taken up in distilled THF (10ml) prior to analysis by GPC and mass spectrometry.

Quantitative analyses of nitrophenols and chloride ions were made on the 0.1M NaOH solutions without acidification, just dilution of the samples with phosphate buffer and water respectively.

Dioxin Production

2-(2'-Chlorophenoxy)phenol was examined for any evidence of cyclisation to dibenzo[1,4]dioxin on reacting with gaseous NO_2 under a wide variety of solvent polarities and pH.

Work-up involved neutralisation of the solutions with 0.1M HCl or $NaHCO_3$ and extraction with benzene. The recovery of dibenzo[1,4]dioxin was almost quantitative and 0.4% yield of the dioxin was the minimum detection limit.

8.2.3. GC/MS

This was provided as part of the departmental mass spectrometry service by kind permission of Dr. E.S.Waight and run by Dr. J.A.Challis.

Samples were analysed by cold on-column injection onto a BP1 or BP15 capillary column using helium as the carrier gas. The column effluent was analysed on a VG 7070 mass spectrometer in electron-impact ionisation mode. A resolution between peaks of 1.5 seconds on a scanning range up to m/z 600 was possible. The resolution time was slightly longer for wider scanning ranges. The capillary column oven was temperature programmed up to 220°C to achieve the best resolution of the sample.

Products were identified by the synthesis of authentic compounds and their subsequent analysis by GC/MS or as a probe sample on the same instrument. Yields were quantified on our own GC system with FID detection.

8.2.4. GPC Analysis

GPC analyses were performed on the same system as hplc analyses (Section 8.2.1.1.) using a PL-Gel, 5μ, 50Å, 300mm×7.5mm (i.d.) column and pre-column, 50mm×7.5mm (i.d.) (Polymer Laboratories, Church Stretton, Shropshire). The eluent used was distilled THF (off potassium) at a flow rate of 1.0 ml/min. 290nm was the monitoring wavelength and an injection loop of 20μl was generally used. Sample preparation has already been described (Section 8.2.2.2.). The column was approximately calibrated using polystyrene standards (Polymer Laboratories).

8.3. Biological Fluids

Blood used for the initial studies in serum and plasma was kindly donated by my colleagues in the Harwood Laboratory after an overnight fast. It was withdrawn intravenously with a wide-bore needle to prevent any haemolysis, into a 50ml syringe by Dr. Alan Swann, Imperial College Health Centre.

For serum the blood was left to clot for thirty minutes before being spun and the serum pipetted out (Dr. Simon Dunmore, Imperial College Biochemistry Department).

For plasma an anticoagulant was immediately added to the blood (50μl of Heparin Sodium Injection, 25000 units in 1ml (Evans), per 25ml of blood). The blood was then spun after standing for one hour at room temperature.

Further studies in plasma were made in out-dated plasma collected from the National Blood Transfusion Service. This Plasma contained a Citrate Phosphate Dextrose anticoagulant (CPD-A1). This plasma was converted into serum by addition of calcium chloride solution sufficient to achieve 0,02M in the plasma. A complex forms between the calcium and citrate which allows the plasma protein to clot and be removed (after 30 mins at 25^{o}C). Hence studies could be undertaken on plasma and serum from the same source.

8.4. Preparative

General and Instrumentation

Reagents were obtained from commercial sources unless otherwise stated. All solvents and reagents were purified where necessary by standard techniques[131].

The physical properties of compounds were determined on the following instruments. Infra-red spectra were measured on a Perkin-Elmer 298 grating spectrometer with polystyrene calibration. Proton NMR spectra on a Varian EM360A/60 MHz or Jeol FX-90Q/90 MHz spectrometer, tetramethylsilane as the internal standard. Melting points were measured on a Gallenkamp hot-stage apparatus and were uncorrected. Mass spectra were provided by the departmental service using a VG 7070 instrument, usually in electron-impact ionisation mode. Elemental microanalyses were provided by Mr. K Jones of the Chemistry department. pH measurements were made on a pTI6 universal digital pH meter, calibrated using standard buffer solutions.

2-(2'-Chlorophenoxy)phenol (32)

Sodium 2-chlorophenoxide was prepared by dissolving 2-chlorophenol in an equimolar quantity of sodium hydroxide solution, evaporating the solution to dryness and drying in vacuo.

Finely divided copper powder was prepared by adding zinc dust to an equimolar quantity of copper(II)sulphate solution at 60-80^{o}C and filtering off the brick red powder precipitated[132].

Sodium 2-chlorophenoxide (0.35g, 2.3mmol) was refluxed in 2-chlorophenol (5.0g,b.p. 176°C) with freshly prepared copper powder (0.20g, 3.1mmol, 1.3eq) for 60 hours under argon. The reaction mixture was allowed to cool, filtered through silica to remove the copper and the 2-chlorophenol was removed by Kugelrohr distillation in vacuo. Column chromatography on silica with dichloromethane -petroleum ether (b.p. 60-80°C) (1:1) as eluent gave 2-(2'-chlorophenoxy)phenol (32)[133-135] as a white crystalline solid (220mg, 43%) (Found: C, 65.5; H, 4.3. Calc. for $C_{12}H_9O_2Cl$: C, 65.3; H, 4.1%); ν_{max} (nujol mull) 3520br (HO), 1240 cm^{-1} (C-Ostr); δ_H (90MHz, $CDCl_3$) 6.7 (1H, brs, OH), 7.1 (8H, m, aromatic protons); m/z 220 (M^+, 100%), 185 (78, M-Cl), 222 (M^+, 32).

Dibenzo[1,4]dioxin (33)

This compound was a product in the synthesis of 2-(2'-chlorophenoxy)phenol (32) and column chromatography under identical conditions also gave dibenzo 1,4 dioxin (33) as a white crystalline solid (180mg, 43%); m.p. 117-118°C (lit.[136], 119°C); δ_H (90MHz, $CDCl_3$) 6.85 (s, aromatic protons); m/z 184 (M^+, 100%).

2-Chloro-4-nitrophenol (34)

2-Chlorophenol (1.0g, 7.8mmol) was stirred with sodium acetate (3.2g, 39mmol, 5eq) in dry distilled dichloromethane (50ml) at ice temperature. N_2O_4 (0.5ml, 15.6mmol, 2eq) was added and the mixture stirred for one hour[18]. The reaction solution was washed with ice-cold

solutions of water, 5% sodium carbonate and water (all 2×50ml) before being dried over $MgSO_4$. The dichloromethane was removed by rotary evaporation at 25°C and column chromatography on silica with dichloromethane-petroleum ether (b.p. 60-80°C) (4:1) gave 2-chloro-4-nitrophenol (34) as a yellow crystalline solid (250mg, 18%); m.p. 111-112°C (lit.[136], 111°C); ν_{max} (nujol mull) 3396 (HO), 1530, 1340 cm^{-1} (NO_2str); δ_H (90MHz, $CDCl_3$) 6.2 (1H, brs, OH), 7.12 (1H, d, J_{56} 9.3Hz, 6-H), 8.14 (1H, dd, J_{35} 2.2Hz, J_{56} 9.3Hz, 5-H), 8.30 (1H, d, J_{35} 2.2Hz, 3-H); m/z 173 (M^+, 100%), 175 (M^+, 33).

2-Chloro-6-nitrophenol (35)[120]

2-Chlorophenol (0.58g, 0.45M) and potassium hydrogen sulphate (0.68g, 0.5M) were dissolved in water (10ml). To this ice-cold stirred solution was added concentrated sulphuric acid (1.72g, 0.93ml, 1.75M) followed by concentrated nitric acid (0.32g, 0.22ml, 0.5M), no temperature increase was observed. The mixture was stirred at 0°C for five minutes, allowed to warm to 20°C and stirred for 10 hours. The reaction solution was then extracted with diethyl ether (2×20ml), dried over $MgSO_4$ and purified by column chromatography (CH_2Cl_2/60-80°C petroleum ether, 8:2, silica) to give 2-chloro-6-nitrophenol (35) as a yellow crystalline solid (70mg, 9%); m.p. 68-69°C (lit.[136], 70°C); ν_{max} (nujol mull) 3326 (HO), 1540, 1350 cm^{-1} (NO_2str); δ_H (90MHz, $CDCl_3$) 6.96 (1H, t(dd), J_{34} 8.4Hz, J_{45} 8.8Hz, 4-H), 7.71 (1H, dd, J_{35} 1.64Hz, J_{34} 8.4Hz, 3-H), 8.07 (1H, dd, J_{35} 1.64Hz,

J_{45} 8.8Hz, 5-H); m/z 173 (M^+, 100%), 175 (M^+, 32), 156 (7, M-17).

2-(2'-Chlorophenoxy)-4-nitrophenol (36)

To a stirred solution of 2-(2'-chlorophenoxy)phenol (32) (400mg, 1.81mmol) with sodium acetate (2.0g, 24mmol, 13eq) in dry distilled dichloromethane in a flask fitted with a drying tube was added N_2O_4 (50µl, 1.55mmol, 0.86eq)[18]. The mixture was stirred at ice temperature for 60 minutes and then at room temperature for 60 minutes. The reaction mixture was filtered, the dichloromethane removed under reduced pressure and column chromatography (benzene, silica) gave 2-(2'-chlorophenoxy)-4-nitrophenol (36) as an orange oil (79.0mg, 19%) (Found: C, 54.7; H, 3.5; N, 5.1. $C_{12}H_8NO_4Cl$ requires: C, 54.3; H, 3.0; N, 5.3%. Accurate Mass Measurement. Found: 265.0136. $C_{12}H_8NO_4Cl$ requires: 265.0142); ν_{max} (nujol mull) 3320 (HO), 1540, 1350 (NO_2str), 1290 cm^{-1} (C-Ostr); δ_H (90MHz, $CDCl_3$) 7.0-8.5 (multiplet); m/z 265 (M^+, 100%), 267 (M^+, 33), 230 (27, M-Cl).

2-(2'-Chlorophenoxy)-6-nitrophenol (37)

This compound was a product in the synthesis of 2-(2'-chlorophenoxy)-4-nitrophenol (36) and column chromatography under identical conditions also gave 2-(2'-chlorophenoxy)-6-nitrophenol (37) as a yellow oil (31.9mg, 7.8%) (Found: C, 54.4; H, 3.3; N, 5.3. $C_{12}H_8NO_4Cl$ requires: C, 54.3; H, 3.0; N, 5.3%. Accurate Mass Measurement. Found: 265.0136. $C_{12}H_8NO_4Cl$ requires:

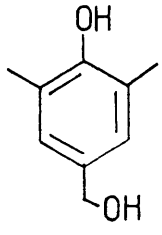
265.0142); ν_{max} (nujol mull) 3250 (HO), 1535, 1360 (NO_2str), 1280 cm^{-1} (C-Ostr); δ_H (90MHz, $CDCl_3$) 7.0-8.5 (multiplet); m/z 230 (100%, M-Cl), 265 (M^+, 90), 213 (39, M-17).

3,5-Dimethyl-4-hydroxybenzaldehyde (38)[122]

2,4,6-Trimethylphenol (273mg, 2.0mmol) was stirred in alkaline methanol (0.87g NaOH in 20ml) under nitrogen. To this solution iodine (1.04g, 4.1mmol, 2eq) in methanol (7ml of the 20ml above) was added dropwise over 10 minutes. The reaction mixture was then stirred under nitrogen for two hours. The reaction mixture was then poured into water (100ml), neutralised with 1M hydrochloric acid and the methanol removed under reduced pressure. The solution was then extracted with diethyl ether (2×50ml), washed with saturated sodium bisulphite solution to remove any iodine, washed repeatedly with water and dried over sodium sulphate. The product was purified by column chromatography on silica using diethyl ether-petroleum ether (b.p. 40-60°C) (5:2) as the eluent to give 3,5-dimethyl-4-hydroxybenzaldehyde (38) as a white crystalline solid (5mg, 2%); m.p. 112-113°C (lit.[136], 115-116°C); ν_{max} (nujol mull) 3230br (HO), 1660 cm^{-1} (CO); δ_H (90MHz, $CDCl_3$) 2.3 (6H, s, -C<u>H</u>$_3$), 5.27 (1H, s, OH), 7.55 (2H, s, 2-H and 6-H), 9.8 (1H, s, -C<u>H</u>O); m/z 149 (100%, M-H), 150 (M^+, 65), 121 (16, M-CHO).

Reduction of 3,5-Dimethyl-4-hydroxybenzaldehyde (38)

3,5-Dimethyl-4-hydroxybenzaldehyde (38) (2mg, 13μmol) was stirred in sodium dried diethyl ether (6ml) in dry apparatus under argon. To this solution lithium aluminium hydride (10mg, 0.3mmol, 80eq) was added. The suspension was stirred overnight at room temperature. The reaction was quenched by adding water (2ml) dropwise. The solution was then made acidic with 1M hydrochloric acid and extracted with diethyl ether. GC/MS showed there to be only diethyl ether and one other substance in this extract. The mass spectrum of this product was consistant with it being the benzyl alcohol reduction product (39) of 3,5-dimethyl-4-hydroxybenzaldehyde (38); m/z 152 (M^+, 100%), 134 (34, M-18). This was not a product of NO_2 oxidation of 2,4,6-trimethylphenol.



(39)

Periodic Acid Oxidation of 2,4,6-Trimethylphenol[121]

A solution of 2,4,6-trimethylphenol (0.2g, 1.5mmol) in water-ethanol (4:1, 80ml) was mixed with a solution of periodic acid (1g, 30mmol) in water (20ml) at room temperature. After five minutes unconsumed oxidant was destroyed by the addition of ethylene glycol (0.2g), prior to extraction with dichloromethane (4×20ml). The extracts were freed from iodine by washing with saturated aqueous sodium thiosulphate solution. The extracts were then

washed with water (4×20ml) and dried (magnesium sulphate) before being evaporated to dryness. The product mixture was treated with cold petroleum ether (b.p. 40-60°C) and the Diels-Alder dimer (40) of 2-hydroxy-2,4,6-trimethyl-3,5-cyclohexadien-1-one (23) separated as a crystalline product (40mg, 20%); m.p. 173-174°C (lit.[137], 182-183°C); ν_{max} (nujol mull) 3480 (HO), 3430 (HO), 1712 (CO), 1680 (conj CO) (lit.[137], 3490, 3400, 1710, 1684 cm^{-1}); m/z 152 (84%, M/2), 110 (74), 109 (50), 304 (M^+, 14). GC/MS of the remaining petroleum ether mixture showed there to be a product identified as 4-hydroxy-2,4,6-trimethyl-2,5-cyclohexadien-1-one (24); m/z 137 (100%), 43 (64), 152 (M^+, 50), 109 (49).

Appendix. Standard Reactivity Index

The reactivity of a wide-range of compounds has been examined under the following standard set of conditions. 10ml of a 10^{-2}M substrate solution in 0.1M NaOH was reacted with 200 ppm gaseous NO_2 at a flow rate of 80 ml/min for 10 mins using the fritted-glass bubbler at 25°C. Exceptions to the above conditions are noted with the specific entry.

Substrates have been arranged according to their chemical functionalities and repetition of entries has been avoided. It may therefore be necessary to look in many categories to find a compound of interest. Compounds are listed under the following categories:-

Phenols

Amines

Amino-Acids

Heterocycles

Thiols/Disulphides

Miscellaneous

Table 41. Phenols

Substrate	$[NO_2^-]/[NO_3^-]$
2-Methoxyphenol	>50
2,4,6-Trichlorophenol	>50
Phenol	>50 (est.640)[a]
2,4,6-Triiodophenol	42
2,6-Ditertbutyl-4-nitrophenol (5% MeCN)	39
2,4,6-Trimethylphenol	35
Bis(2-hydroxyphenyl)methane	45
2-(2'-Chlorophenoxy)phenol (5% MeCN)	37
2-Chlorophenol	16
Pentachlorophenol	17
2-Nitrophenol	8.9
4-Nitrophenol	2.6

[a] Substrate dependence data (Figure 7, Section 2.4.3.)

Table 42. Amines

Substrate	$[NO_2^-]/[NO_3^-]$
N-(1-Naphthyl)ethylenediamine dihydrochloride (10% MeCN)	>50
1-Naphthylamine (20% MeCN)	23
Aniline	15
Triethylamine	50
DABCO	9.0
Pyrrolidine	11.8
Piperazine	12.1
N-Butylamine	1.0

Table 43. Amino-Acids

Substrate	$[NO_2^-] / [NO_3^-]$
L-Tyrosine	>50
L-Cysteine	>50
L-Histidine	40
L-Tryptophan	13
L-Proline	7.5
L-Cystine	1.4
L-Alanine	1.1
L-Threonine	1.2
L-Lysine	1.0
Glycine	1.1
L-Leucine	1.2
L-Serine	1.2
L-Phenylalanine	1.1
L-Arginine	1.1
D,L-Methionine	1.0
L-Aspartic Acid	1.1
L-Glutamic Acid	1.1
S-Methylcysteine (330 ppm NO_2)	1.0

Table 44. Heterocycles

Substrate	$[NO_2^-] / [NO_3^-]$
Imidazole	7.0
Indole (10% MeCN)	6.3
3-Methylindole (0.1M SDS, pH 9.4)	6.5
Pyrrole	3.2

Table 45. Thiols/Disulphides

Substrate	$[NO_2^-] / [NO_3^-]$
Thiophenol	>50
Glutathione	19
Glutathione Disulphide	>50

Table 46. Miscellaneous

Substrate	$[NO_2^-] / [NO_3^-]$
L-Ascorbic Acid	$>$ 50
α-Tocopherol (Vitamin E)	$>$ 50
(10^{-3}M, 0.1M SDS, 10% MeCN)	
Uric Acid	$>$ 50
Phenothiazine	$>$ 50
Dibenzo[1,4]dioxin	1.3
Creatine	0.9
Creatinine	1.0
N-Butanol	1.1
Tert-Butanol	1.0
Ammonia	1.1
α-D(+)Glucose (330 ppm NO_2)	1.2

References

1. RSC Environment Group Symposium, "Chemical Aspects of Acid Rain", London, 30th. May 1985.
2. W.A. Pryor, G.J. Gleicher, J.P. Cosgrove, and D.F. Church, J. Org. Chem., 1984, 49, 5189.
3. L. Eberson and F. Radner, Acta Chem. Scand., Ser. B, 1985, 38, 343.
4. V. Norman and C.H. Keith, Nature, 1965, 205, 915.
5. P. Gray and A.D. Yoffe, Chem. Rev., 1955, 55, 1069.
6. Y. Rees and G.H. Williams, Adv. Free Radical Chem., 1969, 3, 199.
7. C.W. Buaschlicher, Jr., A. Komornicki, and B. Roos, J. Am. Chem. Soc., 1983, 105, 745.
8. C.H. Bibart and G.E. Ewing, J. Chem. Phys., 1974, 61, 1284.
9. B.C. Challis and S.A. Krytopoulos, J. Chem. Soc., Perkin Trans. 2, 1978, 1296.
10. L. Eberson and F. Radner, Acta Chem. Scand., Ser. B, 1980, 34, 739.
11. T.F. Redmond and B.B. Wayland, J. Phys. Chem., 1968, 72, 1626.
12. F.A. Cotton and G. Wilkinson, "Advanced Inorganic Chemistry", 4th. Edn., John Wiley and Sons, New York, 1980, p. 426.
13. G.A. Olah, S.C. Narong, and R.L. Pearson, Synthesis, 1978, 6, 452.
14. H. Shechter, Record of Chemical Progress, 1964, 25, 55.

15. A.I. Titov, Tetrahedron, 1963, 19, 557.

16. T. Yoshida and K. Nambia, J. Fac. Eng. Univ. Tokyo, Ser. A, 1970, 8, 60.

17. W.A. Pryor, J.W. Lightsey, and D.F. Church, J. Am. Chem. Soc., 1982, 104, 6685.

18. E.H. White, J. Am. Chem. Soc., 1955, 77, 6008.

19. E.H. White, J. Am. Chem. Soc., 1955, 77, 6011.

20. E.H. White, J. Am. Chem. Soc., 1955, 77, 6014.

21. R. Huisgen and H. Reimlinger, Liebigs Ann. Chem., 1956, 599, 161.

22. R. Huisgen and C. Ruchardt, Liebigs Ann. Chem., 1956, 601, 21.

23. E.H. White in "Chemistry of the Amino Group", Ed. S. Patai, Interscience, New York, 1968, p. 407.

24. E.H. White and W.R. Feldman, J. Am. Chem. Soc., 1957, 79, 5832.

25. B.C. Challis and S.A. Krytopoulos, J. Chem. Soc., Perkin Trans. 1, 1979, 299.

26. J.H. Ridd, Quarterly Reviews, 1961, 15, 418.

27. B.C. Challis, J.R. Milligan, and R.C. Mitchell, J. Chem. Soc., Chem. Commun., 1984, 1050.

28. J. Garcia, J. Gonzalez, R. Segura, and J. Vilarrasa, Tetrahedron, 1984, 40, 3121.

29. B.R. Glover, Ph.D. Thesis, University of London, 1986.

30. J.R. Milligan, Ph.D. Thesis, University of London, 1984.

31. C. Monti-Bragadin, M. Tamaro, and E. Banfi, Antimicrob. Agents Chemother., 1974, 6, 655.

32. F. Radner, Acta Chem. Scand., Ser. B, 1983, 37, 65.

33. L. Eberson and F. Radner, Acta Chem. Scand., Ser. B, 1984, 38, 861.

34. L. Eberson and F. Radner, Acta Chem. Scand., Ser. B, 1985, 39, 357.

35. M. Ali and J.H. Ridd, J. Chem. Soc., Perkin Trans. 2, 1986, 327.

36. A.T. Cocks and A.J. Crane, CEGB Report No. TPRD/L/2753/N84, March 1985.

37. B.E. Saltzman, Anal. Chem., 1954, 26, 1949.

38. F.P. Scaringelli, E. Rosenberg, and K.A. Rehme, Environ. Sci. Technol., 1970, 4, 924.

39. M.R. Jacobs and S. Hochheiser, Anal. Chem., 1958, 30, 426.

40. B.E. Saltzman and A.F. Wartberg, Jr., Anal. Chem., 1965, 37, 1261.

41. J.T. Shaw, Atmospheric Environment, 1967, 1, 81.

42. M. Buck and H. Stratman, Staub-Reinhalt Luft, 1967, 27, 265.

43. G.B. Morgan, C. Golden, and E.C. Tabor, J. Air Pollut. Contr. Assoc., 1967, 17, 300.

44. F. Nietruch and K.-E. Prescher, Fresenius' Z. Anal. Chem., 1969, 244, 294.

45. H.-J. Crecelius and W. Forweg, Staub-Reinhalt Luft, 1970, 30, 294.

46. T. Nash, J. Chem. Soc. (A), 1970, 3023.

47. T. Nash, Atmospheric Environment, 1970, 4, 661.

48. C. Huygen and P.H. Steerman, Atmospheric Environment, 1971, 5, 887.

49. C. Huygen, Anal. Chem., 1970, 42, 427.

50. L.J. Purdue, J.E. Dudley, J.B. Clement, and R.J. Thompson, Environ. Sci. Technol., 1972, 6, 152.

51. J. Kann, O. Tauts, R. Kalve, and T. Paalme in "N-Nitroso Compounds in the Environment", Eds. P. Bogovski and E.A. Walker, IARC Scientific Publication No. 9, IARC, Lyon, 1974, p. 180.

52. J. Alary, P. Bourbon, P. Chovin, C. Delaunay, J. Eclasson, and J.-C. Lepart, Water, Air and Soil Pollution, 1974, 3, 555.

53. H. Hartkamp and G. Nitz, Staub-Reinhalt Luft, 1974, 34, 439.

54. C. Huygen and R.W. Lanting, Atmospheric Environment, 1975, 9, 1027.

56. Y. Yanagisawa and H. Nishimura, Journal of Japan Society of Air Pollution, 1980, 15, 179.

57. H. Kersting, H. Heberer, and G. Bittersohl, Z. Gesamte Hyg. Ihre. Grenzgeb, 1980, 26, 177.

58. J. Nair and V.G. Gupta, Atmospheric Environment, 1981, 15, 107.

59. P. Chovin and C. Delaunay, Comptes-Rendus de L'Academie des Sciences, 1974, 278-D, 137.

60. A. Gold, Anal. Chem., 1977, 49, 1449.

61. A.J. Apling, F.S.M. Rogers, and K.J. Stevenson, Report No. LR 396(AP), Warren Spring Laboratory, Department of Industry.

62. S.A. Nyarady and R.E. Sievers, J. Am. Chem. Soc., 1985, 107, 3726.

63. S.A. Nyarady, R.M. Barkley, and R.E. Sievers, Anal. Chem., 1985, 57, 2065.

64. I. Smith, Report No. ICTIS/TR10, IEA Coal Research, London, October 1980.

65. H. Chiodi and J.G. Mohler, Environ. Res., 1985, 37, 355.

66. M.P. Doyle and J.W. Hoekstra, J. Inorg. Biochem., 1981, 14, 351.

67. R.A. Ehrman, M. Treshow, and I.M. Lytle, Am. Indust. Hygiene Assoc. J., 1972, 751.

68. H. Kosaka, K. Imaizumi, K. Imai, and I. Tyuma, Biochimica et Biophysica Acta, 1979, 581, 184.

69. M.P. Doyle, R.K. Pickering, T.M. der Weert, J. Hoekstra, and D. Potter, J. Biol. Chem.,1981, 256, 393.

70. H. Kosaka and M. Uozumi, Biochimica et Biophysica Acta, 1986, 871, 14.

71. E.M. Postlewait and M.G. Mustafa, Journal of Toxicology and Environmental Health, 1981, 7, 861.

72. H. Oda, H. Tsubone, A. Suzuki, T. Ichinose, and K. Kubota, Environ. Res., 1981, 25, 294.

73. P. McDonald and G.A. Hamilton in "Oxidation in Organic Chemistry", Ed. W.S. Trahanovsky. Organic Chemistry. A Series of Monographs, Volume 5-B, Academic Press, New York, 1973, p. 97.

74. M.L. Mihailovic and Z. Cekovic in "The Chemistry of the Hydroxyl Group, Part 1", Ed. S. Patai, Interscience, London, 1971, p. 505.

75. H. Musso, Angew. Chem. Internat. Edn., 1963, 2, 723.

76. A.I. Scott, Quarterly Reviews, 1965, 19, 1.

77. D.H.R. Barton, A.M. Deflorin, and O.E. Edwards, J. Chem. Soc., 1956, 530.

78. S.A. Weiner and L.R. Mahoney, J. Am. Chem. Soc., 1972, 94, 5029.

79. W.A. Prütz, J. Butler, and E.J. Land, Int. J. Radiat. Biol., 1983, 44, 183.

80. W.A. Prütz, H. Mönig, J. Butler, and E.J. Land, Arch. Biochem. Biophys., 1985, 243, 125.

81. B.O. Lingren, Acta Chem. Scand., 1960, 14, 1203, 2809.

82. G. Brunton, H.W. Cruse, K.M. Riches, and A. Whittle, Tetrahedron Lett., 1979, 12, 1093.

83. M. Alawi, Fresenius' Z. Anal. Chem., 1984, 317, 372.

84. N.E. Skelly, A.C. Oomens, and F.G. Schuurhuis, J. Chromatogr., 1984, 284, 503.

85. E. Müller, R. Mayer, B. Narr, A. Rieker, and K. Scheffer, Liebigs Anal. Chem., 1961, 645, 25.

86. W.A. Hunter and M. Morse, J. Am. Chem. Soc., 1926, 48, 1615.

87. D.P. Lee, J. Chromatogr. Sci., 1982, 20, 203.

88. J.H. Kershaw and D. Chamberlain, Ind. Eng. Chem., Anal., 1942, 14, 312.

89. N.S. Bayliss and D.W. Watts, Aust. J. Chem., 1963, 16, 927.

90. P.W. Atkins, "Physical Chemistry", Oxford University Press, Oxford, 1978, p. 871.

91. G.R. Smith and W.A. Guillory, J. Mol. Spectroscopy, 1977, 68, 223.

92. E.D. Morris and H.S. Johnston, J. Chem. Phys., 1967, 47, 4282.

93. W.A. Guillory and H.S. Johnston, J. Chem. Phys., 1965, 42, 2457.

94. H. Kominyana and H. Inoue, Chem. Eng. Sci., 1980, 35, 154.

95. M. Grätzel, A. Henglein, and S. Taniguchi, Ber. Bunsenges. Phys. Chem., 1969, 73, 646.

96. R.E. Huie and P. Neta, J. Phys. Chem., 1986, 90, 1193.

97. W.K. Wilmarth, D.M. Stanbury, J.E. Byrd, H.N. Po, and C.P. Chua, Coord. Chem. Rev., 1983, 51, 155.

98. S. Steenken and P. Neta, J. Phys. Chem., 1982, 86, 3661.

99. L.L. Miller, G.D. Nordblom, and E.A. Mayeda, J. Org. Chem., 1972, 37, 916.

100. "Encyclopedia of Electrochemistry of the Elements", Eds. A.J. Bard and H. Lund, Marcel Dekker Inc., New York, 1978.

101. Reference 74., p. 515.

102. L. Eberson, Adv. Phys. Org. Chem., 1982, 18, 79.

103. W.A. Pryor, D.F. Church, C.K. Govidan, and G. Crank, J. Org. Chem., 1982, 47, 156.

104. O. Hammerisch and V.D. Parker, Adv. Phys. Org. Chem., 1984, 20, 55.

105. J. Butler, E.J. Land, W.A. Prütz, and A.J. Swallow, J. Chem. Soc., Chem. Commun., 1986, 348.

106. D.L.H. Williams, Chem. Soc. Rev., 1985, 14, 171.

107. J.H. Fendler, "Membrane Mimetic Chemistry", John Wiley and Sons, New York, 1982.

108. L.J.C. Love, J.G. Haborta, and J.G. Dorsey, Anal. Chem., 1984, 56, 1132A.

109. "Documenta Geigy - Scientific Tables", Eds. C. Diem and C. Lentner, 7th. Edn., J.R. Geigy S.A., Basle, Switzerland, 1970.

110. D.D.M. Wayner, G.W. Burton, K.U. Ingold, and S. Locke, FEBS Lett., 1985, 187, 33.

111. "CRC Handbook of Biochemistry, Selected Data for Microbiology", Ed. H.A. Sober, 2nd. Edn., CRC, Cleveland, Ohio, 1970.

112. B.C. Challis and M. Tehrani, personal communication.

113. I. Franklin, Ph.D. Thesis, University of London, 1979.

114. H. Marsh, Jnr. and G. Dryhurst, J. Electroanal. Chem. Interfacial Electrochem., 1979, 95, 81.

115. "Heterocyclic Compounds", Ed. R.C. Elderfield, Wiley, New York, Volume 7, pp. 708-711.

116. R.J. Sundberg, "The Chemistry of Indoles", Organic Chemistry. A Series of Monographs, Ed. A.T. Blomquist, Academic Press, New York, 1970.

117. "Eight-Peak Index of Mass Spectra", 3rd. Edn., The Mass Spectrometry Data Centre, The Royal Society of Chemistry, Nottingham, 1983.

118. H. Budzikiewicz, C. Djerrassi, and D.H. Williams, "Mass Spectrometry of Organic Compounds", Holden-Day Inc., San Francisco, 1967.

119. Y. Hoshika, J. Chromatogr. Sci., 1981, 19, 444.

120. C.A. Bunton, E.D. Hughes, C.K. Ingold, D.I.H. Jacobs, M.H. Jones, G.J. Minkoff, and R.I. Reed, J. Chem. Soc., 1950, 2628.

121. E. Alder, G. Andersson, and E. Edman, Acta Chem. Scand., Ser. B, 1975, 29, 909.

122. K. Omura, J. Org. Chem., 1984, 49, 3046.

123. W.W. Kaeding, J. Org. Chem., 1963, 28, 1063.

124. R. Pummerer, Chem. Ber., 1914, 47, 1472.

125. A.A. Moroz and M.S. Shvartsberg, Russ. Chem. Rev. (Engl. Transl.), 1974, 43, 679.

126. T. Kawaki and H. Hishimoto, Bull. Chem. Soc. Jpn., 1972, 45, 1499.

127. H. Weingarten, J. Org. Chem., 1964, 29, 3624.

128. R.A. Abramovitch, Adv. Free Radical Chem., 1962, 2, 87.

129. R. Bolton and G.H. Williams, Adv. Free Radical Chem., 1975, 5, 1.

130. R.S. Barratt, Analyst, 1981, 106, 817.

131. D.D. Perrin, W.L.F. Armarego, and D.R. Perrin, "Purification of Laboratory Chemicals", 2nd. Edn., Pergamon, Oxford, 1982.

132. R.Q. Brewster and T. Gröening, Org. Syn. Coll. Vol. 2, 1943, 445.

133. E. Biller, B. Haas, R. Schlegel, and F.-P. Schmook, Ger. Offen., 211760.

134. H.P. Crocker, Ger. Offen., 2005883.

135. A.H. Widiger, Jr. and R.L. Johnson, U.S. Patent, 3405184.

136. "Dictionary of Organic Compounds", Chapman and Hall, New York, 5th. Edn., 1982.

137. E. Alder, J. Dahlen, and G. Westin, Acta Chem. Scand., 1960, 14, 1580.